

Radon levels in South African homes - design  
elements for a national survey and initial  
results from directed sampling

by

Abbey Matimba Maheso



*Thesis presented in partial fulfilment of the requirements for  
the degree of Master of Science (Physics) in the Faculty of  
Science at Stellenbosch University*

Supervisor: Prof R.T. Newman

Co-supervisor: Prof R. Lindsay

March 2021

# Declaration

By submitting this thesis electronically, I declare that the entirety of the work contained therein is my own, original work, that I am the sole author thereof (save to the extent explicitly otherwise stated), that reproduction and publication thereof by Stellenbosch University will not infringe any third party rights and that I have not previously in its entirety or in part submitted it for obtaining any qualification.

March 2021

Date: .....

Copyright © 2021 Stellenbosch University

All rights reserved.

# Abstract

## Radon levels in South African homes - design elements for a national survey and initial results from directed sampling

Abbey Matimba Maheso

*Departement of Physics,*

*University of Stellenbosch,*

*Private Bag X1, Matieland 7602, South Africa.*

Thesis: MSc (Physics)

March 2021

Radon ( $^{222}\text{Rn}$ ) is an inert, colourless, odourless radioactive gas that is generated by the alpha decay of radium ( $^{226}\text{Ra}$ ), a radionuclide in the uranium ( $^{238}\text{U}$ ) decay series. Radon ( $^{222}\text{Rn}$ ) is the primary source of environmental radiation exposure posing significant risks to human health. The World Health Organization (WHO) estimates that between 3 and 14% of lung cancers are attributable to radon and its progeny. There are a number of factors contributing in a multiplicative manner to the radon levels inside dwellings (e.g. underlying soil and geology, building materials, building construction).

An overview of existing data on indoor radon levels across South Africa and national radon surveys conducted around the world is presented. The approach strategies adopted to achieve public acceptance of radon detectors in dwellings is presented and discussed. An investigation

*ABSTRACT*

---

into the most appropriate technology to use for short- and long-term indoor radon measurements was undertaken. As part of this, results from measurements with track-etch, electret ion-chamber and Airthings™ detectors were critically compared.

Radon measurements were carried in workplaces, homes and schools. The radon concentration recorded in workplaces (offices and laboratories) ranged from  $32.2 \pm 5.2 \text{ Bqm}^{-3}$  to  $87.0 \pm 10.1 \text{ Bqm}^{-3}$ . The levels recorded in Gauteng homes ranged from  $2.4 \pm 0.3 \text{ Bqm}^{-3}$  to  $102.5 \pm 11.7 \text{ Bqm}^{-3}$ . The levels recorded in schools and homes in Western Cape ranged from  $12.3 \pm 2.8 \text{ Bqm}^{-3}$  to  $143.7 \pm 17.0 \text{ Bqm}^{-3}$  and from  $0.0 \pm 0.0 \text{ Bq m}^{-3}$  to  $126.9 \pm 14.6 \text{ Bqm}^{-3}$ , respectively.

Results of the surveys showed that radon concentration levels in most of the dwellings were low, whilst in areas close to granite outcrops the levels were found to be relatively high. The overall annual mean effective dose rate from radon and its decay progenies was estimated to be  $0.6 \pm 0.4 \text{ mSvy}^{-1}$  which yields an excess lifetime cancer risk of around  $1.7 \pm 1.1 \times 10^{-3}$ . These values are below the recommended action levels. The study recommends that the highly populated areas, especially those close to granite outcrops, should be prioritised for the future indoor radon survey. The radon measurements should preferably be made during the winter seasons using electret ion-chamber and track-etch detectors. Access to homes can be gained through the door-to-door approach, invitations and school outreach.

# Uittreksel

## Radonvlakke in Suid-Afrikaanse huise - ontwerpelemente vir 'n nasionale opname en aanvanklike resultate van gerigte steekproefneming

*(“Radon levels in South African homes - design elements for a national survey and initial results  
from directed sampling”)*

Abbey Matimba Maheso

*Departement Fisika,*

*Universiteit van Stellenbosch,*

*Privaatsak X1, Matieland 7602, Suid Afrika.*

Tesis: MSc (Fisika)

Maart 2021

Radon ( $^{222}\text{Rn}$ ) is 'n inerte, kleurlose, reuklose radioaktiewe gas wat ontstaan deur die alfa-verval van radium ( $^{226}\text{Ra}$ ), 'n radionuklid in die uraan ( $^{238}\text{U}$ ) vervalreeks. Radon ( $^{222}\text{Rn}$ ) is die primêre bron van blootstelling aan die omgewingstraling wat beduidende risikos vir die mens se gesondheid inhou. Die Wêreldgesondheidsorganisasie (WGO) skat dat tussen 3 en 14% van longkanker gevalle aan radon en sy afvalprodukte te wyte is. Daar is 'n aantal faktore wat op 'n vermenigvuldigende manier bydra tot die radonvlakke in huise (bv. onderliggende grond en geologie, boumateriaal, boukonstruksie).

## UITTREKSEL

---

'n Oorsig van bestaande data oor radonvlakke regoor Suid Afrika en nasionale radonopnames wat oor die hele wêreld gedoen word, word aangebied. Die benaderingsstrategie wat aangewend word om openbare aanvaarding van radondetektore in wonings te bewerkstellig, word aangebied en bespreek. 'n Ondersoek na die mees geskikte tegnologie om vir kort- en langtermyn radonmetings binnenshuis te gebruik, is onderneem. As deel hiervan is resultate van metings met spoor-ets, elektret ionokamer en Airthings™ detektore krities vergelyk.

Radonmetings is by werkplekke, binne huise en by skole. Die radonkonsentrasie wat by werkplekke (kantore en laboratoriums) aangeteken is, wissel van  $32.2 \pm 5.2 \text{ Bqm}^{-3}$  tot  $87.0 \pm 10.1 \text{ Bqm}^{-3}$ . Die vlakke wat in Gautengse huise aangeteken is, het gewissel van  $2.4 \pm 0.3 \text{ Bqm}^{-3}$  tot  $102.5 \pm 11.7 \text{ Bqm}^{-3}$ . Die vlakke wat in skole en huise in die Wes-Kaap aangeteken is, wissel van  $12.3 \pm 2.8 \text{ Bqm}^{-3}$  tot  $143.7 \pm 17.0 \text{ Bqm}^{-3}$  en van  $0.0 \pm 0.0 \text{ Bqm}^{-3}$  tot  $126.9 \pm 14.6 \text{ Bqm}^{-3}$ , onderskeidelik.

Resultate van die opnames het getoon dat die radonkonsentrasievlakke in die meeste wonings laag was, terwyl die vlakke relatief hoog in gebiede naby graniet "outcrops" was. Die totale jaarlikse gemiddelde effektiewe dosis as gevolg van radon en sy afvalprodukte word beraam op  $0.6 \pm 0.4 \text{ mSvy}^{-1}$  wat 'n oormaat lewenslange kankerrisiko oplewer van ongeveer  $1.7 \pm 1.1 \times 10^{-3}$ . Hierdie waardes is laer as die aanbevole aksievlakke. Die studie beveel aan dat die meer bevolkte gebiede, veral die naby graniet "outcrops" voorkeur moet geniet in toekomstige binnenshuise radonopnames. Radon metings moet verkieslik gedurende die winterseisoen geskied met behulp van elektriese ionokamer-en spoor-etsdetektors. Toegang tot huise kan verkry word deur die deur-tot-deur-benadering, uitnodigings en skooluitreike.

# Acknowledgements

I would like to thank God for giving me the strength to complete this work. I would like to thank Stellenbosch University for granting me a full scholarship to pursue my Master's degree. I wish to thank the Centre for Nuclear Safety and Security (CNSS), for funding this work.

I wish to thank various people for their contribution to this thesis. First of all, I would like to express my very great appreciation to my principal supervisor, Professor Richard Thomas Newman for his enduring support and guidance. I would like to extend my thank you to my co-supervisor Professor Robbie Lindsay at the University of Western Cape. I also express my heartiest gratitude and cordial thanks to the iThemba LABS for allowing us to use their venue for the school outreach campaign and all the personnel who I worked with during the school outreach campaign. I would be honored to mention thier names; Mrs Luchricia Sidukwana, Mr Hilton Tobias and Mr Ambrose Yaga.

Owing recognition to the individuals for the diverse contributions in the completion of this work: Dr Atsile Ocwelwang, Dr Rikus Le Roux, Prof. Jacques Bezuidenhout, Miss Lebogang Phefo, Miss Tarryn Bailey, Miss Paballo Moshupya, Mr Mashamba Madzhiga and last but not least Mr Ryno Botha. A very special thanks to the friend of mine, Nompumelelo Ngejane who has been encouraging along the way. Finally, I wish to thank my parents, siblings, and church members, for all the prayers, generous support and encouragement.

## List of Figures

2.1	The distribution of nuclides as a function of neutron numbers $N$ and proton numbers $Z$ [All08]. . . . .	6
2.2	Decay chain showing how uranium-238 radionuclide decays to a stable lead-206 nuclide. . . . .	8
2.3	The Bragg curve shows the distance travelled by the alpha particles emitted by radon in the air. Image downloaded from <a href="https://en.wikipedia.org/wiki/Bragg_peak">https://en.wikipedia.org/wiki/Bragg_peak</a> . . . . .	9
2.4	Electromagnetic spectrum showing radiation in the environment. . . . .	11
2.5	RAD7 detector. . . . .	21
2.6	The cross section of the E-PERM system [Kot90]. . . . .	23
2.7	South African $10 \times 10$ km grid map showing areas where indoor radon was measured. The data was obtained from table 2.9. . . . .	37
2.8	The log-normal distribution transformed to normal distribution. . . . .	39
3.1	Voltage reader used for measuring initial $V_i$ and final $V_f$ voltages from the electrets. . . . .	41
3.2	Left, E-PERM (S-chamber) in opened position. Right, E-PERM in closed position. . . . .	43
3.3	(a) CR-39 polycarbonate plastic element, (b) A 43 mm diameter plastic holder [Par20]. . . . .	46
3.4	The ParcRGMs inside the radon-proof bags. . . . .	47
3.5	The Airthings™ radon detector. . . . .	48
3.6	The measurement setup for campaign-A1. . . . .	51
3.7	(a) The setup of SSTs (EICs) in the workplace, (b) in an office under normal conditions, (c) in the confined laboratory without any windows. . . . .	52
3.8	Two sets of LLT-OO (EICs) and ParcRGMs were placed side-by-side. . . . .	53
3.9	(a) Four sets of LST-OO, SLT (EICs) and ParcRGMs were deployed in parallel and placed away from the wall ( $>0.5$ m). (b) Three sets of LST-OO and ParcRGM were deployed in parallel and placed next to the wall ( $<0.5$ m). . . . .	54
3.10	Four sets of LST-OO (EICs) and ParcRGMs were deployed and placed next to one another. . . . .	55
3.11	(a) Three LST-OO (EICs), two LLT-OO (EICs), two SST (EICs), and three SLT (EICs) were deployed in parallel with nine ParcRGMs. (b) Three sets of LST-OO (EICs) and ParcRGM were placed close to the wall ( $<0.5$ m). . . . .	56



3.12	Two LST (EICs) and four ParcRGMs were deployed in parallel and placed next to one another. . . . .	57
3.13	The Airthings™ radon detectors placed next to three short term electrets. . . . .	58
3.14	Three Airthings™ radon detectors placed next to one another. . . . .	58
3.15	Gauteng map showing soil type. . . . .	60
3.16	Radon locations in the City of Johannesburg. . . . .	63
3.17	Radon locations in the City of Tshwane. . . . .	64
3.18	Radon locations in the City of Ekurhuleni . . . . .	65
3.19	The Graetz X5C plus™ dosimeter. . . . .	66
3.20	Western Cape map showing the geology. . . . .	67
3.21	Western Cape map showing the radon locations in homes and schools. . . . .	68
4.1	Indoor radon concentration as a function of walls and height. . . . .	72
4.2	Radon levels in offices and laboratories located at Stellenbosch University. . . . .	74
4.3	Results of two sets of LLT-OO and ParcRGM. . . . .	76
4.4	Results of SST, LST-OO and ParcRGM. . . . .	77
4.5	Results of LST-OO and ParcRGM deployed in parallel and placed next to the wall (<0.5 m). . . . .	78
4.6	Results of LST-OO and ParcRGM in room 2024. . . . .	79
4.7	Results showing of two LST-OO , three LLT-OO, three SST, and two SLT that were deployed along with nine ParcRGM. . . . .	80
4.8	Results showing SLT and ParcRGM. . . . .	81
4.9	Results showing SST and Airthings radon detectors for a week measurement. . . . .	82
4.10	Screenshots taken from a smartphone showing weekly radon average levels for each detector. . . . .	83
4.11	The indoor radon data plotted in EXCEL showing hourly measurements for each detector. . . . .	84
4.12	Frequency distribution of radon in homes around Gauteng. . . . .	86
4.13	Radon concentrations in living rooms and bedrooms. . . . .	87
4.14	Linear regression of the relationship between indoor radon concentration in living rooms and bedrooms for 22 homes. . . . .	88
4.15	Box plots showing indoor radon concentration as a function of the building materials. . . . .	89
4.16	Average indoor radon concentration as a function of the surrounding soil type in the selected study areas. . . . .	90

4.17	Average indoor radon concentration as a function of the surrounding geology in the selected study areas. . . . .	91
4.18	Indoor radon concentration as a function of the surrounding geology in Paarl area [Lin08]. . . . .	92
4.19	Indoor radon concentration in homes located next to mine area. . . . .	93
4.20	Indoor radon concentration when using E-PERM system from campaign 1A. . . . .	94
4.21	Indoor radon concentration when using E-PERM system from campaign B. . . . .	94
4.22	Frequency distribution for indoor radon in homes and schools in Western Cape. . . . .	96
4.23	Box plots showing indoor radon concentration as a function of the room type. . . . .	97
4.24	Box plots showing indoor radon concentration as a function of the building materials. . . . .	98
4.25	Indoor radon concentration as a function of the surrounding geology in Cape Flats area. . . . .	99
4.26	Indoor radon concentration as a function of the surrounding geology in Vredenburg, Western Cape [Rou19]. . . . .	100
F.1	Cost comparison between the electret detector and track etch detector for long-term measurements (3-months). . . . .	129

## List of Tables

2.1	$^{222}\text{Rn}$ daughters and their radiation energies [Rob13]. . . . .	15
2.2	Different building materials with estimates of radium concentration [Ham71]. . .	18
2.3	The advantages and disadvantages of different radon measuring detectors [Rad15].	24
2.4	The advantages and disadvantages of different radon measuring detectors (con- tinues) [Kri17]. . . . .	25
2.5	Action levels in different countries [WHO09] . . . . .	27
2.6	Methods for measuring indoor radon concentration [Fri05, Iva13, Jón15, IAE19]. .	30
2.7	Methods for measuring indoor radon concentration (continues) [Dow17, Car19, Vuk18, IAE19]. . . . .	31
2.8	Methods for measuring indoor radon concentration (continues), [Lem01, IAE19].	32
2.9	The summary of the finding from case studies around South Africa [Lin08, Rou19, Leu02] . . . . .	36
3.1	E-PERM™ configurations with their respective constants and measuring peri- ods. [Rad15]. . . . .	42
3.2	Campaign-A1 experimental setup. . . . .	51
3.3	Number of houses in Gauteng that were sampled for indoor $^{222}\text{Rn}$ measurements.	61
3.4	The indoor gamma-ray background radiation ( $\text{nGyh}^{-1}$ ) for each house in 3 inves- tigated regions. . . . .	66
4.1	Summary statistics for data in Figure 4.1. . . . .	73
4.2	The radon levels in different locations. . . . .	75
4.3	The relative percentage difference between the detectors in room 1059. . . . .	78
4.4	The relative percentage difference between the detectors in room 2024. . . . .	80
4.5	Descriptive statistics for each Airthings Wave radon detector. . . . .	84
4.6	Day and night results of indoor radon levels. . . . .	85
4.7	Annual mean effective dose (E) and mean lifetime risk for indoor radon exposure in the different campaigns. . . . .	102
B.1	Building characteristics for each home in Gauteng . . . . .	110
B.2	Additional information about homes in Gauteng. . . . .	111
B.3	Additional information about homes in Gauteng (continued). . . . .	112
C.1	The photographs taken from each home in Gauteng showing the building materials of the house (outside), living room and bedroom. . . . .	114

D.1	The information about the building materials of schools and homes in Western Cape. . . . .	123
D.2	The information about the building materials of schools and homes in Western Cape (continued). . . . .	124
D.3	Additional information of schools and homes in Western Cape. . . . .	125
D.4	Additional information of schools and homes in Western Cape (continued). . . . .	126
E.1	Lithology description in Western Cape (Paarl) . . . . .	127
E.2	Lithology description in Western Cape (Cape Flats) . . . . .	127

# Contents

<b>1</b>	<b>Introduction</b>	<b>1</b>
1.1	Background	1
1.2	Objectives	2
1.3	Thesis structure	2
1.4	Project mind map	4
<b>2</b>	<b>Literature review</b>	<b>5</b>
2.1	Radioactivity	5
2.1.1	General properties of nuclei	5
2.2	Radioactive decay of a radionuclide	6
2.2.1	Alpha decay	8
2.2.2	Beta decay	10
2.2.3	Gamma rays	10
2.3	Radiation around us	10
2.3.1	Non-ionising radiation	11
2.3.2	Ionising radiation	11
2.4	Radiation exposure and associated dose	12
2.4.1	Absorbed dose	12
2.4.2	Equivalent dose	12
2.4.3	Effective dose	13
2.4.4	Annual mean effective dose rate due to radon	13
2.4.5	The excess lifetime risk	14
2.5	Physical and chemical properties of radon	14
2.6	Radon migration	16
2.6.1	Radon emanation	16
2.6.2	Radon transport and exhalation	16
2.6.3	Radon entry into buildings	17
2.6.4	Radon from the building materials	17
2.7	Health effects of radon	19
2.8	Overview of radon measurement systems	20
2.8.1	Active radon systems	20

2.8.2	Passive radon detectors . . . . .	22
2.9	Overview of a national indoor radon survey worldwide . . . . .	26
2.10	South African existing indoor radon data . . . . .	33
2.11	Log-normal distribution and indoor radon . . . . .	38
<b>3</b>	<b>Data collection and methodology</b>	<b>40</b>
3.1	An overview of the instruments used for radon detection. . . . .	40
3.1.1	E-PERM™ System . . . . .	40
3.1.2	ParcRGM™ system . . . . .	46
3.1.3	Airthings™ radon monitor system . . . . .	48
3.1.4	Geographic Information Systems (GIS) . . . . .	49
3.2	Indoor <sup>222</sup> Rn measurements in workplaces . . . . .	49
3.2.1	Campaign-A description . . . . .	49
3.2.2	Selected study area . . . . .	50
3.2.3	Campaign-A1 experimental setup . . . . .	50
3.2.4	Campaign-A2 experimental setup . . . . .	53
3.2.5	Indoor <sup>222</sup> Rn measurements using Airthings™ radon monitors. . . . .	57
3.3	Indoor <sup>222</sup> Rn measurements in homes located in Gauteng . . . . .	59
3.3.1	Campaign-B description . . . . .	59
3.3.2	Selected study area . . . . .	59
3.3.3	Approach strategies to homeowners . . . . .	61
3.3.4	Deployment procedure . . . . .	61
3.3.5	Collection procedure . . . . .	62
3.3.6	Gamma-ray background radiation measurements . . . . .	65
3.4	Indoor <sup>222</sup> Rn measurements in homes and schools around Western Cape . . . . .	67
3.4.1	Campaign-C description . . . . .	67
3.4.2	Selected study area . . . . .	67
3.4.3	Distribution and collection of radon detectors . . . . .	70
<b>4</b>	<b>Results and Discussion</b>	<b>72</b>
4.1	Campaign A: Results of indoor radon concentration in homes, schools and work- places . . . . .	72
4.1.1	Campaign A1: results of indoor radon concentration in workplaces. . . . .	72

4.1.2	Campaign A2: a comparison results between E-PERM and ParcRGM systems . . . . .	75
4.1.3	Comparison between Airthings Wave and E-PERM . . . . .	82
4.1.4	Seasonal variation of indoor radon using EIC (SST) . . . . .	82
4.1.5	Day and night variation of indoor radon using Airthings Wave . . . . .	83
4.2	Campaign B: Results of $^{222}\text{Rn}$ from homes in Gauteng. . . . .	86
4.3	Campaign C: Results of $^{222}\text{Rn}$ from homes and schools in Western Cape. . . . .	95
4.4	Annual effective dose estimation of indoor $^{222}\text{Rn}$ . . . . .	102
<b>5</b>	<b>Conclusion</b>	<b>103</b>
5.1	Summary of main findings . . . . .	103
5.2	Recommendations . . . . .	104
<b>6</b>	<b>Appendices</b>	<b>106</b>
<b>A</b>	<b>Questionnaire</b>	<b>106</b>
<b>B</b>	<b>Gauteng homes: building materials information</b>	<b>110</b>
<b>C</b>	<b>Gauteng homes: photographs showing the building materials</b>	<b>114</b>
<b>D</b>	<b>Western Cape schools and homes: building materials information</b>	<b>122</b>
<b>E</b>	<b>Western Cape lithology information</b>	<b>127</b>
<b>F</b>	<b>Cost-Effectiveness of radon detectors</b>	<b>128</b>

# Chapter 1

## 1 Introduction

### 1.1 Background

This MSc thesis focuses on the design of South Africa's national indoor radon survey and the development of an indoor radon measuring system. All of the measurements in this MSc Thesis were analysed at the Health Physics Laboratory (HPL) which is located at the Department of Physics at Stellenbosch University (South Africa). This thesis deals with measurements of indoor radon in homes, schools, and workplaces (offices, and laboratories). Radon is common indoors and outdoors. It arises in soil and geology with a radium and uranium content. Radon is transported through diffusion and advection processes to the atmosphere and into the indoor environment. Radon builds up indoors depending on the building materials and ventilation. This study investigated the correlation between building materials and indoor radon levels.

Epidemiological studies have shown that elevated radon indoors can cause lung cancer and are ranked second as a cause of lung cancer death after smoking. Countries around the world have started regulating indoor radon concentrations and are establishing their reference levels for indoor radon. They accomplished this through national indoor radon surveys. There is no national radon survey program in South Africa. However, the National Nuclear Regulator (NNR) in South Africa has set a reference level of  $300 \text{ Bqm}^{-3}$ . In 2018, a project was initiated by the Center for Nuclear Safety and Security (CNSS) in South Africa to design a national radon survey. The University of Stellenbosch was successful in getting funding to carry out the project. The thesis also provides an overview of national indoor radon survey programs in other countries and uses this information to inform a future national indoor radon survey for South Africa. The thesis also includes a desktop-based survey of existing South African indoor radon levels.

The measurement of indoor radon gas and its daughters in the air is necessary, especially on radiological protection to prevent human beings from health risks associated with radon gas. Various methodologies and technologies can be used to measure radon gas indoors, and their advantages and disadvantages are also described. The common methods known for indoor radon measurement are called active and passive methods. Electret Passive Environmental Radon



Monitor (E-PERM) and Alpha Track detectors were mainly used to conduct the measurements of indoor radon gas for this study.

## 1.2 Objectives

This research discusses the factors to consider when designing the national indoor radon survey. It aims to assist the national authorities and inform them of the strategies to be considered for future indoor radon surveys. Here are the objectives which will be covered throughout the research:

- to conduct studies of the types of radon survey programmes that have been carried out in other countries;
- to conduct indoor radon measurements in homes, schools and workplaces;
- to identify the hotspots and sources of elevated radon activity; and
- to design a strategy and plan for indoor radon mapping in Republic of South Africa.

## 1.3 Thesis structure

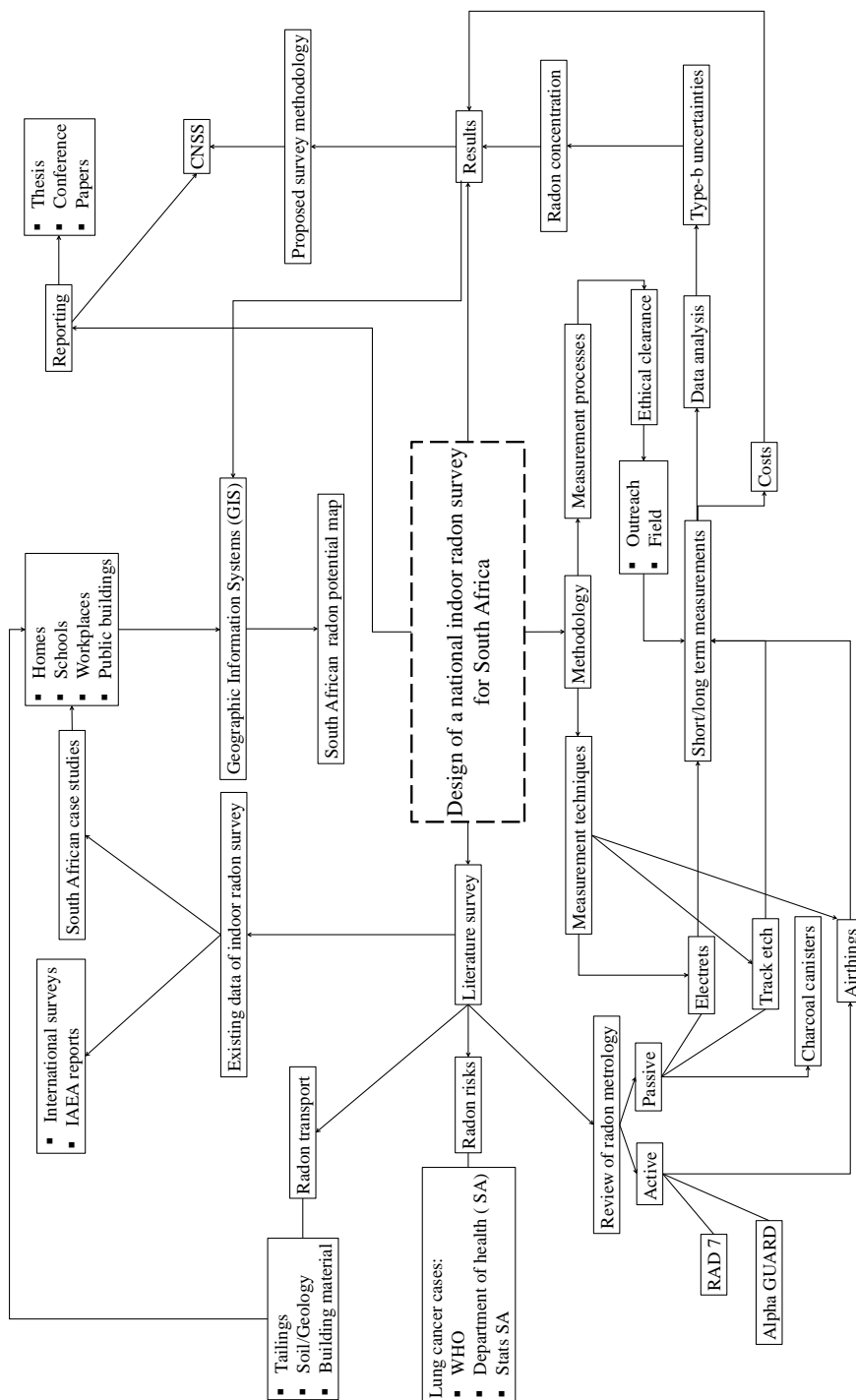
This section give the outline of the thesis and each chapter is carefully summarised. The mind-map diagram of the research is attached at the end of this section.

- **Chapter 2** begins by giving background theory of radioactivity and decay series. It also covers the different types of radiation and decay modes. Radon indoors is further discussed by explaining its physical and chemical properties. The emanation and inhalation of radon gas and its daughters are further examined. This chapter will also cover the sources of radon in air and the health risks associated with indoor radon. This chapter will also present an overview of instruments used for measuring indoor radon and discuss their advantages and disadvantages for each radon detector. The last two sections of this chapter will cover an overview of radon national surveys conducted in other countries and the case studies conducted in South Africa.
- **Chapter 3** outlines the research methodology. How the indoor radon measurements were carried out will be discussed explicitly here. This chapter will discuss how, for each campaign, detectors were deployed in buildings. The use of Geographic Information Systems

(GIS) to generate radon maps for South Africa will be discussed. Will also investigate the inter-comparison measurements between different radon instruments.

- **Chapter 4** presents the experimental results of the research. The results of the indoor radon concentration obtained from each campaign will be discussed. From the soil map that was generated using the qGIS software, the correlation between the indoor radon and soil type will be discussed. The correlation between indoor radon gas and building materials will be discussed as the building materials also contribute to indoor radon gas. The results obtained from the inter-comparison measurements will also be discussed since different types of radon detectors have been used to measure radon gas indoors.
- **Chapter 5** The thesis will be concluded with the presentation of suggestions for a national indoor radon survey in South Africa.

### 1.4 Project mind map



## Chapter 2

### 2 Literature review

#### 2.1 Radioactivity

##### 2.1.1 General properties of nuclei

Radioactivity is defined to be the spontaneous emission of a stream of particles or electromagnetic rays in nuclear decay [Moe80]. This form of radiation can be understood by exploring the atomic nucleus. In theory, an atom is made up of three particles which are protons (positively charged), neutrons (no charge), and electrons (negatively charged). The electrons are located on outside of the atom inside electron shells, and both protons and neutrons are located at the centre of an atom called a nucleus. A typical diameter of an electron cloud and nucleus is  $10^{-10}$  m and  $10^{-14}$  m, respectively [Kra88].

An atoms is electrically neutral if the number of protons denoted by ( $Z$ ) is equal to the number of electrons. The number of protons identifies the element. And the mass of an atom is practically provided by its nucleus, protons and neutrons denoted by ( $N$ ). The atomic mass number is denoted by ( $A$ ) and can be determined as  $A=Z+N$ . A specific number of protons and neutrons together inside a nucleus forms a unique nuclide denoted by  ${}^A_ZX_N$ , where  $X$  is the chemical symbol of the element. In this thesis, all nuclides will be symbolised as  ${}^AX$ , for example, uranium element with an atomic mass number of 238 will be expressed as  ${}^{238}\text{U}$ .

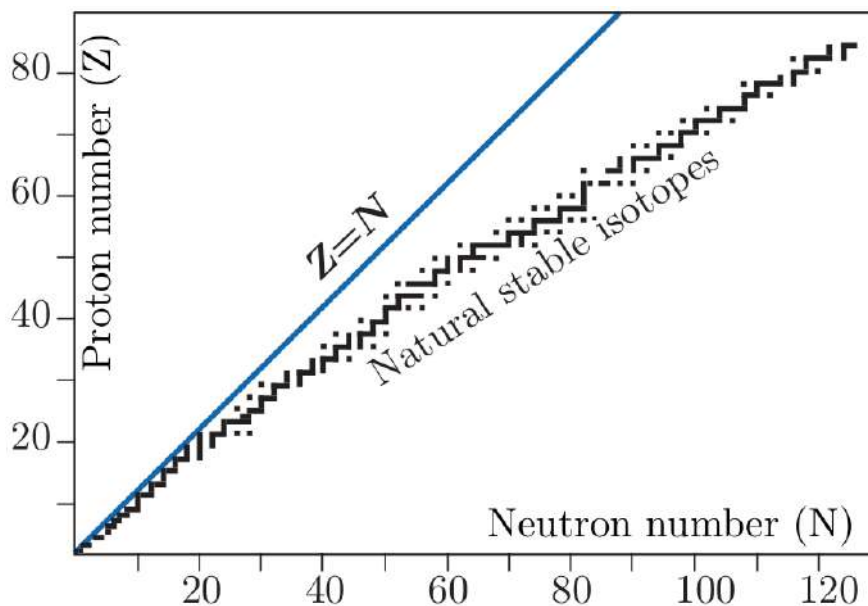


Figure 2.1: The distribution of nuclides as a function of neutron numbers  $N$  and proton numbers  $Z$  [All08].

Nuclides with the same atomic number  $Z$  are called isotopes. Many isotopes of different elements are unstable and tend to disintegrate until they reach stability, this process is called radioactivity. For  $Z > 82$ , all the known nuclides are unstable. In Figure 2.1 the black line region represents the belt of stability, all nuclides in this region are stable. All other nuclides are unstable and decay spontaneously in various ways. An unstable nuclide which undergoes radioactive decay is called a radionuclide.

## 2.2 Radioactive decay of a radionuclide

The discovery of radioactivity dates back to 1896 when the physicist named Henri Becquerel noticed the rays emitted from a uranium grain penetrated a paper and created an image on a photographic plate [Kra88]. The radioactive decay process occurs when the radionuclide disintegrates due to instability, as a result, radiation or energy is emitted. Three types of radiation can be emitted in the radioactive processes namely, alpha particles, beta particle, and gamma rays.

It is important to consider the rate of radioactive decay when dealing with a radionuclide. The

rate of radioactive decay is determined using the half-life  $T_{1/2}$  of a radionuclide. The half-life is the time required for the disintegration of half of the atoms in a radioactive substance. The activity of a quantity of radioactive material is the number of nuclear decays per second and is expressed in Becquerel (Bq).

In a case where an unstable radionuclide decays to a stable nuclide, the number of radioactive atoms denoted by  $N_t$  after time  $t$  can be determined by:

$$N_t = N_0 e^{-\lambda t} \quad (2.1)$$

where  $N_0$  is the initial number of atoms and  $\lambda$  is a parameter known as the decay constant given by equation:

$$\lambda = \ln(2)/T_{1/2} \quad (2.2)$$

where  $T_{1/2}$  is the half-life of the radionuclide.

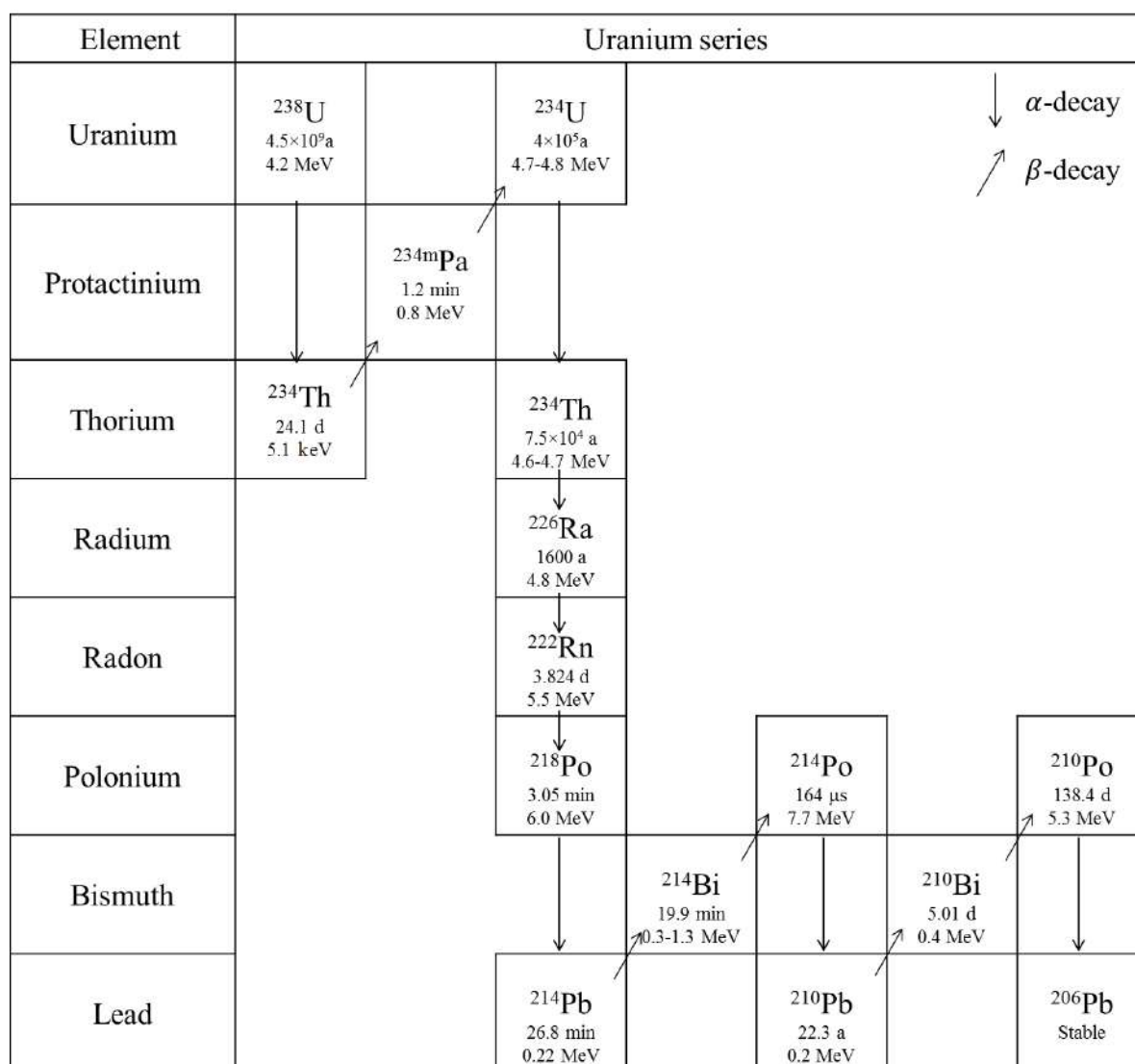


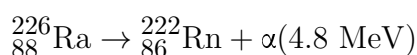
Figure 2.2: Decay chain showing how uranium-238 radionuclide decays to a stable lead-206 nuclide.

### 2.2.1 Alpha decay

Alpha particles are composed of two neutrons and two protons released from the nucleus, which gives these particles the same form as a helium nucleus with a mass number of 4. The emission of an alpha particle changes the parent nucleus by reducing the atomic number by 2, and the atomic mass number by 4. The alpha decay equation may be described in equation 2.3.



where X and Y represents a parent nucleus and daughter nucleus, respectively. A typical example of an alpha decay:



When dealing with the alpha particles it is important to consider the stopping power, which is defined as the energy loss by a particle in material corresponding to the path length travelled by the particle in the material. For 5.00 MeV alpha particles, the stopping power in air is 1.23 MeV cm<sup>-1</sup> [Fil19]. An alpha particle interacts strongly with matter and stops within 100 μm in most materials. In the air, alpha particles may travel only a few centimetres, a 5.49 MeV alpha particle travels approximately 4 cm in air as illustrated in Figure 2.3.

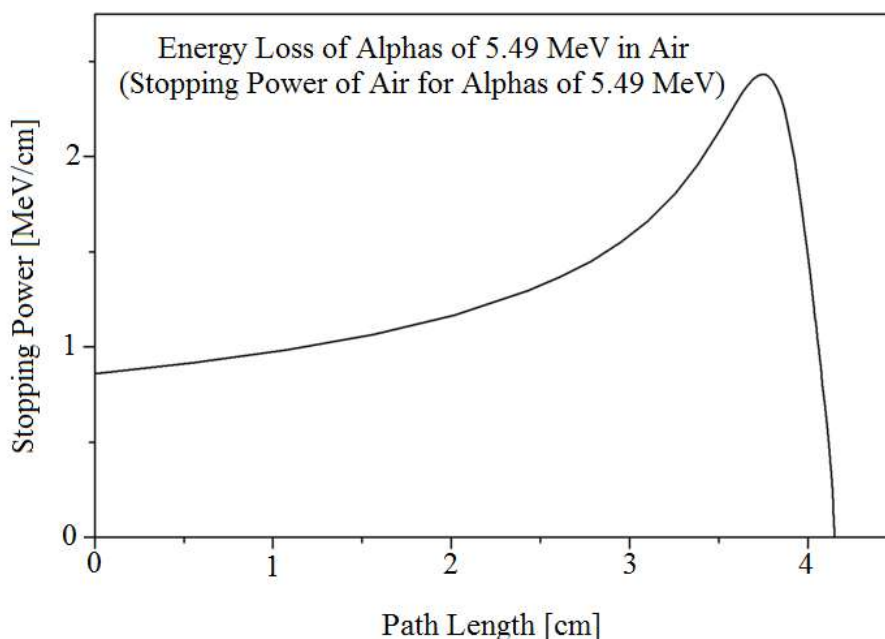


Figure 2.3: The Bragg curve shows the distance travelled by the alpha particles emitted by radon in the air. Image downloaded from [https://en.wikipedia.org/wiki/Bragg\\_peak](https://en.wikipedia.org/wiki/Bragg_peak).



### 2.2.2 Beta decay

When a high-speed electron or positron is emitted in the decay of a radioactive isotope this process is called beta decay. The beta decay occurs in two modes known as beta-plus  $\beta^+$  and beta-minus  $\beta^-$ . Beta particles in the air travel larger distances and move deeper into the matter than for alpha particles with the same initial kinetic energy.

### 2.2.3 Gamma rays

Gamma rays are form of high energy electromagnetic radiation with energies ranging from a few keV to approximately 8 MeV and can go much higher [Bus11]. The interaction of gamma rays with matter can be explained through the processes of the photoelectric effect, Compton scattering and pair production. Gamma radiation released from natural sources also known as background radiation is largely due to primordial radionuclides, mainly from the  $^{232}\text{Th}$  and  $^{238}\text{U}$  series, and their decay products, as well as  $^{40}\text{K}$ . Another source of gamma rays is due to secondary radiation from atmospheric interaction with cosmic ray particles.

## 2.3 Radiation around us

Our everyday life is exposed to some amount of radiation. The sources of radiation can be subdivided into terrestrial (from materials in the earth), artificial (from man-made activities) and cosmic (from cosmic ray interaction with air). Radon gas in air is the main contributor to the dose to people, and it contributes to the greatest amount of natural radiation [WHO09]. Radiation is listed as ionising or non-ionising.

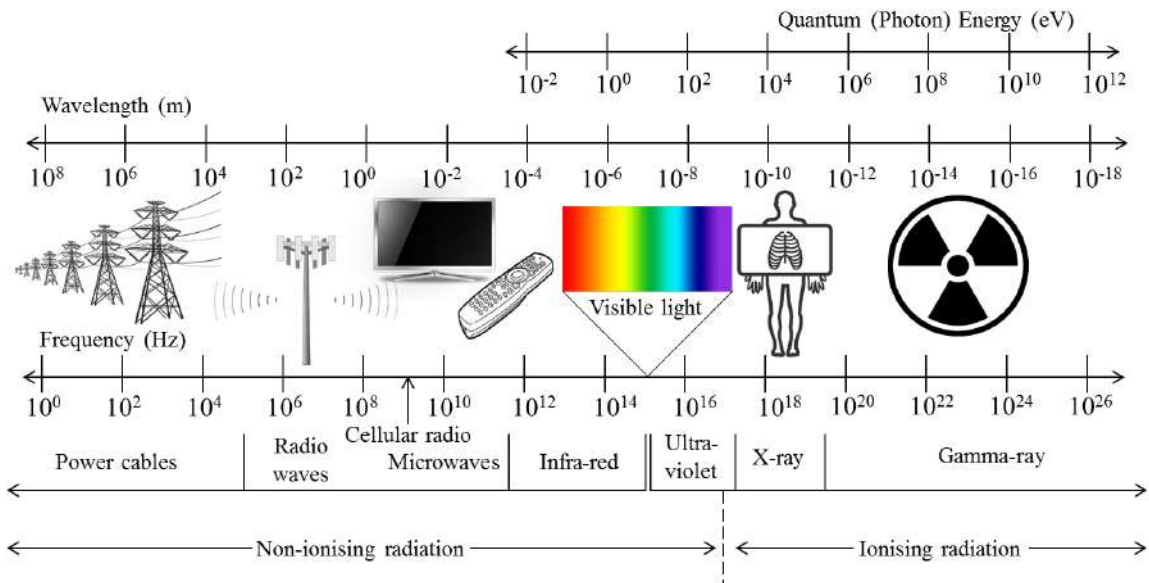


Figure 2.4: Electromagnetic spectrum showing radiation in the environment.

### 2.3.1 Non-ionising radiation

Non-ionising radiation is a form of radiation with less quantum photon energy to remove electrons from atoms and molecules. Non-ionising radiation has lower frequency and longer wavelength as illustrated in Figure 2.4. These types of radiation are divided into three regions namely, optical, thermal, and non-thermal. The optical region is extended into visible light, infrared, and ultraviolet. The thermal region is extended into microwaves and radio waves. The non-thermal region covers extremely low frequencies [Wil16].

### 2.3.2 Ionising radiation

Ionising radiation is defined to be high-energy radiation that carries sufficient quantum photon energy to ionise atoms and molecules, the process is referred to as ionisation. During the ionisation process, an electron is knocked off from an atom. When the particles and photons are emitted by a radioactive source they form ionising radiation. Examples of ionising radiation include  $\alpha$ -particles,  $\beta$ -particles, X-rays, and  $\gamma$ -rays radiation. Ionising radiation is characterised

by a short wavelength and high frequency. This radiation can move through matter and alter it as it passes through. As the ionising radiation passes through an atom, an atom gets ionised. Ionising radiation is regarded as more dangerous than non-ionising radiation. Ionising radiation is much more dangerous because it can ionise the atoms of the DNA molecules and cause disruption in major cellular functions. Once broken, the proteins that are coded by that fragment of DNA cannot be repaired, leading to many serious health hazards like cancer.

## 2.4 Radiation exposure and associated dose

Determining the effect of radon exposure to personnel is important. The radiometric quantities and effects that the radiation dose produces must be measured. This section deals with dosimetric quantities known as dose and also discusses how to calculate the annual effective dose using radon concentration. Here are some categories of dosimetric quantities to be discussed in this section; the absorbed dose, the equivalent dose and the effective dose.

### 2.4.1 Absorbed dose

Absorbed dose is a measure of the energy absorbed by a medium from any type of radiation per unit mass. It is denoted by symbol  $D$ . The SI unit of absorbed dose is gray (Gy) defined to be joule per kilogram ( $\text{Jkg}^{-1}$ ), and one gray is equal to one joule per kilogram [Kno00].

$$1 \text{ Gy} = 1 \text{ Jkg}^{-1} \quad (2.4)$$

The absorbed dose can be used to measure the physical or chemical effects created by radiation exposure in an absorbing material. The original unit of absorbed dose is radiation absorbed dose (rad) defined to be  $100 \text{ ergs gram}^{-1}$ , and one gray is equal to 100 rad.

$$1 \text{ Gy} = 100 \text{ rad} \quad (2.5)$$

### 2.4.2 Equivalent dose

In order to determine how much damage may be done to the tissue or the level of the potential hazard we use equivalent dose denoted by  $H$ . The SI unit of equivalent dose is Sievert (Sv) also defined to be joule per kilogram ( $\text{Jkg}^{-1}$ ). The equivalent dose can be used as a measure of biological effect of a particular type of radiation on organs or tissues. The equivalent dose is the

product of the absorbed dose  $D$  and the quality factor denoted by  $QF$ . The  $QF$  depends on the radiation type involved.

$$H = D \times QF \quad (2.6)$$

The quality factor depends on the type of radiation, for example,  $\alpha$ -particles and  $\beta$ -particles of typical energies have the  $QF$  of 20 and 1, respectively [ICRP 60]. The original unit of equivalent dose is rem (roentgen equivalent man), and one sievert is equal to 100 rem.

$$1 \text{ Sv} = 100 \text{ rem}$$

### 2.4.3 Effective dose

Effective dose (Sievert) is calculated for the whole body. It is the product of equivalent dose ( $H$ ) and tissue weighting factors ( $w_T$ ) which is different for specified tissues and organs of the human body (lungs, gonads, bone marrow and skin). The tissue weighting factors are needed because different organs have different levels of sensitivity to radiation.

$$E_D = \sum H \times w_T \quad (2.7)$$

Effective dose is used to assess the potential for long-term effects that might occur in the future and is expressed in millisieverts (mSv).

### 2.4.4 Annual mean effective dose rate due to radon

Annual mean effective dose rate  $E$  ( $\text{nSv}^{-1}$ ) can be determined using equation 2.8 which is based on the UNSCEAR model [UNS00]:

$$E = RnC \times F \times H \times T \times D \quad (2.8)$$

where:

- $RnC$  is the mean indoor radon concentration in air given in Becquerel per cubic meter ( $Bqm^{-3}$ );
- $F = 0.4$  is the equilibrium factor defined as the ratio of the radon daughters to the radon concentration in air [Nad19];
- $H = 0.8$  is the home occupancy factor. Khalil et al. [Kha19] determined the occupancy factors for universities and schools to be 0.22 and 0.16, respectively;
- $T = 8760 \text{ hy}^{-1}$  is the number of hours in a year; and
- $D = 9 \text{ nSv per } Bqm^{-3}h^{-1}$  is the dose conversion factor as per ICRP.

#### 2.4.5 The excess lifetime risk

The excess lifetime risk can be calculated as an estimate of the probability of developing lung cancer due to radon exposure over the mean lifetime using equation 2.9:

$$\text{Risk} = E(\text{nSvy}^{-1}) \times DL(y) \times RF(\text{Sv}^{-1}) \quad (2.9)$$

where:

- $DL = 64$  years is an average life expectancy in South Africa; and
- $RF = 0.05 \text{ Sv}^{-1}$  as the fatal risk factor as per The International Commission on Radiological Protection [ICR08].

## 2.5 Physical and chemical properties of radon

Radon is a naturally occurring radioactive gas found in nature. It is colourless, odourless and tasteless and is chemically inert. Radon belongs in the group of noble gases in the periodic table of elements and is the 86<sup>th</sup> element with an atomic mass number of 222. At room temperature, radon is very dense and is classified as the heaviest of the noble gases. Radon is directly produced from the decaying radionuclide called radium-226, which is generally found in soil and rocks.

Radon exists naturally in three radionuclides of its 39 isotopes generally called actinium, thoron,

and radon with the atomic symbol  $^{219}\text{Rn}$ ,  $^{220}\text{Rn}$ , and  $^{222}\text{Rn}$ , respectively. However, this research focuses only on radon referred to as  $^{222}\text{Rn}$ . At 0 °C and 1 atm, the density of radon is  $9.73 \text{ gL}^{-1}$ , which is 7.5 times denser than air. Since radon is not stable, with the half-life of 3.824 days it undergoes a radioactive decay process and produce other radionuclide known as radon daughters or radon progeny. The radon daughters include polonium, lead and bismuth as indicated in Table 2.1.

The unit for measuring radon activity concentration in air is called Becquerel per cubic meter ( $\text{Bqm}^{-3}$ ) named after physicist Henri Becquerel, where 1 Becquerel represents one nuclear disintegration per second. Another common unit used for measuring radon is pico-curies of radioactivity per litre ( $\text{pCiL}^{-1}$ ) and is related to Becquerel by equation 2.10:

$$1 \text{ pCiL}^{-1} = 37 \text{ Bqm}^{-3} \quad (2.10)$$

Table 2.1:  $^{222}\text{Rn}$  daughters and their radiation energies [Rob13].

Radionuclide	Half-life		Radiation energies (MeV)		
			$\alpha$	$\beta$	$\gamma$
$^{222}\text{Rn}$	3.824 day	Gas	5.49	-	-
$^{218}\text{Po}$	3.11 min	Solid	6.00	-	-
$^{214}\text{Pb}$	26.8 min	Solid	-	1.02	0.35
			-	0.70	0.30
			-	0.65	0.24
$^{214}\text{Bi}$	19.7 min	Solid	-	3.27	0.61
			-	1.54	1.77
			-	1.51	1.17
$^{214}\text{Po}$	$1.64 \times 10^{-4} \text{ s}$	Solid	7.69	-	-

## 2.6 Radon migration

Since radon is a gas, it is highly mobile and can move from the soil and building materials if it enters the pore space after being formed by the decay of  $^{226}\text{Ra}$  in the soil particles or building material. The release of radon from soils, rocks and the building materials, is described through emanation, transport, and exhalation processes. This section discusses how radon is transported from outdoors into buildings.

### 2.6.1 Radon emanation

All radon gas is produced from soil or rocks with minerals such as uranium or radium. The fractional grains of soil containing radium atom produces a newly formed radon atom, then about 10% to 50% of radon atoms escape from the grains to pore spaces between the mineral grains [Ott92]. Some fraction of radon dissolve in water between grain other are absorbed in the mineral grain. The emanation of radon depends on various factors. This includes radium content in a mineral grain, grain size, pore space property, soil moisture and temperature [Bos03].

### 2.6.2 Radon transport and exhalation

The radon gas accumulated in the pore space is then transported through advective flow and diffusion to the surface. Diffusion is governed by Fick's law which describes the migration from high concentration pores toward low concentration pores and is given by equation 2.11 [Phe20].

$$f = -D_M \nabla C \quad (2.11)$$

where

- $f$  is the radon activity flux density in  $\text{Bqm}^{-2}\text{s}^{-1}$ ;
- $D_M$  is the molecular diffusion coefficient in  $\text{m}^2\text{s}^{-1}$ ; and
- $\nabla C$  is the gradient of radon activity concentration in  $\text{Bqm}^{-4}$ .

On the other hand, the advective flow is governed by Darcy's law and it describes how the flow is induced by pressure difference, the flow will occur from higher pressure towards lower pressure

and is given by equation 2.12 [Spe04].

$$\vec{v} = -\frac{k}{\mu_a} \vec{\nabla} P_a \quad (2.12)$$

where

- $\vec{v}$  is fluid flow per unit cross section ( $\text{m}^3\text{m}^{-2}\text{s}^{-1}$ );
- $k$  is the intrinsic permeability of the soil ( $\text{m}^2$ );
- $\mu_a$  is dynamic viscosity of air in Pascal seconds (Pas); and
- $P_a$  is the air pressure in Pascal (Pa).

The radon gas that has been transported to the ground surface (soil, rocks, or building materials) is exhaled to the atmosphere. The rate at which the radon gas is exhaled depends on the geological characteristics of the study area, soil porosity and texture, soil temperature and type of the building materials.

### 2.6.3 Radon entry into buildings

The amount of radon gas found indoors mostly comes from outdoor (rocks and soil). Since radon is gaseous at room temperature, it will flow through cracks and, or openings in walls and floors of dwellings [Zub16]. The building materials also contribute to indoor radon gas, for example, tiles, ceramics, carpets, porcelains, and marbles. In general, the outdoor radon levels in the air are very low (2 - 20  $\text{Bqm}^{-3}$ ) compared to the indoor radon levels. The radon gas then can build up indoors over time. Indoor radon concentrations have been found to range between 20  $\text{Bqm}^{-3}$  to 110 000  $\text{Bqm}^{-3}$  with a world average of 40  $\text{Bqm}^{-3}$  [WHO09].

### 2.6.4 Radon from the building materials

The primary source of indoor radon is soil gas, but it is also considered that the building materials contribute to indoor radon gas. In most cases, radon exhaling from building materials does not contribute significantly to indoor radon levels as compared with soil gas [Kel01]. The building materials that are widely used in dwellings include cement bricks, red-clay bricks, gravel aggregates, and igneous rocks [Tre18]. Radon can be released into the indoor environment by



building materials containing  $^{226}\text{Ra}$ . It is important to measure the radon released from the building materials used for the construction of the dwellings. In some countries, the national legislation sets limits on naturally occurring sources of radiation that are allowed in building materials. Table 2.2 shows the estimates of radium concentration data that was obtained in the United Kingdom buildings. Generally, high concentrations of  $^{226}\text{Ra}$  found in the building materials result in elevated indoor radon concentrations.

Table 2.2: Different building materials with estimates of radium concentration [Ham71].

Materials	Radium concentration ( $\text{Bqkg}^{-1}$ )
Aerated concrete	89.0
Clay Bricks	52.0
Concrete block with fly ash	65.0
Flint aggregate	2.2
Granite aggregate bricks	11.0
Granite bricks	89.0
Gravel aggregate	7.4
Natural gypsum	23.0
Phosphogypsum	120.0
Vermiculite	93.0

## 2.7 Health effects of radon

Naturally occurring gaseous radionuclides like  $^{222}\text{Rn}$  can be easily inhaled directly by humans. The health problem of indoor radon in human beings is linked to the inhalation of radon daughters. Since  $^{222}\text{Rn}$  gas is radioactive, it decays further to produce its daughters which are also radioactive. The daughters can also attach to dust particles in the air vapour and trace gases of indoor gas. When  $^{222}\text{Rn}$  gas is inhaled, most of the  $^{222}\text{Rn}$  can immediately be exhaled, whereas its decaying daughters are retained in the human lungs. These radioactive daughters continue to decay in the lungs and release energy bursts in a form of alpha particles. These  $\alpha$ -particles subsequently interacts with biological tissues in the lungs. During interactions of alpha particles and lung tissues, the deoxyribonucleic acid (DNA) can be altered and damaged. As a result, lung cancer can develop through gene mutation and a rapid increase in damaged cells which replicate to form a tumour.

Several studies have identified radon as the second main contributor to causing lung cancer after cigarette smoking [UNS08]. Tobacco smokers who are living in the dwellings with higher radon levels are at more risk of lung cancer than non-smokers who are living in the dwelling with higher radon levels. The World Health Organization (WHO) estimates that between 3 and 14% of lung cancers are attributable to radon and its progeny [WHO09]. In 2006, a study conducted in the UK indicated that about 3.3% of lung cancer deaths were due to radon in homes. About 1 in 7 of the deaths from radon-related lung cancer was due to radon and not by active smoking. The remainder was due to radon and active cigarette smoking as cancer could have been prevented by avoiding exposure to either factor [Gra09].

Radon in homes and workplaces is associated with an increase in the risk of lung cancer in the general population [WHO17]. Some workers and members of the public can also be also exposed to higher radon concentration in their workplaces. This includes workers in mines, water treatment plants, tourist caves, schools, pre-schools, hospitals, etc. Radon exposure for both workers and members of the public in such buildings is managed through the use of regulations and reference levels. Data from the Chinese [Lub04], European [Dar05] and North American [Kre05] indoor radon studies consistently indicate that the lung cancer risk increases approximately linearly with increased long-term exposure to radon.

## 2.8 Overview of radon measurement systems

Since radon is a noble gas, it cannot be detected by human senses. The only way to detect radon gas is through the detection of nuclear radiation. Systems for measuring indoor radon concentration have been developed over the years. These measurement systems are divided into two classes namely active and passive. Active radon detectors require electric power to operate and involve the pumping of radon gas into the detector. On the other hand, passive radon detectors can operate without any electric power. This section gives an overview of radon detectors that are commonly used for measuring indoor radon concentrations. The advantages and disadvantages of each detector are also listed.

### 2.8.1 Active radon systems

#### **RAD7**

The RAD7 monitor is a solid-state alpha detector equipped with a 0.7 litre hemispherical sample cell coated with an electrical conductor. The solid-state alpha detector is located at the centre of the hemispherical cell as indicated in Figure 2.5. The electrical conductor inside the hemisphere cell is charged with a high voltage power circuit to a potential of 2 kV to 2.5 kV and an electric field is created inside the volume of the hemispherical chamber. The radon gas is pumped into the chamber through an inlet filter and fills the hemisphere. Then radon decays inside the chamber and emits alpha particles and its daughters build up. The electric field propels the positively charged daughter ( $^{218}\text{Po}$ ) to the detector. When this  $^{218}\text{Po}$  alpha decays, the alpha is measured by the silicon detector that also measures the energy of the alpha (= 6 MeV). Similarly, it can measure the emission energy from the  $^{214}\text{Po}$  decay further down the radon decay chain. Then the detector converts alpha pulses into electrical signals [Saa18]. The RAD7 has the capability for continuous monitoring of radon concentrations from  $4 \text{ Bqm}^{-3}$  to  $750\,000 \text{ Bqm}^{-3}$  [Dur20].

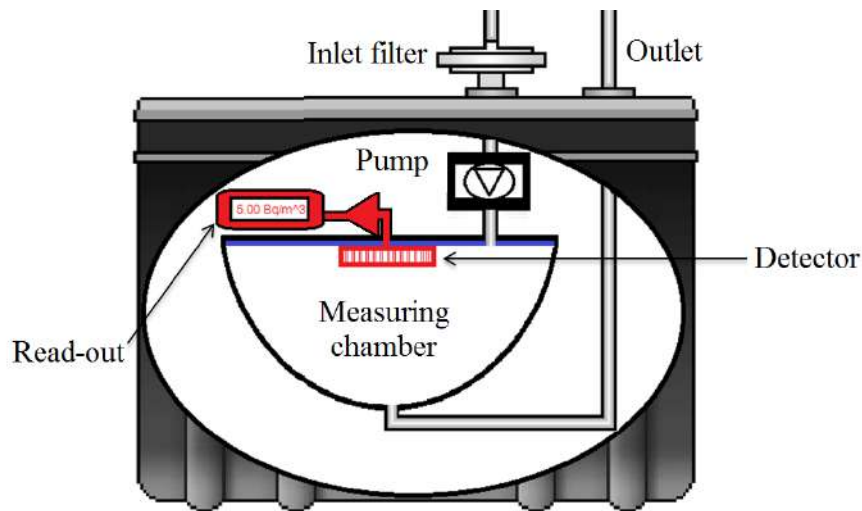


Figure 2.5: RAD7 detector.

### AlphaGUARD

The AlphaGUARD radon detector is a continuous monitoring system equipped with a 0.62-litre pulse-counting ionisation chamber [Deh12]. The ionisation chamber is held with the potential of +750 V (anode) and the electric field is created when voltage is applied across the electrodes of ionisation chamber. Radon gas enters the ionisation chamber and decays to produce its daughters and alpha particles. The air inside the chamber get ionised by alpha particles, the positive ions gets attracted to the cathode and negative ions get attracted to the anode. As a result, an electric current is induced and detected by a sensitive current measuring device placed between the anode and cathode. The AlphaGUARD has the capability for continuous monitoring of radon concentrations from  $0 \text{ Bq m}^{-3}$  to  $50\,000 \text{ Bq m}^{-3}$  [Sap12].

### Airthings™ radon detector

Airthings™ is a battery-powered smart radon gas detector that uses radon sensor which consists of a passive diffusion chamber to detect alpha particles [Bal20]. Inside the chamber there is a photodiode sensor, which is the semiconductor with two-terminal components whose electrical characteristics are light-sensitive. The chamber is coated with a chromium-plate on the outside which prevents unwanted particles to enter the chamber. When air enters through a 0.2 mm filter, only radon gas and its daughters allowed from entering the chamber. Then radon decays inside the detector and alpha particles are detected by the photodiode sensor. The

Airthings™ radon detector is a versatile detector which can also detect the temperature and humidity. The Airthings™ has the capability for continuous monitoring of radon concentrations from  $2 \text{ Bqm}^{-3}$  to  $2 \text{ MBqm}^{-3}$  [Air18].

## 2.8.2 Passive radon detectors

### Charcoal canister

The active charcoal canister is made up of a tin box filled with activated carbon. Activated charcoal has a high affinity for vapours and gases like radon. When the canister is exposed to air, radon gas enters the detector and undergoes the radioactive decay to produce its daughters. Radon and its daughters get absorbed by carbon in the canister. Then radon daughters emit gamma rays inside the charcoal canister. After the desired exposure period, the canister is analysed in the laboratory using gamma-ray spectrometry for counting the gamma-rays released by radon daughters. Three gamma-rays energies are used for counting the gamma rays emitted by radon daughters, namely 295 keV and 352 keV (energies of  $^{214}\text{Pb}$  photons) and 609 keV (energy of  $^{214}\text{Bi}$  photon) [Pan14].

### Track etch

Passive track-etch monitors detect the alpha particles from the radioactive decay of radon and its daughters. The track etch monitor is made up of a poly-allyl-diglycol-carbonate (PADC) film which is highly sensitive to alpha particles [Mos19]. The sensitive film is covered with container which allows  $^{222}\text{Rn}$  to diffuse into it. The alpha radiation from radon and its progeny cause radiation damage in the film by leaving tracks. After the desired exposure period, the track etch film is analysed in the laboratory using optical microscopy for counting the tracks caused by radon and its daughters. During the analysis, a film is etched in a hot caustic solution to make these tracks visible [Bát15]. The tracks can be counted with an optical microscope and the radon concentration can be determined. The track etch radon monitors can be exposed for 2 to 3 months. The track-etch has the capability for monitoring of radon concentrations from  $5 \text{ Bqm}^{-3}$  to  $15 \text{ MBqm}^{-3}$  [Tas15].

### Electret ionisation chambers

The electret ionisation chamber (EIC) employs an electret, a plastic disk made of Teflon<sup>®</sup> material [Bau97]. The electret carries a electrostatic charge with an initial surface voltage of around 700 V. When the electret is mounted on the ionisation chamber, an electric field is created inside the opened chamber as illustrated in Figure 2.6. Radon diffuses through a filter which is designed to trap all radon daughters. Radon with the half-life of 3.85 days decays further and produces its daughter and alpha particles which ionises the air inside the chamber [Rad15]. The electret collects the negatively charged ions generated during the ionisation process that occurs inside the chamber. These ions are drawn to the surface of the electret where they cause a reduction in its surface charge. The electret is discharged at a rate proportional to the radon concentration [Kot90]. The loss of charge on the surface of the electret during the exposure period determines the average radon concentration in the location where the devices were located. Using different combination of electret ionisation chambers it is possible to measure radon concentrations ranging from 1 Bqm<sup>-3</sup> to 3 MBqm<sup>-3</sup> [Kot90].

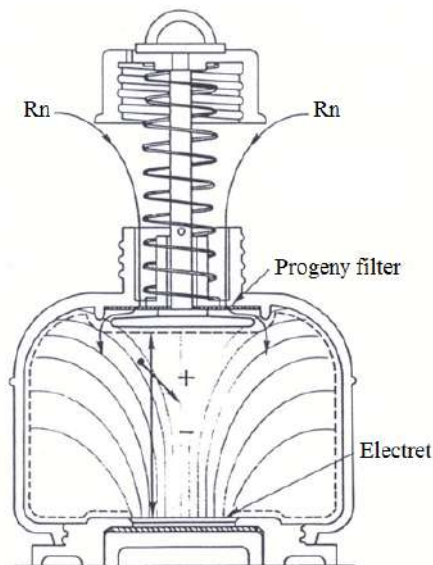


Figure 2.6: The cross section of the E-PERM system [Kot90].

Table 2.3: The advantages and disadvantages of different radon measuring detectors [Rad15].

Detector Type	Advantages	Disadvantages
RAD7	<ul style="list-style-type: none"> <li>• Make quick reading</li> <li>• Can determine the energy of each alpha particle</li> </ul>	<ul style="list-style-type: none"> <li>• Expensive</li> <li>• Cannot be easily transported via mail</li> <li>• Requires to be calibrated every year</li> </ul>
Track-etch	<ul style="list-style-type: none"> <li>• Low cost</li> <li>• Can be easily transported via mail</li> <li>• Safe for home use, Track-etch film is non-toxic</li> <li>• Can be deployed by anyone</li> </ul>	<ul style="list-style-type: none"> <li>• Tracks can be hard to count accurately</li> <li>• Can only be used for long term testing</li> <li>• Water entering device causes wrong readings</li> <li>• Detectors must be sent to a laboratory for analysis</li> </ul>
Electret ionisation chamber	<ul style="list-style-type: none"> <li>• Electret can be re-used until voltage falls below 200 volts</li> <li>• Electret can be recharged</li> <li>• Suitable for short-term and long-term measurements</li> <li>• Temperature and humidity independent</li> </ul>	<ul style="list-style-type: none"> <li>• Results require correction for the gamma-ray background radiation and altitude at which testing took place</li> <li>• Can be accidentally discharged by touching or surface contamination</li> <li>• Surface Potential Electret Reader (SPER) voltage reader requires calibration each year</li> </ul>

Table 2.4: The advantages and disadvantages of different radon measuring detectors (continues) [Kri17].

Detector Type	Advantages	Disadvantages
Airthings	<ul style="list-style-type: none"> <li>• Tracks radon levels in real time</li> <li>• Suitable for long-term and short-term measurements</li> <li>• Easy to install and set up</li> </ul>	<ul style="list-style-type: none"> <li>• More expensive than conventional radon testing methods</li> <li>• Uses Bluetooth only</li> </ul>
Charcoal	<ul style="list-style-type: none"> <li>• Compact, convenient and economical</li> <li>• Can be used for 48-hour test</li> <li>• Can be easily mailed to the laboratory for analysis</li> <li>• Passive, does not require power</li> <li>• Quick and accurate analysis</li> </ul>	<ul style="list-style-type: none"> <li>• Limited to short-term</li> <li>• Provides no indication of changes in radon during measurement</li> <li>• Hard to detect tampering</li> <li>• Detectors must be sent to a laboratory for analysis</li> </ul>
AlphaGUARD	<ul style="list-style-type: none"> <li>• Relatively good precision</li> <li>• Can track hourly variation</li> <li>• Can indicate tapering of ventilation</li> <li>• Option to download or print on site</li> </ul>	<ul style="list-style-type: none"> <li>• Expensive</li> <li>• Requires annual calibration</li> <li>• Can only test one room at a time</li> </ul>



## 2.9 Overview of a national indoor radon survey worldwide

Over the years, indoor radon surveys have been conducted in many countries. The radon surveys were mainly conducted in homes. Since radon is not only a problem in dwellings, the surveys have also been conducted in workplaces including office buildings, schools and factories. The method used in one country was observed to be widely different from the method used in other countries, these methods are discussed in table 2.6, table 2.7 and table 2.8. This might be on account of different factors like the country's geology, building styles, climatic parameters and ventilation conditions. This section will cover the overview of national indoor radon surveys conducted worldwide. This will include the reference levels adopted per country, sampling design, sampling procedure, measurement techniques used, measurement duration and quality assurance.

### 2.9.1 Reference levels for radon

The reference level is defined as the level of activity concentration above which it is not acceptable to allow exposures to occur and under which safety management will continue to be implemented [Vuk18]. The level value depends on the amount of exposure, which varies with the countries. The reference levels help countries to identify possible health hazards related to indoor radon exposure and to take steps to minimise exposure.

Radon-related risk can be estimated with a reference level. The areas where the average concentration of radon is higher than the national average concentration, are referred to as radon prone areas (RPA). There is no level of radon considered safe. Several countries chose their national action levels based on results from indoor radon surveys. The United States Environmental Protection Agency has set the radon action level at  $148 \text{ Bqm}^{-3}$  [EPA03]. The National Nuclear Regulator (NNR) in South Africa has adopted the reference level at  $300 \text{ Bqm}^{-3}$ .

The action level represents the maximum acceptable levels of indoor radon to minimise the risk to people and warn them when the mitigation action is required. WHO indicates that indoor radon exposure is a major and growing public health threat in homes, and recommends that countries adopt reference levels of the gas of  $100 \text{ Bqm}^{-3}$ . Health Canada revised the National Building Code of Canada (NBCC) recommendations in 2007, by reducing indoor radon from  $800 \text{ Bqm}^{-3}$  to  $200 \text{ Bqm}^{-3}$ . However, both World Health Organisation (WHO) and International Atomic Energy Agency (IAEA) have shown that concentrations below  $200 \text{ Bqm}^{-3}$  have also been

associated with lung cancer [WHO09]. Table 2.5 show some action levels that have been adopted in some countries.

Table 2.5: Action levels in different countries [WHO09]

Country	Action levels in Bq m <sup>-3</sup>
Argentina	400
Austria	400
Belgium	400
Bulgaria	500
Canada	800
China	400
Czech Republic	400
Denmark	200
Ecuador	400 to 600
Finland	400
France	400
Georgia	200
Germany	100
Greece	400
Ireland	200
Kyrgyzstan	200
Latvia	200
Lithuania	400
Netherlands	30
Norway	200
Peru	200 to 600
Romania	400
Russia	400
Slovenia	400
Sweden	200
Switzerland	1000
United Kingdom	200
USA	148

### 2.9.2 Mapping methods for indoor radon

Several stages are considered for mapping indoor radon. The first stage is to define the objectives which include two forms of maps which are contour maps and class maps. The contour maps show the geographical distribution of the levels of the quantity of interest, for example, geological characteristics or soil types. On the other hand, the class-map shows whether the standard regarding the quality of interest is satisfied, for example, to indicate the probability that the dwelling will exceed the reference level. Also, the existing indoor radon data is collected and reviewed.

Countries like Ireland [Syn06] and Iran [Mar15] used uniform grid sampling by choosing their sampling unit to be  $10 \text{ km} \times 10 \text{ km}$  square and  $5 \text{ km} \times 5 \text{ km}$  square, respectively. According to a Norwegian study [Jen02], grid sampling was not suitable because of scattered populated areas. Instead of grid sampling, the dwellings were randomly chosen from each participating municipality. In Greece and Lithuania [Mor99], population density sampling strategy was considered. In Lithuania, dwellings were randomly selected on a whole territory followed by preferential sampling regions with higher population and/or higher radon levels. In France, a selection was based on the hospital with a higher number of lung cancer patients [Bay04]. In some countries, the selection method was based on the geological characteristics and soil types [Kie97], [Yar12].

### 2.9.3 Sampling procedure

After the sampling area was identified, homeowners were informed and invited to participate in the survey. This was achieved through multiple approaches, for example, in Greece, a door-to-door approach was used in order to minimise non-response and bias [Nik02]. In Cyprus, homeowners were reached by phone calls to get their agreement for participating in the survey [Ana03]. In Iceland, volunteers were reached via a webpage or by phone. In the Austrian survey, dwellings were randomly selected through telephone register [Fri05].

### 2.9.4 Measurements duration

Since  $^{222}\text{Rn}$  is gas, its level fluctuates as a function of time of day. Short-term indoor measurements of a few hours or a few days may not be considered a reliable indicator of long term average values [IAE19]. To obtain accurate results of long term average values, long-term measurements

are recommended. Long-term measurements can take between 3 to 12 months. Integrated measurements lasting for one-year are usually preferred to obtain good estimates of the mean radon concentration. Alpha track detectors and electret ion-chambers are recognised by Health Canada for long-term measurements. In most countries, a measuring period of 3 months is recommended as per national practices to meet homeowners' expectations. However, most of the short-term monitoring devices can be used for screening if a radon problem is suspected.

### 2.9.5 Seasonal variation

Buildings are generally less ventilated during the winter season than in summer. The Stack Effect is generated due to indoor/outdoor pressure difference [Joj09]. This accounts for  $^{222}\text{Rn}$  gas accumulating in indoor spaces rather than outdoors. Studies show that tests conducted in the winter months tend to give higher results than the annual average, and tests conducted in summer months produce lower results. A similar variation can be observed for day/night variation. Soil emanation activity during late night/early morning hours is higher than the emanation activity during the day [Kha13].

Other countries like Korea [Kim03] conducted both summer and winter measurements and obtained seasonal correction factors. The seasonal correction factor is needed to adjust measurements taken over periods other than twelve months. In some countries, either summer or winter measurement were conducted, and the seasonal factors are used to compare seasonal variation. However, it is recommended that the measurements must be taken in the winter season to obtain maximum radon concentrations.

### 2.9.6 Quality assurance

Conducting quality assurance and quality control activities is recommended to assure confidence in the radon monitoring programme. This can include the handling of radon detectors during transportation. Some steps can be taken during sampling to ensure the accuracy of the results by reducing uncertainties. In other countries, the quality of measurements was ensured through inter-comparisons, inter-calibration and parallel measurements [How07]. Some countries have a testing scheme for radon detectors, to ensure that they meet the required standard of accuracy.

Table 2.6: Methods for measuring indoor radon concentration [Fri05, Iva13, Jón15, IAE19].

Country	Approach methods	Measuring methods
Argentina	<p>Cities with highest population were prioritised.</p> <p>The survey began in mine dwellings. Houseowners agreed to participate. Each householder was provided with the questionnaire.</p> <p>Most measurements were carried out in dwellings constructed from bricks and concrete.</p>	<p>Passive track etch detectors with exposure period of three (3) months. The measurements were preferably performed in the winter.</p> <p>Short term detectors (activated charcoal detectors and electret detectors) were used for the purpose of making initial screening measurements.</p>
Australia	<p>Homes were selected randomly from an electoral register.</p> <p>Questionnaires were sent to each participant along with one radon detector. The detectors were placed in the living rooms.</p>	<p>The detectors used for radon survey were track-etch radon detectors and were exposed for 12 months.</p>
Austria	<p>Dwellings were selected at random from the telephone directory.</p> <p>Two detectors were placed in each dwelling in the most frequently used rooms.</p> <p>Questionnaires were distributed together with the detectors.</p>	<p>Three detector systems were used: track-etch detectors, electrets and charcoal detectors with liquid scintillation counting measurement.</p> <p>Three-month measurements were performed using track-etch and three-days using charcoal detectors. All measurements were made in spring and autumn.</p>
Bulgaria	<p>The survey was population based. The dwellings were randomly selected by using a door-to-door approach for contacting families and distributing detectors.</p> <p>Detectors were deployed on the ground floor. The detectors were placed in the living room and in children's rooms or bedrooms.</p> <p>The measurements were completed in 2775 dwellings.</p>	<p>The measurements were performed with track-etch detectors).</p>

Table 2.7: Methods for measuring indoor radon concentration (continues) [Dow17, Car19, Vuk18, IAE19].

Country	Approach methods	Measuring methods
Canada	A market research company was contracted to recruit participants for the survey. Participants were recruited randomly by telephone. Each participant received a radon detector and a questionnaire.	All measurements were to be carried out for a minimum period of three months during the summer season.
Iceland	The Icelandic Radiation Safety Authority (IRSA) advertised on its web site. IRSA staff also asked family, friends and colleagues to participate. The detectors were sent to homeowners. Survey was also conducted in schools, workplaces, and kindergartens.	The detectors used were alpha track detectors.
Iran	Postcodes were used for selecting homes. The radon detectors were distributed by trained staff. Two radon detectors were placed in separate rooms (living room and bedroom).	Track-etch detectors were used in the survey.
Ireland	Participant were randomly selected at from the register of electors. A total of 12 649 dwellings were surveyed for indoor radon gas.	Track-etch detectors were used in survey for 12 months.
Italy	The door-to-door approach was adopted for contacting the participants.	Alpha track detectors (LR-115 type II) were used for a period of 12 months.
Montenegro	The survey was geographically and population based. Detectors were deployed in the living room or bedroom on ground floor or first floor	Track-etch detectors were used in the survey for six month.

Table 2.8: Methods for measuring indoor radon concentration (continues), [Lem01, IAE19].

Country	Approach methods	Measuring methods
Netherlands	Homes were randomly selected. Each participant received two passive detectors: one radon detector and one thoron progeny detector and a questionnaire.	Track-etch detectors were used in the survey for at least one year.
United States of America	Homes were randomly selected. Environmental Protection Agency (EPA) assisted homeowners in placing the detectors in their homes. Questionnaires were distributed together with the detectors.	Track-etch detectors were used in the survey

## 2.10 South African existing indoor radon data

Numerous pilot studies have been carried out in indoor radon surveys in South Africa. These studies include measurements of the radon levels in soil, water, and air. No national-scale study on indoor radon has been conducted in South Africa so far. This section gives an overview of existing studies overview of indoor radon in South Africa.

### Indoor radon along the West Coast, Western Cape [2019]

The indoor radon measurements were performed in 52 houses located in Vredenburg and Saldanha [Rou19]. The houses were randomly selected and the homeowners were approached to get permission for measurement. E-PERM electret chambers were used to measure radon and exposed for a minimum of 3 days. The monitors were placed in the most occupied rooms like the living rooms. The average values for indoor radon levels were  $58.7 \text{ Bqm}^{-3}$  in Vredenburg and  $38.6 \text{ Bqm}^{-3}$  in Saldanha.

### Radon in mine dwellings, Gauteng [2017]

Indoor radon gas measurements were performed in mine dwellings located in a gold mining area of Gauteng Province [Kam17]. The  $^{222}\text{Rn}$  gas activity in indoor air was measured using the AlphaGUARD Radon Professional Monitor. The measurements were performed in two mine villages namely, West Village and East Village. The detectors were deployed 1 m above the ground in six houses, three houses were located in the west village and the other three in the east village. The measurements were taken in 24 hours. The average activity of  $119.6 \text{ Bqm}^{-3}$  was obtained from the mining area. The maximum indoor radon level found in the mining area was  $472 \text{ Bqm}^{-3}$ .

### Radon in-air in a spa resort, Western Cape [2016]

The radon activity levels in-air were measured at Montagu in the Western Cape [Bot16]. The study aimed to estimate the associated effective dose received by the employees and visitors at the Avalon Springs thermal spa resort. The measuring method that was employed was E-PERM™ (Electret Passive Environmental Radon Monitor). The electrets were deployed for 5 days at different locations. These locations were described to be the Grand Suite, hot-tub, indoor pool, pumping room and, cocktail bar. The indoor radon concentration levels ranged from a



minimum of  $33 \pm 4 \text{ Bqm}^{-3}$  to a maximum of  $523 \pm 26 \text{ Bqm}^{-3}$ . The annual occupational effective dose due to the inhalation of radon progeny ranged from  $0.16 \pm 0.01 \text{ mSv}$  to  $0.40 \pm 0.02 \text{ mSv}$ .

### **Radon in-air in wine cellars, Western Cape [2014]**

In Western Cape, nine wine cellars were selected for the study of radon in-air [Bot17]. The measuring techniques used in this study were passive electret (E-PERM) from Rad Elec Inc. and RAD7 detector. The short-term electret ion-chambers were deployed for 6 to 10 days at each location within the nine wine cellars. Two RAD7 detectors were used to perform continuous radon in-air activity concentration measurements for 2 days. The radon levels ranged from  $12 \pm 4 \text{ Bqm}^{-3}$  to  $770 \pm 40 \text{ Bqm}^{-3}$ .

### **Paarl Houses, Western Cape [2004]**

In 2004 the indoor radon measurements were performed in Paarl, Western Cape [Lin08]. The study involved school learners and teachers. A total of seven schools participated in this study. The E-PERM were distributed by the researchers to at least 200 localities in Paarl. The detectors were deployed in the houses and exposed for at least seven days. The living rooms were preferred as the perfect place to deploy the detector. The information about the house characteristics was obtained through a questionnaire. The deployments and collection were supervised by the researchers for quality assurance. The results yielded an average value of  $115 \text{ Bqm}^{-3}$  with a minimum of  $8 \text{ Bqm}^{-3}$  and a maximum of  $801 \text{ Bqm}^{-3}$ .

### **Cango Caves, Western Cape [2005]**

During the summer of 2004 and 2005, the radon levels were measured in the Cango Caves in the Western Cape Province [Nem05]. Two measuring methods used in this study were E-PERM and the RAD7. Short-term electrets were exposed for 24 hours inside the caves. The RAD7 was exposed in a large section of the caves for 2 hours, this was performed during the day and overnight. The results for the radon activity levels ranged from  $800 \text{ Bqm}^{-3}$  to  $2600 \text{ Bqm}^{-3}$ .

### **Goldfields, Free State [1998]**

The University of the Free State conducted an indoor radon study in 1998 [Eli98]. The study involved the potential radiation hazards from gold mines in the Free State province. The envi-

ronmental radon gas measurements were taken around Goldfields mine. The aim was to identify the areas with high radon concentration greater than  $200 \text{ Bqm}^{-3}$ . The three measuring techniques used in this study were passive track etch, AlphaGUARD Radon Professional Monitor, and E-PERM. The exposure period was at least 2 to 3 months, 24 hours, and, seven weeks, respectively. The environmental radon levels were measured indoors and outdoors. The results seemed to confirm that the natural radon levels in the Free State Goldfields do not differ much from non-mining areas. No excessively high indoor radon concentration greater than  $200 \text{ Bqm}^{-3}$  was detected.

### **South African indoor radon study by Leuschner et al. [1989-1991]**

In this study, about 1855 houses in South Africa were measured for radon levels [Leu02]. Two types of passive detectors used in this study were passive track etch and passive charcoal canisters. The track etch monitors were exposed for two months and the charcoal canisters were exposed for seven days. The average indoor radon concentration was about  $70 \text{ Bqm}^{-3}$  with a maximum of  $842 \text{ Bqm}^{-3}$ . In  $<1\%$  of houses radon levels were above  $400 \text{ Bqm}^{-3}$  and in  $3 - 4\%$  of houses radon levels were above  $200 \text{ Bqm}^{-3}$ . The main contributing factors for higher radon levels were associated with wooden floors, radium content in the soil, and the underlying geology.

Table 2.9: The summary of the finding from case studies around South Africa [[Lin08](#), [Rou19](#), [Leu02](#)]

Location	Province	Sample Size	Average	Maximum	Reference
Vredenburg	Western Cape	33	59	200	<a href="#">[Rou19]</a>
Saldahna	Western Cape	19	37	90	<a href="#">[Rou19]</a>
Paarl (2005)	Western Cape	200	115	801	<a href="#">[Lin08]</a>
Cape Town	Western Cape	134	13	52	<a href="#">[Leu02]</a>
Paarl (1989)	Western Cape	60	85	842	<a href="#">[Leu02]</a>
Malmesbury	Western Cape	59	42	150	<a href="#">[Leu02]</a>
Beaufort-West	Western Cape	62	79	184	<a href="#">[Leu02]</a>
George	Western Cape	91	64	143	<a href="#">[Leu02]</a>
Akasia	Gauteng	7	57	97	<a href="#">[Leu02]</a>
Bedfordview	Gauteng	16	20	72	<a href="#">[Leu02]</a>
Boksburg	Gauteng	116	66	212	<a href="#">[Leu02]</a>
Germiston	Gauteng	143	116	297	<a href="#">[Leu02]</a>
Johannesburg	Gauteng	284	49	197	<a href="#">[Leu02]</a>
Roodepoort	Gauteng	6	61	130	<a href="#">[Leu02]</a>
Randfontein	Gauteng	45	92	185	<a href="#">[Leu02]</a>
Randburg	Gauteng	13	122	440	<a href="#">[Leu02]</a>
Soweto	Gauteng	150	56	131	<a href="#">[Leu02]</a>
Krugersdorp	Gauteng	53	77	273	<a href="#">[Leu02]</a>
Sandton	Gauteng	16	50	106	<a href="#">[Leu02]</a>
Centurion	Gauteng	16	61	136	<a href="#">[Leu02]</a>
Hartbeespoort	Gauteng	28	59	145	<a href="#">[Leu02]</a>
Nababeep	Northern Cape	88	87	393	<a href="#">[Leu02]</a>
Springbok	Northern Cape	67	78	340	<a href="#">[Leu02]</a>
Brits	North West	30	42	119	<a href="#">[Leu02]</a>
Stilfontein	North West	72	62	131	<a href="#">[Leu02]</a>
Rustenburg	North West	10	33	48	<a href="#">[Leu02]</a>
Parys	Free State	44	66	595	<a href="#">[Leu02]</a>
Richards Bay	KwaZulu-Natal	76	38	120	<a href="#">[Leu02]</a>
Phalaborwa	Limpopo	8	61	79	<a href="#">[Leu02]</a>

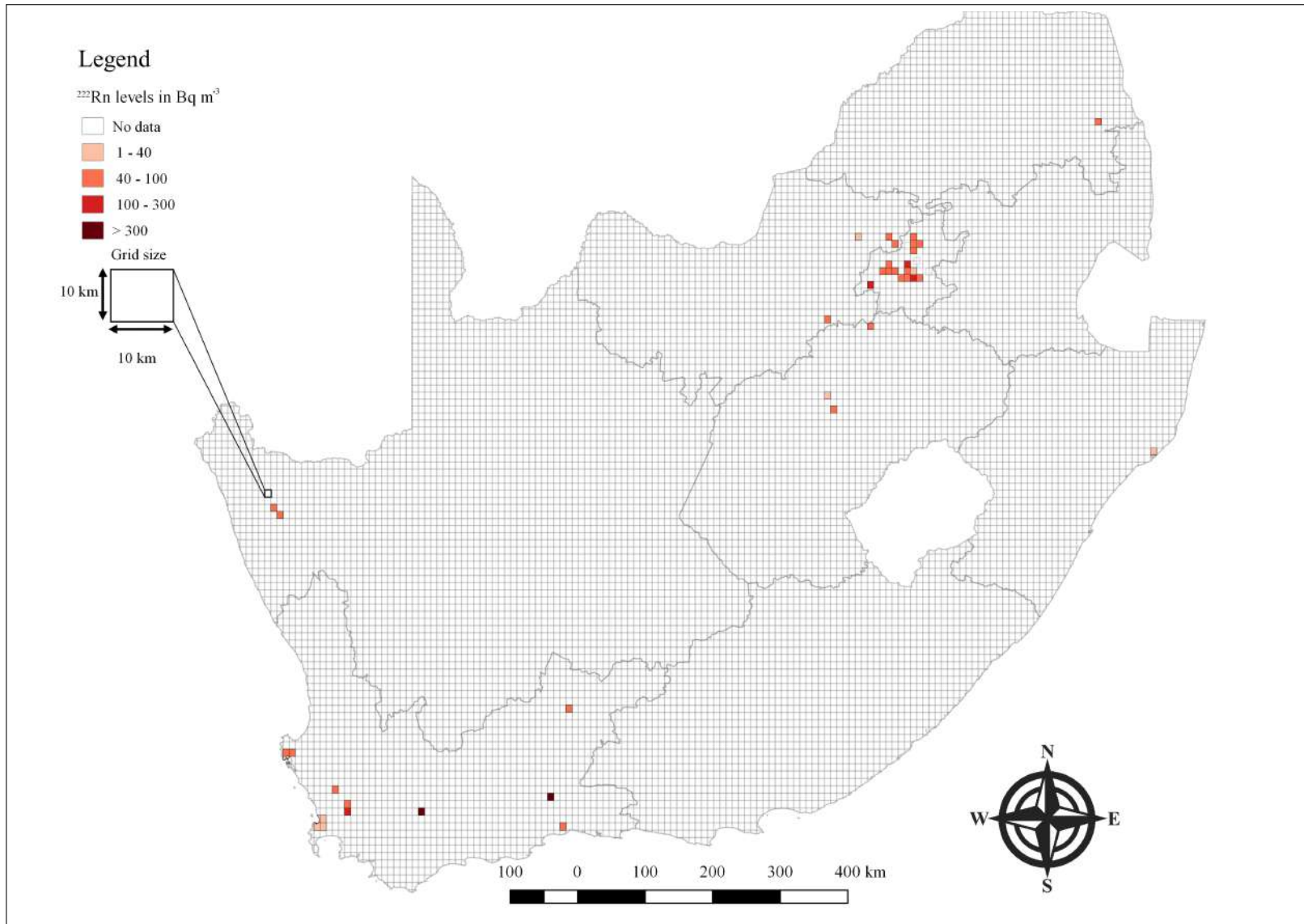


Figure 2.7: South African 10 × 10 km grid map showing areas where indoor radon was measured. The data was obtained from table 2.9.

## 2.11 Log-normal distribution and indoor radon

Many studies have shown that indoor radon levels follows a log-normal distribution [Bos19]. Log-normal distribution is defined to be a continuous probability distribution of random variable whose logarithm is normally distributed. In simple terms if the original data of indoor radon follows log-normal distribution then the natural logarithm of the data follow normal distribution. So, if the original data of variable is

$$x_1, x_2, x_3, \dots, x_i$$

When combining all data points, the resulting probability distribution function  $p(x)$  for indoor radon concentration ( $x$ ) can be approximately expressed as 2.13 [Rim18]

$$p(x) = \frac{1}{x\sqrt{2\pi\sigma^2}} \exp\left(\frac{-[\ln(x) - \mu]^2}{2\sigma^2}\right) \quad x > 0; \sigma > 0 \quad (2.13)$$

where  $\sigma$  and  $\mu$  are the fitting parameters,  $\sigma$  is the standard deviation which represents the spread of the distribution, and  $\mu$  is the mean value of the data [Rim18]. Figure 2.8 illustrates how the log-normal (left) and normal distribution (right) look like. Two curves on the left (red and black) follow log-normal distribution and have the same value for  $\mu$  and different values for  $\sigma$ , respectively. The spread of the curve changes with the  $\sigma$  value. This indicates that the shape of a curve depends on the  $\sigma$  value. The following properties must hold for the distribution to be log-normal: the values must be always positive and the distribution must be always right-skewed. To get the log-normal distribution on the right, simply take the natural logarithm of original data of log-normal distribution.

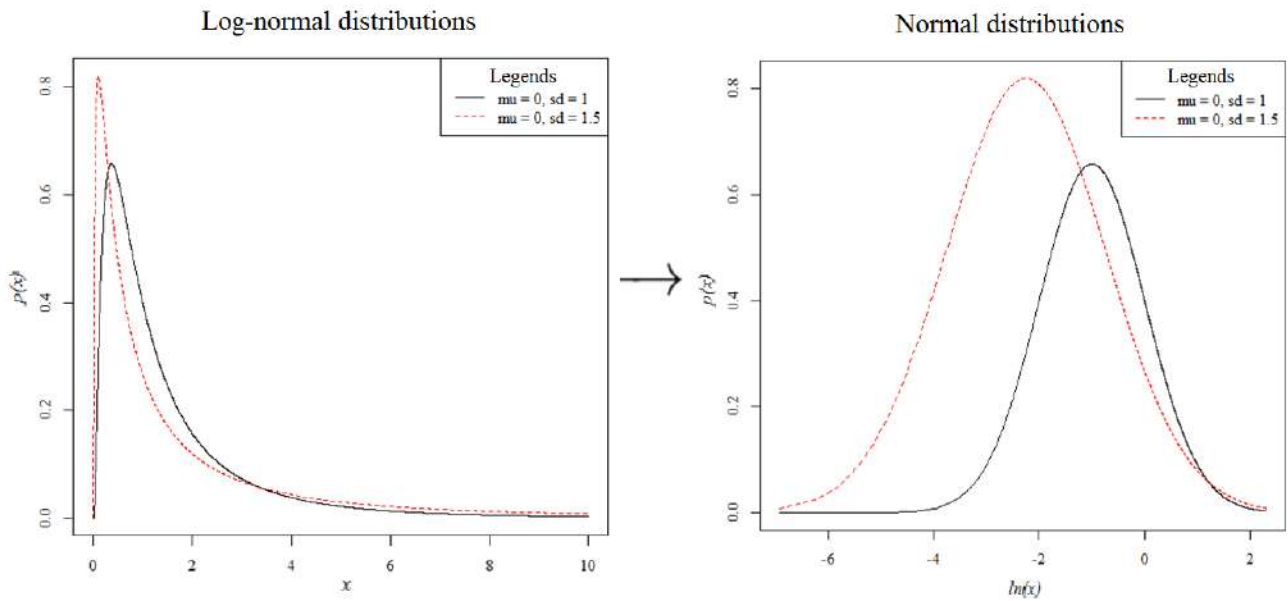


Figure 2.8: The log-normal distribution transformed to normal distribution.

In a case of indoor radon levels, the log-normality test is necessary for estimating the mean value of indoor radon concentration and for determining the probability that the indoor radon will exceed the recommended reference radon concentration [Pan19]. In some European countries, studies show that the mean concentration of indoor radon ranges from less than  $10 \text{ Bqm}^{-3}$  to over  $100 \text{ Bqm}^{-3}$  with the typical standard geometric deviation ranging from the value of  $2 \text{ Bqm}^{-3}$  to  $3 \text{ Bqm}^{-3}$  [WHO17]. It implies that about 2% to 3% of the cases the indoor radon concentration is expected to be one hundred times the mean. On the other hand, the study conducted in Belgium indicated that the deviation from log-normal is due to outliers determined to be extreme levels of indoor radon [Cin15]. The log-normal distribution showed a good fit for indoor radon concentrations [Zub16].

## Chapter 3

### 3 Data collection and methodology

In this chapter, the different measuring techniques for indoor  $^{222}\text{Rn}$  concentration are discussed. This chapter will also describe the approach and systems used for the selection of study areas. The procedures for the measurement of indoor  $^{222}\text{Rn}$  concentration will be discussed for each campaign.

#### 3.1 An overview of the instruments used for radon detection.

Radon is undetectable by human senses but by radon detectors there must be a limit of how high the levels may be. There are several ways to measure radon concentrations indoors. The radon measuring instruments used for indoor radon measurements in this study are discussed in this section.

##### 3.1.1 E-PERM™ System

###### 3.1.1.1 E-PERM™ preparation processes

E-PERMs (Electret Passive Environmental Radon Monitors) from Rad Elec™ were used in this study. An E-PERM sometimes referred to an electret ion-chamber (EIC), normally comes in a keeper cover for preventing voltage loss due to ions in the air. Each electret's surface was carefully examined for any dust or fibre contamination. The surface of each electret was cleaned using a jet of nitrogen air. The cleaning was done at the SU Physics Department workshop. The cleaning procedure was also repeated for cover keepers and the E-PERM™ ion chambers. For this research, all electret ion-chambers (EICs) were prepared in the Health Physics Laboratory (HPL) located inside the Merensky Building.

The **S**urface **P**otential **E**lectret **R**eader (SPER) from Rad Elec™ was used to read out the voltage across the surface of each electret as illustrated in Figure 3.1. An electret was carefully placed in the circular receptacle in the SPER voltage reader and a metal slider in the SPER voltage reader was manually moved to expose the electret to the voltage sensor. The voltage on the electret was

digitally displayed on the LCD panel on the SPER voltage reader. The voltage measurement was repeated three times for each electret. The values were recorded in the logbook as initial voltages ( $V_i$ ).



Figure 3.1: Voltage reader used for measuring initial  $V_i$  and final  $V_f$  voltages from the electrets.

After measuring the initial voltage, an electret was removed from the receptacle and quickly placed into the closed ion chamber. Depending on the duration of the measurements (short- or long-term), an electret was attached to the ionisation chamber; either S-chamber or L-OO chamber. Different E-PERM<sup>TM</sup> configurations are shown in Table 3.1, with their associated constants ( $C_1$ ,  $C_2$  and  $C_3$ ). The  $C_1$  and  $C_2$  are calibration constants and  $C_3$  is a constant to take the gamma-ray background into account.



Table 3.1: E-PERM<sup>TM</sup> configurations with their respective constants and measuring periods. [Rad15].

E-PERM <sup>TM</sup> configuration	Constants			Description	Exposure period (days)
	C <sub>1</sub>	C <sub>2</sub>	C <sub>3</sub>		
SST	1.69776	0.0005742	0.087	Short-term electret in the S-chamber	2 - 7
SLT	0.14	0.0000525	0.087	Long-term electret in the S-chamber	30 - 120
LST-OO	0.23327	0.000123	0.12	Short-term electret in the L-OO chamber	15 - 91
LLT-OO	0.02156	0.00001012	0.12	Long-term electret in the L-OO chamber	91 - 365

### 3.1.1.2 E-PERM<sup>TM</sup> deployment procedure

After all electrets were screwed into the bottom of the ionisation chamber (S-chamber or L-OO chamber), the E-PERM<sup>TM</sup> were then transported to the study areas with the ion chamber in a "closed" or "off" position as shown on the right of Figure 3.2. The E-PERMs<sup>TM</sup> were kept closed during transportation to avoid the surrounding air from entering the ion chamber. A plastic trolley-case was generally used for transporting the E-PERMs<sup>TM</sup> from the HPL to the designated study area. The case protected the E-PERMs<sup>TM</sup> from direct exposure to sunlight.

When the E-PERMs<sup>TM</sup> were finally transported to the study area, the E-PERM<sup>TM</sup> unit was turned to the "open" or "on" position by carefully unscrewing the top screw cap as shown on the left of Figure 3.2. Then each E-PERM<sup>TM</sup> was generally placed at least 1.0 m above the ground. The idea was to measure the indoor <sup>222</sup>Rn gas at height inside dwellings where normal breathing occurs. The E-PERM<sup>TM</sup> was also placed at least 0.5 metre away from the building walls, considering the fact that the thoron (<sup>220</sup>Rn) coming from the walls could contribute more when the detector is close to walls.



Figure 3.2: Left, E-PERM (S-chamber) in opened position. Right, E-PERM in closed position.

The serial number at back of each electret was carefully recorded. The date and time at which the E-PERM<sup>TM</sup> was opened was recorded at initial time ( $t_i$ ). Then the temper-indicating tape labelled "DO NOT DISTURB" was placed next to the deployed E-PERM<sup>TM</sup> for alerting people that the indoor <sup>222</sup>Rn measurement was in progress. For each E-PERM<sup>TM</sup> setup, a photograph showing the E-PERM<sup>TM</sup> and the location was taken. The E-PERM<sup>TM</sup> was left exposed to the air for a certain period depending on the intended measuring duration.

### 3.1.1.3 E-PERM<sup>TM</sup> collection procedure

After the predetermined exposure period, the E-PERMs<sup>TM</sup> were collected for analysis in the laboratory. This section describes the E-PERM<sup>TM</sup> collection procedure. A photograph of the E-PERM<sup>TM</sup> at its measurement location was taken. This photograph was compared with the one taken just after deployment to see if the E-PERM was moved. Then the E-PERM<sup>TM</sup> was carefully put to "closed" or "off" position by simply screwing the top screw cap. Immediately after the E-PERM the date and time ( $t_f$ ) was recorded. The serial number on the back of each E-PERM<sup>TM</sup> was also recorded. The E-PERMs<sup>TM</sup> were then transported back to HPL for analysis.

### 3.1.1.4 Equation for calculating the radon concentration

Equation 3.1 was used to calculate radon concentration in air. In cases where the gamma-ray background could not be measured equation 3.2 was instead used. The value of gamma-ray background ( $B_{\gamma c}$ ) was taken as  $32 \text{ Bqm}^{-3}$  [Rad15], [Kot90].

$$\text{RnC} = 37 \cdot \left[ \frac{V_i - V_f}{\text{CF} \cdot T} - (B_{\gamma} \cdot C_3) \cdot \text{ElevCF} \right] \quad (3.1)$$

$$\text{RnC} = 37 \cdot \left[ \frac{V_i - V_f}{\text{CF} \cdot T} \right] - B_{\gamma c} \quad (3.2)$$

$$\text{CF} = C_1 + C_2 \cdot \left( \frac{V_i + V_f}{2} \right) \quad (3.3)$$

$$\text{ElevCF} = 0.79 + \frac{6 \cdot \text{Elevation}}{100000} \quad (3.4)$$

where,

- RnC ( $\text{Bqm}^{-3}$ ) is the mean radon concentration;
- $V_i$  and  $V_f$  are voltages before and after the exposure respectively;
- CF is the calibration factor;
- T is the duration of exposure in days;
- $B_{\gamma}$  is the measured gamma-ray background radiation due to the gamma-ray background

radiation in  $\mu\text{Rh}^{-1}$ . If the gamma-ray background value was measured in  $\text{nGyh}^{-1}$ , it was converted to  $\mu\text{Rh}^{-1}$  by dividing the  $\text{nGyh}^{-1}$  value by 8.7 [Rad15];

- ElevCF is the elevation correction factor in feet (ft):
  - if Elevation<sup>1</sup>  $\leq 4000$  ft (1 219 m), then ElevCF=1
  - if Elevation  $> 4000$  ft (1 219 m) then use equation 3.4;
- and  $C_1, C_2, C_3$  are constants given in Table 3.1.

The E-PERM measurement has three contributing sources of measurement uncertainty:

- $E_1$  is the uncertainty associated with the chamber volume, electrets thickness and other chamber parameters and has been experimentally measured to be 5%

$$E_1 = 5\% \quad (3.5)$$

- $E_2$  is the uncertainty associated with the electret voltage reading

$$E_2 = \frac{100\% \times 1.4}{(V_i - V_f)} \quad (3.6)$$

- $E_3$  is the uncertainty associated with the natural gamma-ray radiation background  $B_\gamma$

$$E_3 = \frac{100\% \times 0.1}{\text{RnC}} \quad (3.7)$$

The total uncertainty,  $E_{\text{tot}}$  (%), associated with each E-PERM measurement was evaluated using Equation (3.8)

$$E_{\text{tot}} = \sqrt{E_1^2 + E_2^2 + E_3^2} \quad (3.8)$$

---

<sup>1</sup>Elevation is the height above sea level where the test was conducted. The average Elevation values were obtained from Google.

### 3.1.2 ParcRGM™ system

#### 3.1.2.1 ParcRGM™ preparation processes

The track-etch ParcRGM detectors were prepared at the ParcRGM (Pty) Ltd offices in Pretoria and couriered to the HPL. Each ParcRGM™ was prepared by cutting CR-39 material into small rectangular blocks as illustrated in Figure 3.3(a). Then each block was placed inside a plastic holder which only allows  $^{222}\text{Rn}$  gas to diffuse in to reach the track-etch material as shown in Figure 3.3(b). Each ParcRGM™ was labelled with a serial number outside the plastic holder for identification. Then each ParcRGMs™ was placed inside a radon-proof protective bag made of Mylar® material and sealed as shown in Figure 3.4.

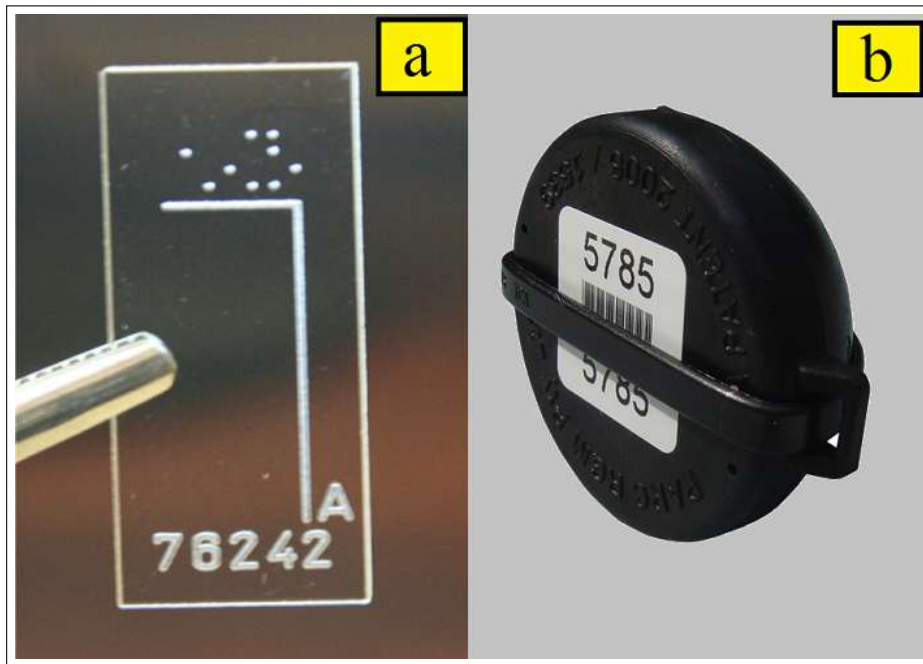


Figure 3.3: (a) CR-39 polycarbonate plastic element, (b) A 43 mm diameter plastic holder [Par20].



Figure 3.4: The ParcRGMs inside the radon-proof bags.

### 3.1.2.2 ParcRGM<sup>TM</sup> deployment procedure

After the ParcRGMs<sup>TM</sup> were transported to the pre-determined location, their radon-proof bags were cut open with a pair of scissors and the ParcRGMs<sup>TM</sup> were carefully removed from their bags. The ParcRGMs<sup>TM</sup> begin to measure indoor  $^{222}\text{Rn}$  gas the moment they are removed from the bag. The date and time were recorded immediately after each ParcRGM<sup>TM</sup> was removed from the bag. The ParcRGMs<sup>TM</sup> were generally deployed in the same way as the E-PERMs<sup>TM</sup>, 1.0 m above the ground and 0.5 m away from the building walls. A photograph showing the ParcRGM<sup>TM</sup> and the location was then taken. A control monitor that came with other ParcRGM<sup>TM</sup> was kept in its radon-proof bag. The ParcRGMs<sup>TM</sup> were left exposed for the intended measuring period.

### 3.1.2.3 ParcRGM<sup>TM</sup> collection procedure

At the end of the measuring period, the date and time were noted, and the photograph was taken to ensure that the ParcRGMs<sup>TM</sup> were not moved during the measuring period. Each ParcRGM<sup>TM</sup> was placed back in its radon-proof bag and the bag was resealed using a sellotape. The ParcRGM<sup>TM</sup> stopped measuring indoor  $^{222}\text{Rn}$  gas immediately after it was placed in the radon-

proof bag. All the ParcRGMs™ were collected and transferred into an appropriate container. A radon-proof bag with the control monitor was cut open and the monitor was removed from its bag and transferred to a container with the rest of other ParcRGMs™. Then the ParcRGMs™ were transported in a container to ParcRGM (Pty) Ltd laboratory for analysis.

### 3.1.3 Airthings™ radon monitor system

The Airthings™ radon detectors were purchased from CareTac (Pty) Ltd. The detector is battery-powered and it comes with two AA batteries installed. The indoor radon gas diffuses into the detector through the air inlets then it decays and emits alpha particles. Then the sensor registers the alpha particles emitted by radon gas. The detection principle of the Airthings™ radon detector is already explained under section 2.8 in Chapter 2. A smartphone with Airthings app was linked to the Airthings smart detector via Bluetooth to read the radon levels as shown in Figure 3.5. The data were automatically uploaded to the Airthings cloud computer servers and later assessed from the online dashboard. The .csv file was downloaded from the dashboard and the data were analysed using the Microsoft EXCEL program.



Figure 3.5: The Airthings™ radon detector.

### 3.1.4 Geographic Information Systems (GIS)

A Geographic Information System (GIS) mapping program (qGIS 2.18, Free Software Foundation, Inc., 51 Franklin Street, Fifth Floor, Boston, MA 02110-1301 USA, downloaded from: [https://docs.qgis.org/2.18/en/docs/gentle\\_gis\\_introduction/introducing\\_gis.html](https://docs.qgis.org/2.18/en/docs/gentle_gis_introduction/introducing_gis.html)) was used to map indoor radon concentrations in this research. GIS provides a convenient way for a range of data to be integrated, including aggregate resource inventory information [Kel15]. All shapefiles were obtained from the Council for Geoscience (CGS) website. A shapefile (.shp) is a vector data storage format for storing the location, shape, and attributes of geographic features. A shapefile is stored in a set of related files and contains one feature class. The shapefiles included soil-type, geology, lithology, population, and administrative type of shapefile.

To help identify the study areas where a radon survey should be performed, the soil and geology shapefiles were incorporated into the qGIS software. The Global Positioning System (GPS) coordinates for the location of the indoor radon measurements were obtained from Google Maps. The coordinate data were geocoded (by transforming the location address and street names into the geographic coordinates) and new shapefiles were created from them. These shapefiles were used to create points on the map for every indoor radon location. All maps in this research were generated using qGIS software.

## 3.2 Indoor $^{222}\text{Rn}$ measurements in workplaces

### 3.2.1 Campaign-A description

This section deals with the indoor radon measurements in workplaces. Universities are educational premises where a wide range of workplaces can be found with a high occupancy factor for members of the public. Radon levels in universities may pose potential long-term health risks to the full-time staff and students. The examined workplaces in this study include offices and laboratories. These places are normally occupied by professional academic staff members and students. The experimental work in this section was divided into two campaigns named campaign-A1 and -A2, respectively.



The aim of campaign-A1 was to

- investigate systematic effects associated with indoor radon measurements, and
- to measure indoor radon in offices.

The aim of campaign-A2 was to

- do long-term measurements using E-PERM<sup>TM</sup> and ParcRGM radon monitors to compare results for radon levels using two completely different measurement techniques;
- investigate day and night variation of indoor <sup>222</sup>Rn gas using Airthings<sup>TM</sup> radon detector and
- to compare Airthings<sup>TM</sup> and at least EIC results.

### 3.2.2 Selected study area

This study campaign was conducted in the offices and laboratories located in the Merensky building at Stellenbosch University. The University is situated in Stellenbosch, a town in the Western Cape with an average elevation of 136 metres above sea level and located about 50 kilometres from Cape Town. The soil types found in Stellenbosch are mainly Lithic Leptosols. The Merensky building is one of the academic buildings located in the Stellenbosch University. It is a three-story building with offices, laboratories and lecture halls. The building materials include granite steps to the entrance, tiled/carpeted corridors, wooden panelling floor tiles and wooden doors.

### 3.2.3 Campaign-A1 experimental setup

A total of 18 short-term electrets ion chambers (SST) were prepared in HPL at the Physics Department, Stellenbosch University. Measurements were made for radon concentrations at various locations and heights within the building during winter (June 2019). The deployment of the EICs was divided into four sets as described in Table 3.2. The experimental setup is shown in Figure 3.6. The radon detectors were deployed in a vertical configuration to investigate indoor radon as a function of height. Other radon detectors were placed next to the wall and away from the wall to investigate the effect of building walls on the radon measurements. The radon detectors were deployed for a week in the same room.

Table 3.2: Campaign-A1 experimental setup.

Code	Number of SST	Description
H	4	Deployed in the vertical position (1.5 m, 2.1 m, 2.7 m and 3.3 m)
W	5	Placed next to buildings walls (<0.5 m)
A	5	Deployed away from buildings walls (>0.5 m)
CW	4	Placed in the corner of buildings walls (<0.5 m)
Total	18	



Figure 3.6: The measurement setup for campaign-A1.

In the same building, the indoor radon concentration was also measured in six offices and four laboratories. In three offices, two SST (EICs) were deployed per office. One detector was placed next to the building's wall and the other was placed away from the building wall as shown in

Figure 3.7(a). In other offices, only one detector was deployed under a normal condition <sup>2</sup> as shown in Figure 3.7(b). Three laboratories were measured for indoor radon gas. One laboratory was a confined space without windows as shown in Figure 3.7(c). All detectors were deployed for a week during the winter season (June 2019).

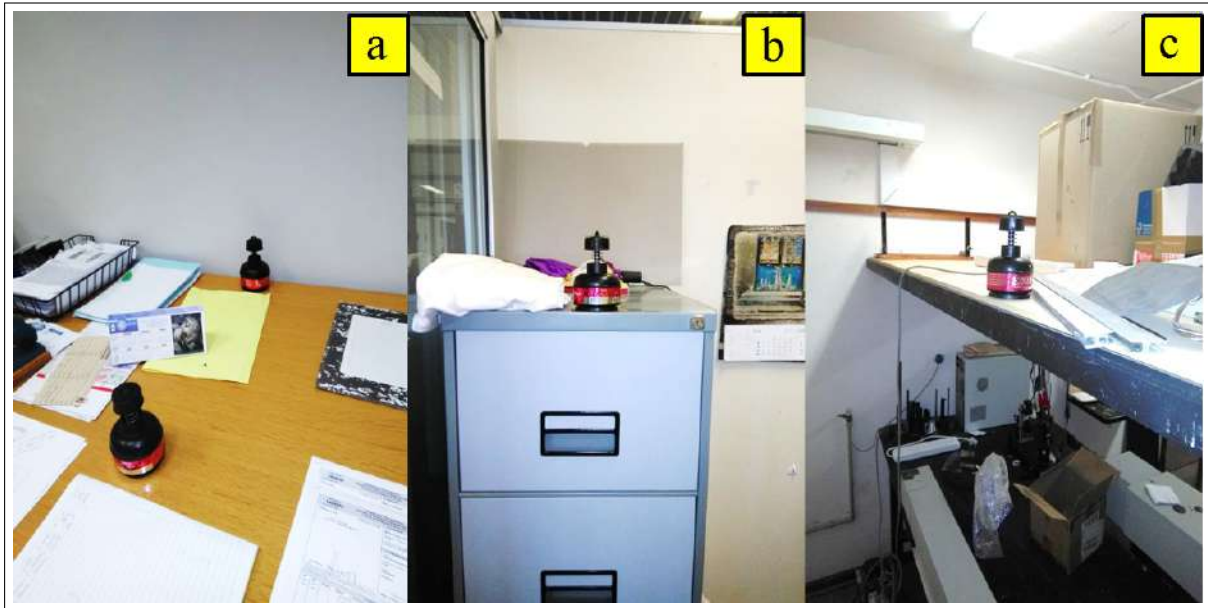


Figure 3.7: (a) The setup of SSTs (EIC) in the workplace, (b) in an office under normal conditions, (c) in the confined laboratory without any windows.

---

<sup>2</sup>normal condition

- More than 1 m above the floor.
- More than 1 m from wall openings that may allow airflow.

### 3.2.4 Campaign-A2 experimental setup

A total of 31 passive electrets (E-PERM) from Rad Elec and 35 passive track-etch monitors from ParcRGM were used in this study. Measurements were made of indoor radon concentrations for three months (March - June 2020). The radon detectors were deployed in 5 locations, 4 locations were laboratories and offices located in the same building at Stellenbosch University and 1 location is a house located around the Stellenbosch area. The E-PERM radon detectors were prepared as described under section 3.1.1.

For each location, EICs and ParcRGMs were placed side-by-side as illustrated in Figure [3.8 - 3.12].

**Location 1: Room 2026 Merensky building, Stellenbosch University.**



Figure 3.8: Two sets of LLT-OO (EICs) and ParcRGMs were placed side-by-side.

**Location 2: Room 1059 (Health Physics Laboratory) Merensky building, Stellenbosch University.**



Figure 3.9: (a) Four sets of LST-OO, SLT (EICs) and ParcRGMs were deployed in parallel and placed away from the wall ( $>0.5$  m). (b) Three sets of LST-OO and ParcRGM were deployed in parallel and placed next to the wall ( $<0.5$  m).

**Location 3: Room 2020 (third-year physics laboratory) Merensky building, Stellenbosch University**



Figure 3.10: Four sets of LST-OO (EICs) and ParcRGMs were deployed and placed next to one another.

**Location 4: Room 2024 (Physics Film Studio) Merensky building, Stellenbosch University.**



Figure 3.11: (a) Three LST-OO (EICs), two LLT-OO (EICs), two SST (EICs), and three SLT (EICs) were deployed in parallel with nine ParcRGMs. (b) Three sets of LST-OO (EICs) and ParcRGM were placed close to the wall ( $<0.5$  m).

**Location 5: House located in Stellenbosch.**

Figure 3.12: Two LST (EICs) and four ParcRGMs were deployed in parallel and placed next to one another.

The EICs and ParcRGMs detectors were collected after three months from each location. ParcRGM detectors were put back in their radon-proof bags as in Figure 3.4 and dispatched to ParcRGM (Pty) Ltd laboratory for analysis. The E-PERMs were collected and analysed in Health Physics Laboratory (HPL) at the Physics Department, Stellenbosch University.

**3.2.5 Indoor  $^{222}\text{Rn}$  measurements using Airthings™ radon monitors.**

One Airthings™ radon monitor was deployed with three SST E-PERMs™ in the laboratory as shown in Figure 3.13. The aim was to compare results from the two types of radon monitor. The measurements were carried out for one week during the summer season (February 2020). The three Airthings™ radon monitors were also used to measure the radon concentration in the house as shown in Figure 3.14. The detectors were activated and allowed to calibrate their sensors for 12 hours before they were paired with the smartphone to start measuring radon. Detector no.3 was placed closer to the walls of the building than no.1. Measurements were carried out during the winter season (August 2020). The house was mostly closed to allow sufficient radon to accumulate indoors. The data from Airthings radon detectors were accessed from the Airthings™ online dashboard (web:<https://www.airthings.com/en/dashboard>) after twenty-one days of measurements and analysed with the Microsoft EXCEL program.





Figure 3.13: The Airthings™ radon detectors placed next to three short term electrets.

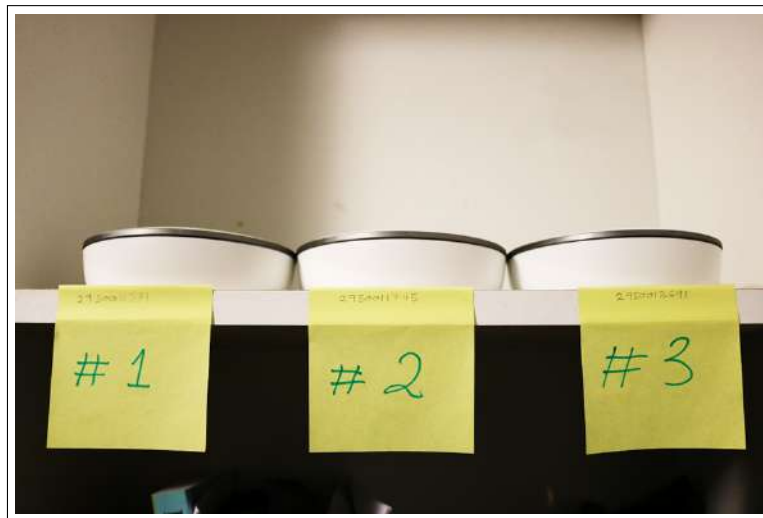


Figure 3.14: Three Airthings™ radon detectors placed next to one another.

### 3.3 Indoor $^{222}\text{Rn}$ measurements in homes located in Gauteng

#### 3.3.1 Campaign-B description

This section deals with the short-term measurement of indoor radon in homes. The aim of this campaign was to

- compare the indoor radon levels in living and bedrooms of selected Gauteng houses;
- investigate the influence of building materials on indoor radon gas and;
- to investigate if there is a correlation between soil type and indoor radon levels.

#### 3.3.2 Selected study area

This study was conducted during the summer season (December 2020) in 22 homes located in Gauteng province. The province has the highest population in the Republic of South Africa (RSA) estimated to be 15.48 million in 2020 (<http://www.statssa.gov.za/>). The houses were selected in four administrative regions. The selection was based on the soil type of each region. An average elevation above the sea level in Gauteng is 1500 metres. The soil types found in Gauteng province are mainly Albic Plinthosol, Haplic Lixisol, Plinthic Acrisol, and Lithic Lep-tosol.

Gauteng province is divided into five main administrative regions namely, the City of Johannesburg, City of Tshwane, Ekurhuleni, Sedebeng and West Rand. This study was conducted in only three regions namely the City of Johannesburg, City of Tshwane and Ekurhuleni. The selection of these three regions was based on the population density per region and the soil/geology type as indicated in Table 3.3. The majority of the houses were single-storey, built with cement or clay bricks.

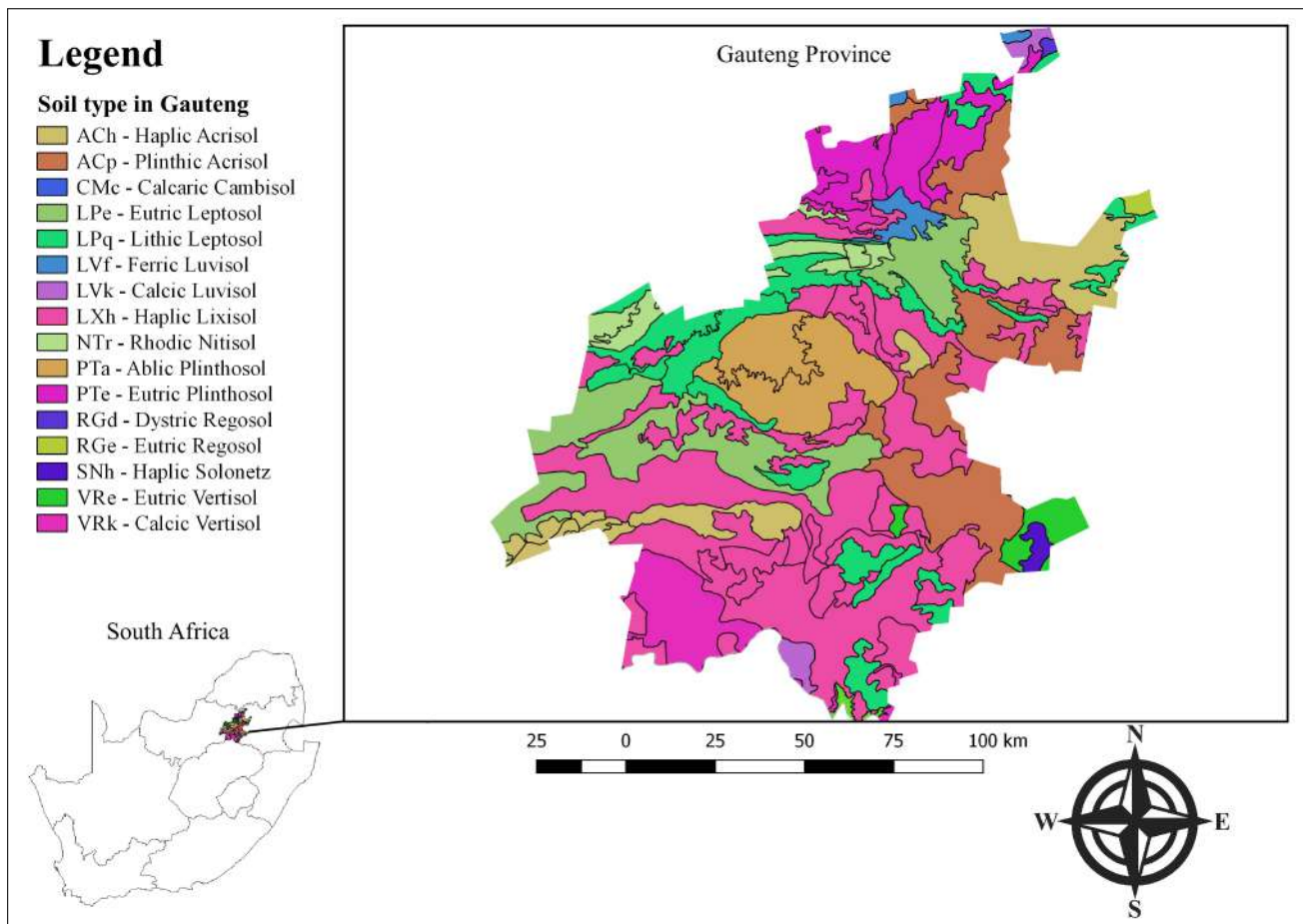


Figure 3.15: Gauteng map showing soil type.

Table 3.3: Number of houses in Gauteng that were sampled for indoor  $^{222}\text{Rn}$  measurements.

Region	Town	Soil type	Geology	No. of house sampled
City of Johannesburg	Midrand	Plinthic Acrisol	Meinhardsraal granite	4
			Transvaal	
			Sand river gneiss	
			Rooiberg Griqualand-West	
City of Tshwane	Atteridgeville	Lithic Leptosol	Transvaal	10
	Lotus Gardens		Sand river gneiss	
			Rooiberg Griqualand-West	
City of Ekurhuleni	Benoni	Albic Plinthosol	ECCA	8
	Daveyton		Witwatersrand	
			Haplic Lixisol	

### 3.3.3 Approach strategies to homeowners

The ethical clearance for surveying homes was obtained from the University of Stellenbosch. The homeowners for the selected homes were approached and were asked for permission for conducting the indoor  $^{222}\text{Rn}$  levels in their homes. After agreeing to participate, each homeowner was asked to complete a consent form. In the consent form, the reason for conducting the survey was clearly stated. Thereafter homeowners were asked to complete a questionnaire. The questionnaire was used to get the information about the characteristics, for example, home address, building materials, age of the house, and the period of occupancy in the house.

### 3.3.4 Deployment procedure

The radon detectors that were used in this survey were short-term electrets in the ion S-chambers (SST) from Rad Elec. All short-term electrets and ion S-chambers were prepared as discussed in section 3.1.1.1. The initial voltage ( $V_i$ ) was measured using the SPER reader, immediately after the homeowner agreed to participate. A short-term electret was then carefully screwed into the S-chamber to form a SST configuration as indicated in Table 3.1. Then for every short-term electret, the serial number on the electret was recorded.

The homeowner was asked to identify a suitable spot in the living room and bedroom to place

the radon detectors. After the homeowner identified a spot for deployment, the radon detector was opened and placed in the selected spot. The detector was generally placed 1.0 m above the ground and 0.5 m away from the walls of the building, however it was not always the case. A photograph of the deployed detector was taken with the permission of the homeowner.

A total of twenty-two homes were sampled. Two detectors were deployed for each house, one in the living room and the second in a bedroom. Each owner was notified about the date and time of the collection of the radon detector. The radon detectors were left in each home for 1 week.

### 3.3.5 Collection procedure

Homeowners were reminded about the collection of the radon detector two days before the actual collection date. This was done through the SMS. The radon detectors were collected from the homes after a week. This was done in the same order as the deployment, for example, if house no.1 was the first to be surveyed and house no.22 was the last to be surveyed. Then a similar order was followed during the collection of the radon detectors, first in house no.1 and house no.22 was the last.

On the date of collection, a photograph of the radon detector setup was taken. Then the radon detector was carefully closed by screwing the top screw cap of the S-Chamber and the serial number on the short-term electret was noted. The date and time were also recorded the moment the radon detector was closed. The final voltage on the short-term electret was measured three times and the values were noted as ( $V_f$ ). After the collection of the radon detectors, the GPS coordinates of the house were recorded. All radon detectors were collected from 22 homes in 3 regions. The locations of the homes surveyed are shown in the Figure 3.16, Figure 3.17 and Figure 3.18.

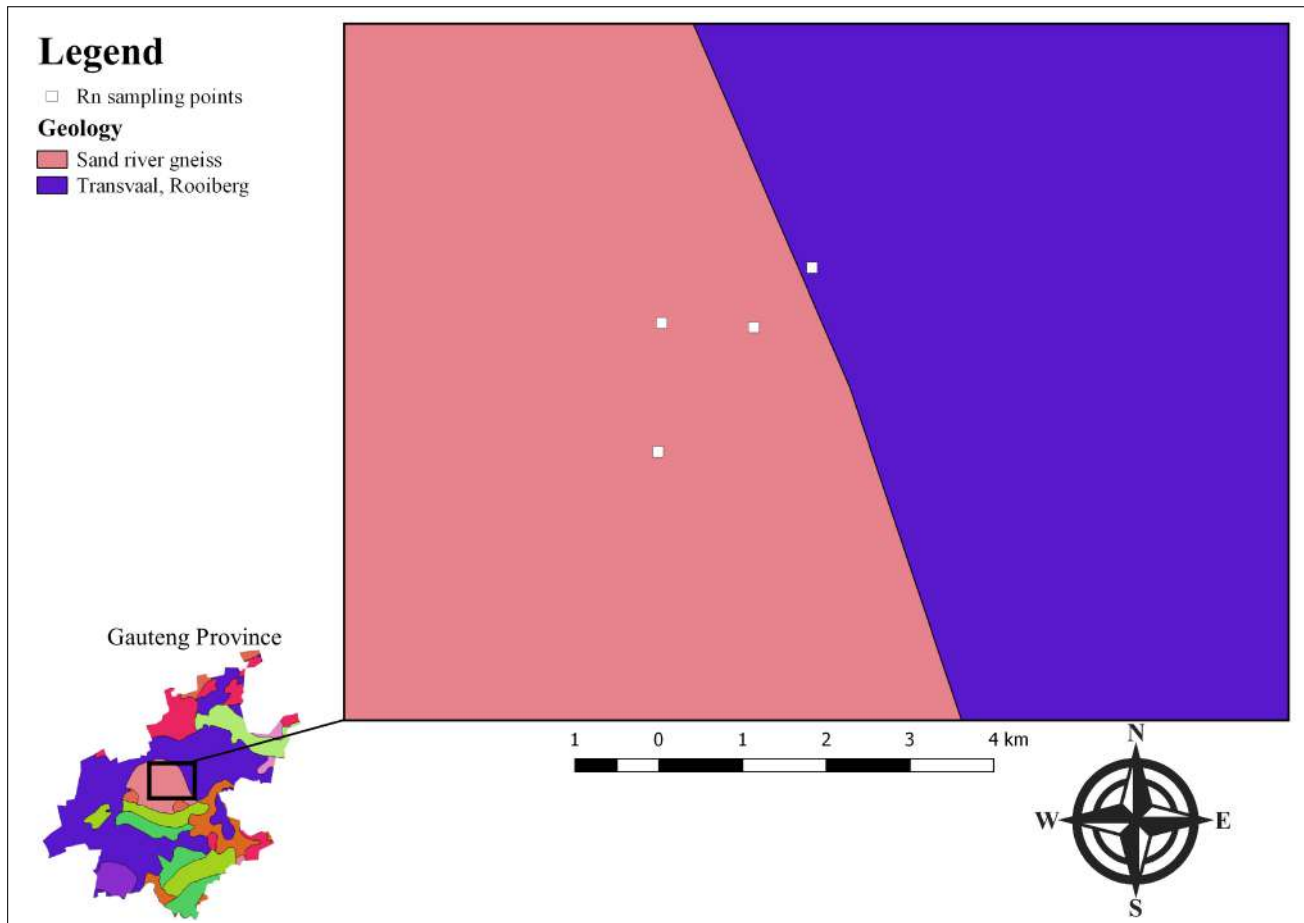


Figure 3.16: Radon locations in the City of Johannesburg.

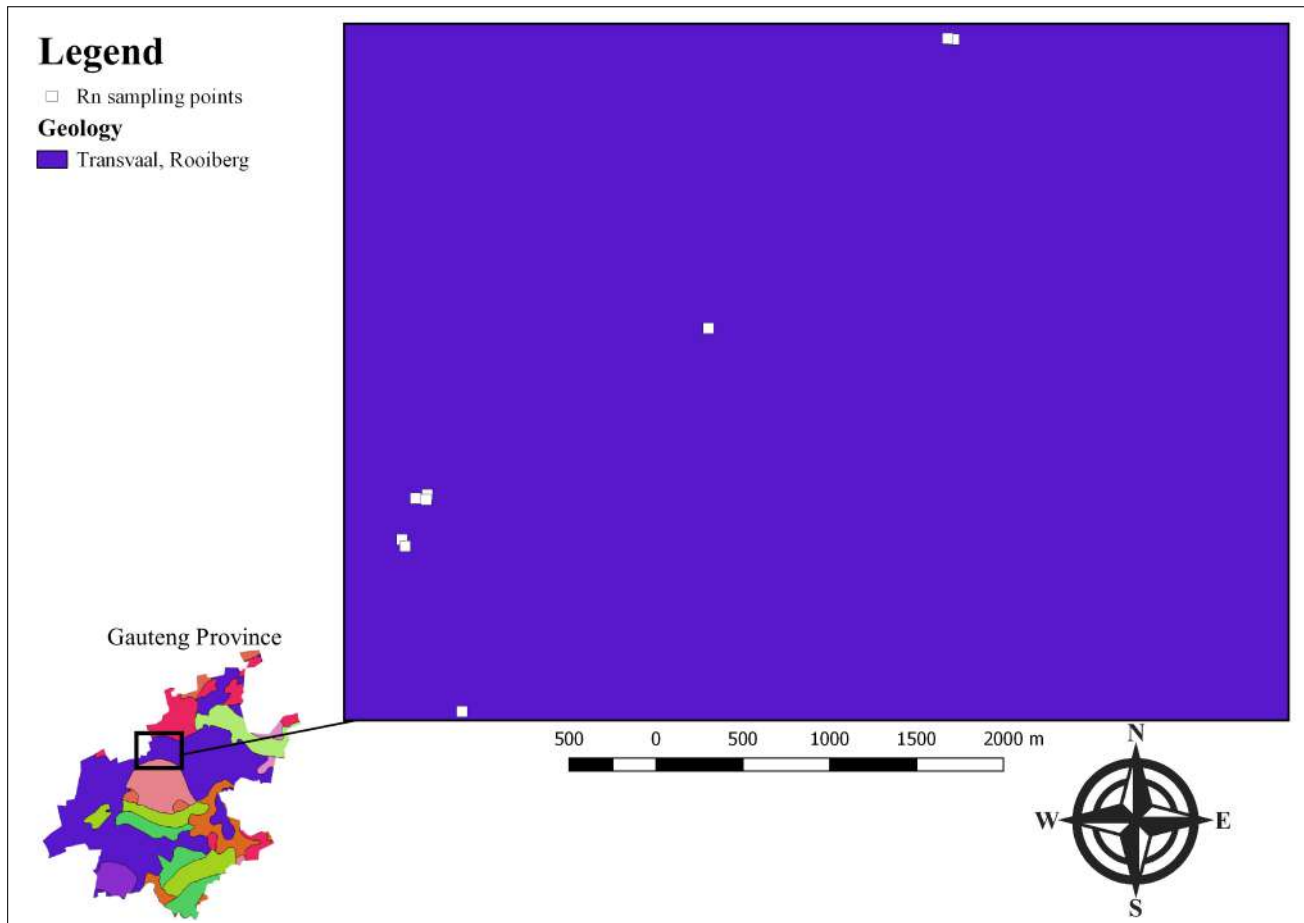


Figure 3.17: Radon locations in the City of Tshwane.

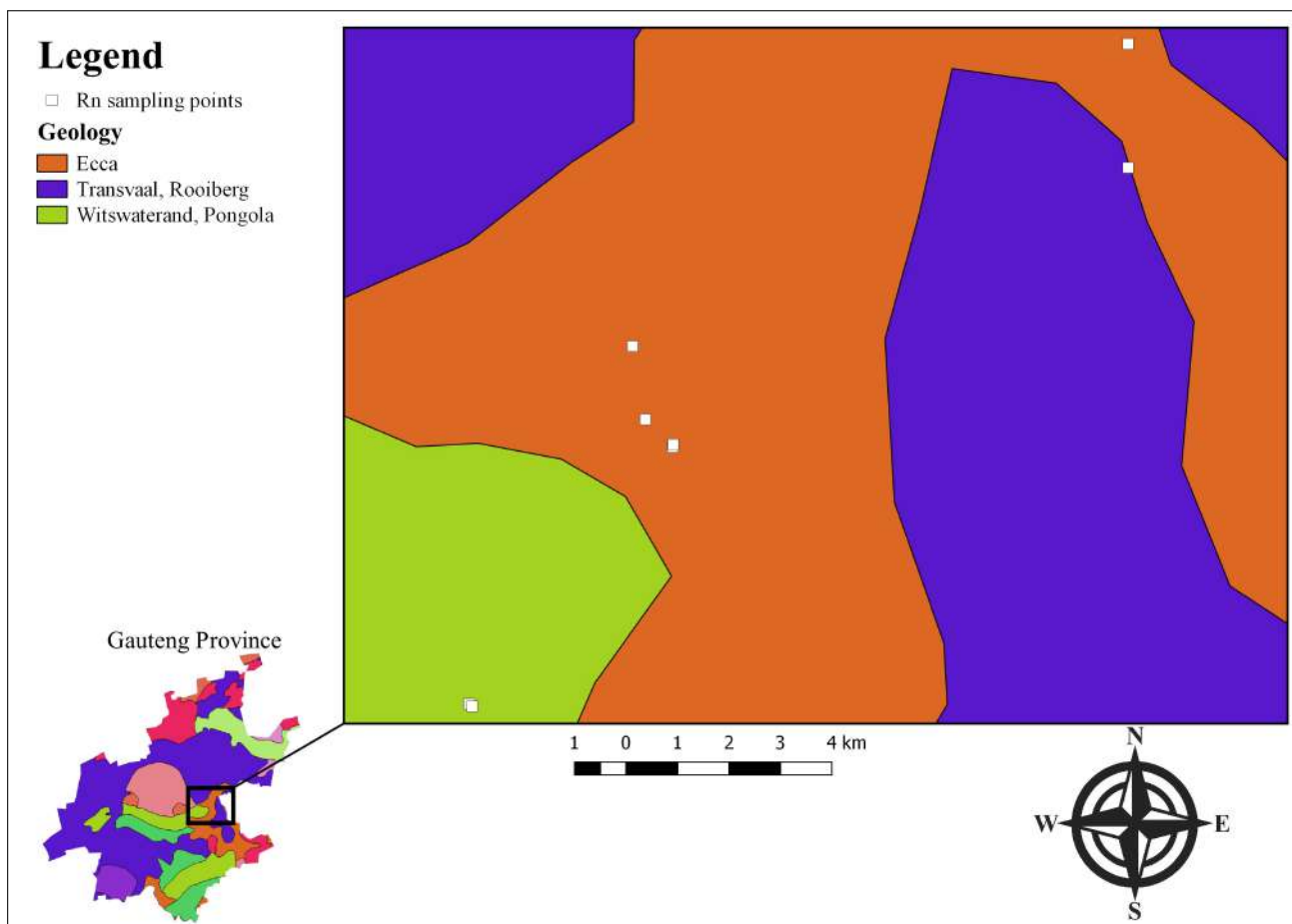


Figure 3.18: Radon locations in the City of Ekurhuleni

### 3.3.6 Gamma-ray background radiation measurements

When measuring the indoor radon concentration using the E-PERM™ system, it is important to consider the gamma-ray background radiation. For this campaign, the gamma-ray dose rates were measured in the homes. From each region, three houses were selected and measured for gamma-ray background radiation. The Graetz X5C plus™ dosimeter illustrated in Figure 3.19 was used to measure the environmental gamma-ray radiation in the air. The dosimeter was placed next to the radon detector for the selected individual homes to measure the ambient gamma-ray background radiation for one hour. At each home, the background gamma-ray measurement was made twice, during the deployment and collection of the radon monitors. The Graetz dosimeter measured the values in units of  $\mu\text{Sv h}^{-1}$ , these values were later converted to  $\text{nGy h}^{-1}$ . The values



measured in three houses for each region are given in Table 3.4. For campaigns A and C the default background gamma-ray of  $32 \text{ Bqm}^{-3}$  was used.



Figure 3.19: The Graetz X5C plus™ dosimeter.

Table 3.4: The indoor gamma-ray background radiation ( $\text{nGyh}^{-1}$ ) for each house in 3 investigated regions.

Location	Day	Region		
		City of Johannesburg	City of Tshwane	Ekurhuleni
House 1	1	120.0	120.0	120.0
	2	120.0	120.0	120.0
House 2	1	120.0	120.0	120.0
	2	120.0	120.0	120.0
House 3	1	130.0	110.0	120.0
	2	120.0	120.0	120.0
	Mean	121.7	118.3	120.0
	SD	4.1	4.0	0.0

### 3.4 Indoor $^{222}\text{Rn}$ measurements in homes and schools around Western Cape

#### 3.4.1 Campaign-C description

This section deals with the indoor measurement of  $^{222}\text{Rn}$  gas in schools and homes. The approach strategies for gaining access to conducting surveys in homes and schools are well discussed. The main aim of this campaign was to

- do short-term indoor  $^{222}\text{Rn}$  measurements in homes and schools and
- to investigate the correlation between indoor  $^{222}\text{Rn}$  gas and the surrounding soil/geology.

#### 3.4.2 Selected study area

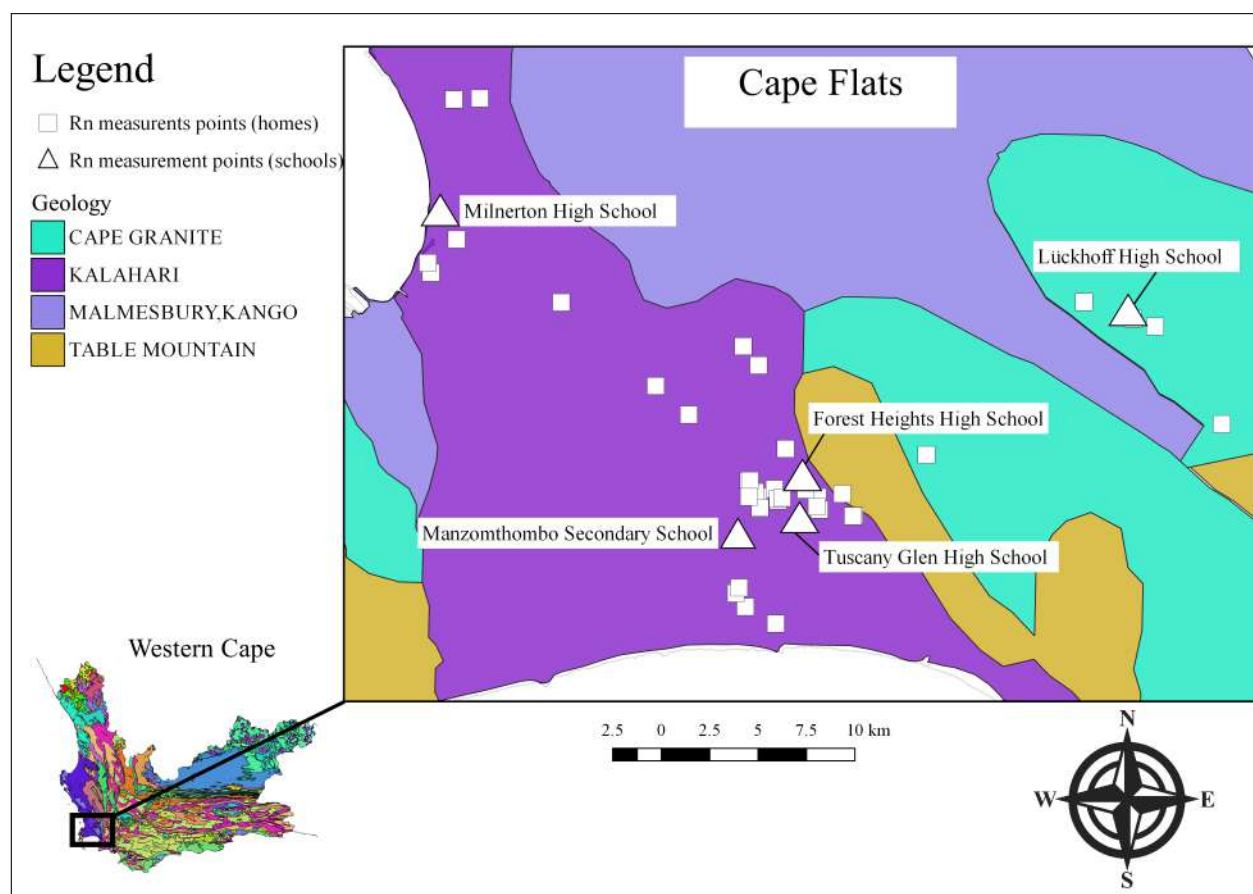


Figure 3.20: Western Cape map showing the geology.

The Western Cape is one of the nine provinces in South Africa with an estimated population of 7 million in 2020. The province is divided into 6 districts namely Cape Winelands, Central Karoo, City of Cape Town, Garden Route, Overberg and West Coast. The elevation ranges from the lowest of 0.0 m to the highest of 2325.0 m, as the Western Cape is largely covered with mountains. Western Cape geology consists of Bokkeveld, Cape granite, Kalahari, Malmesbury, Kango, Gariiep, Table Mountain and Witteberg.

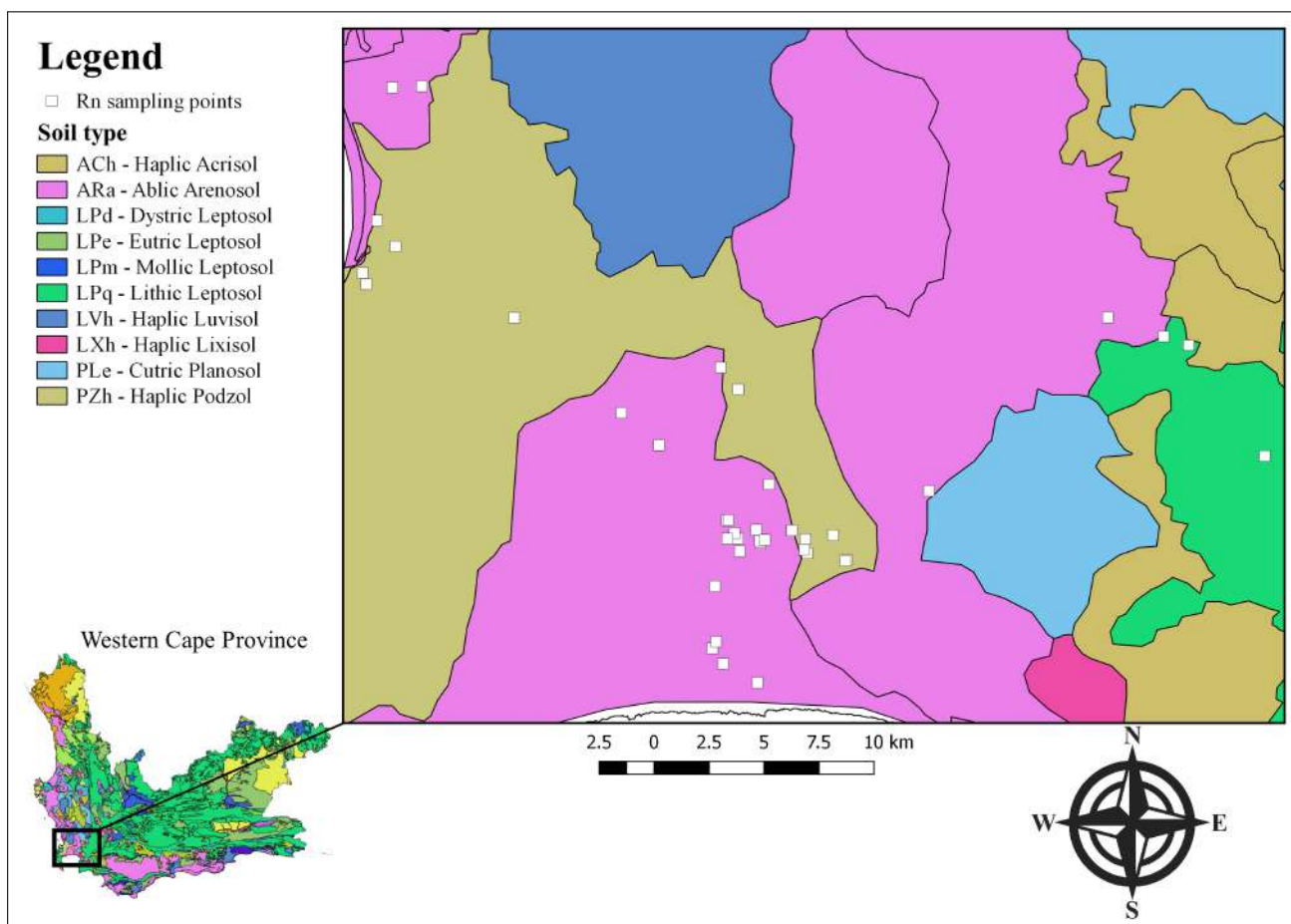


Figure 3.21: Western Cape map showing the radon locations in homes and schools.

The study campaign was only conducted in schools and homes around the City of Cape Town and Cape Winelands regions. The importance of the campaign arises from the fact that these regions are heavily populated. The inhabitants of these regions comprise about 50% of the total population in Western Cape province. Hence it is necessary to investigate the indoor  $^{222}\text{Rn}$  gas in homes and schools around these areas.

### 3.4.2.1 School selection and recruitment processes

In the initial phase of the survey, 10 schools were targeted around the City of Cape Town and the Cape Winelands region. The selection of schools was based on the geology and the population density of the area where the school is located. A total of 10 schools were identified around the City of Cape Town and Cape Winelands. The ethical clearance for conducting the radon survey in school and homes was approved by Stellenbosch University in June 2019. The permission for the recruitment of schools was obtained from the Western Cape Education Department (WCED).

For a selected school, the school principal was invited by e-mail (obtained from the WCED database) to have his/her school participate in the project. The principal was asked to identify five school learners and one school teacher from the school with the following criteria. A participant must

- be in grade 10 or 11 science-stream class
- reside in the vicinity of the school (not more than 5 km away from school).

After the principal agreed for the school to participate, the informed consent form was sent to the principal. Then the principal was asked to distribute the consent forms to the school learners and the teachers. After the learner has agreed to participate in the survey, the learner was given an informed-consent form to give their parents/guardians at home. All participants were asked to give information about their names, age, address and phone numbers. This information was used to organise the transport and the venue where the outreach was held.

### 3.4.2.2 School outreach arrangements

After knowing the number of participants, a venue to meet with the learners was secured. The aim was to assemble all the participants in one venue on the days of an event. iThemba LABS (a National Research Foundation facility, [www.tlabs.ac.za](http://www.tlabs.ac.za)) was approached to make its auditorium and computer laboratory available for the outreach event. The proposal was approved and the event dates were arranged. The management team at iThemba LABS also assisted with

the transportation of the participants from and to their schools. Catering was also arranged for all the participants.

### 3.4.3 Distribution and collection of radon detectors

Day 1 of the event was held at the iThemba LABS on Saturday 31<sup>st</sup> August 2019. A total of forty learners and eight school teachers participated in the outreach programme. All participants signed the attendance register at the beginning each day of the event. The school outreach program lasted for 6 hours. During the program, learners were introduced to the survey program through presentations on radon and the project details.

Instructions on how to handle and deploy the radon detectors was presented to the participants. Afterward, initial voltages were measured from each short-term electret using a SPER voltage reader. Since there was a large number of participants, they were divided into two groups and two SPER voltage readers were used for reading out the voltage on the electrets. The initial voltage on each short-term electret was measured three times and the serial number on the electret was also noted. Then a short-term electret was carefully screwed into the S-chamber to form SST (EIC).

Each learner received a closed SST (EIC) to take home and each teacher received three SST (EICs) to deploy at his/her school. Each participant also received a questionnaire and an information sheet on how to deploy a radon detector. To ensure that each participant followed a correct procedure to deploy the detector, the participant was asked to take photographs of the location and the radon detector before and after deployment. The participants were asked to open the radon detector as soon as they get back to their homes. A total of 46 SST radon detectors were distributed and were deployed in homes and schools in the selected regions.

The participants returned on day 2 (7<sup>th</sup> September 2019), the final day of the outreach event which was held. At the beginning of an event, the method of calculating the radon concentrations was presented to the participants. The participants were then divided into two groups. Each participant returned the closed SST radon detector and the questionnaire in the same order as day 1. For each participant, a short-term electret was unscrewed from the S-chamber and the final voltage was immediately measured three times with the SPER voltage reader. As a part

of the school outreach activity, the participants were engaged in the calculation of indoor radon for their homes and schools. The participants were then grouped according to their respective schools. Each group was given access to the iThemba LABS computer laboratory in order for it to calculate radon levels using Microsoft EXCEL and to prepare a presentation on findings using Microsoft Powerpoint. The event closed with each group making a presentation in the auditorium on its work.

## 4 Results and Discussion

### 4.1 Campaign A: Results of indoor radon concentration in homes, schools and workplaces

#### 4.1.1 Campaign A1: results of indoor radon concentration in workplaces.

A total of 18 SST were deployed in a big laboratory (room 2024) located in the Merensky building at Stellenbosch University to test the impact of building materials (walls) and height (ceilings). To test the effect of building walls on indoor radon, the five radon detectors were placed close to the wall (<0.5 m) and the four radon detectors were placed in a room corner. To measure the indoor radon concentration as a function of height, four radon detectors were deployed in a vertical position at various heights ranging from 1.5 m to 3.3 m from the floor. Five detectors were placed on a table. The measurements were conducted for a week and a summary of the results of these measurements is shown in Figure 4.1 and presented in Table 4.1.

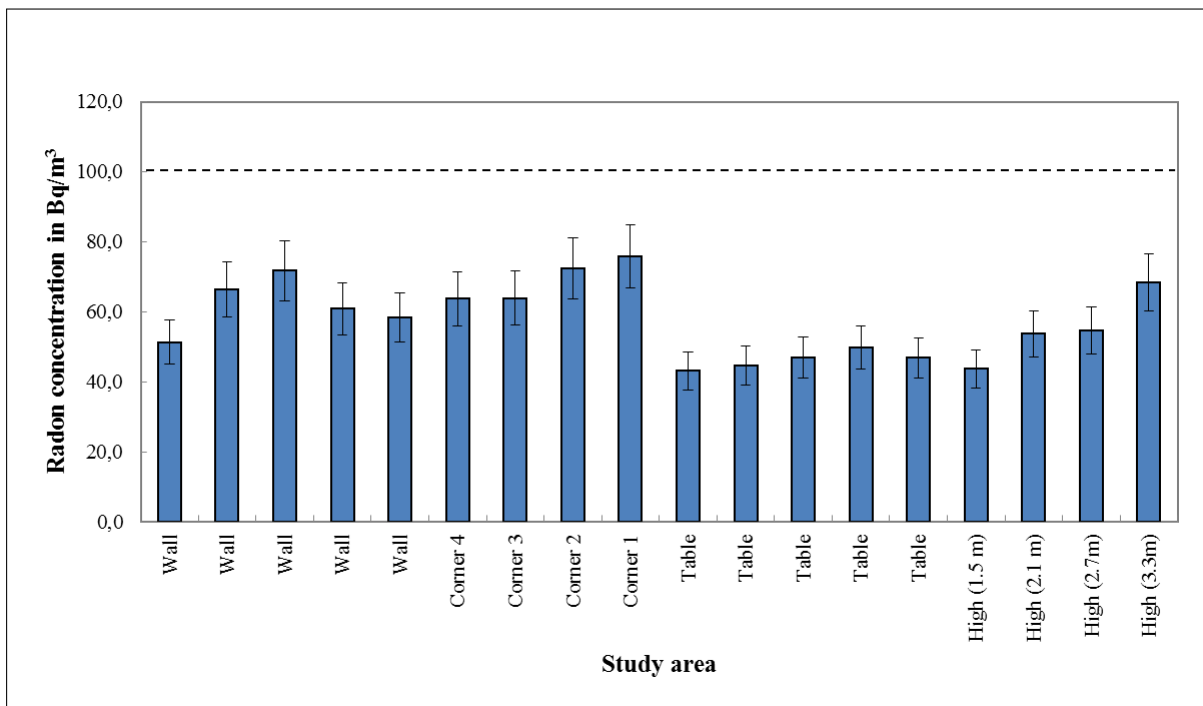


Figure 4.1: Indoor radon concentration as a function of walls and height.

Table 4.1: Summary statistics for data in Figure 4.1.

Descriptive Statistics	Radon concentration (Bqm <sup>-3</sup> )		
	Wall	Corner wall	Table
Mean	61.8	69.0	46.3
Standard Error	3.5	3.1	1.1
Median	60.9	68.2	46.9
Standard Deviation	7.8	6.2	2.5
Sample Variance	60.4	38.1	6.3
Kurtosis	-0.3	-4.4	-0.2
Skewness	-0.1	0.3	0.1
Range	20.4	12.3	6.6
Minimum	51.4	63.7	43.1
Maximum	71.8	76.0	49.7
No of data	5.0	4.0	5.0
Confidence Level(95.0%)	9.6	9.8	3.1

All radon levels were below the action level of 100 Bqm<sup>-3</sup> recommended by WHO (indicated by a black dashed line in Figure 4.1). The radon concentration close to a wall ranged from 51.4 ± 6.3 Bqm<sup>-3</sup> to 71.8 ± 8.5 Bqm<sup>-3</sup> with the mean of 61.8 ± 7.8 Bqm<sup>-3</sup>. The radon concentration in a corner wall ranged from 63.7 ± 7.7 Bqm<sup>-3</sup> to 76.0 ± 9.0 Bqm<sup>-3</sup> with a mean of 69.0 ± 6.5 Bqm<sup>-3</sup>. The radon concentration on the table ranged from 43.1 ± 5.4 Bqm<sup>-3</sup> to 49.7 ± 6.1 Bqm<sup>-3</sup> with the mean of 46.3 ± 2.5 Bqm<sup>-3</sup>.

A comparison between the results of radon concentration close to a wall and away from a wall, showed that the radon concentration close to a wall is greater than the radon concentration away from a wall. The obtained results were expected since the thoron <sup>220</sup>Rn, a natural radioactive decay whose half-life is short (T<sub>1/2</sub>=55.6 s) coming from the walls decays and reach the detector which contribute more when the radon detectors are placed close to a wall. The gamma radiation also contributes to the ionisation process in the radon chamber during measurements, as a result, more voltage in the electrets drops, and this accounts for an increased radon concentration.



The effect of building materials to indoor radon is also observed from the height results. The height results in Figure 4.1 show an increase in radon concentration as the height increases. At the height of 1.5 m, 2.1 m, 2.7 m and 3.3 m, the radon concentrations were found to be  $43.8 \pm 5.5 \text{ Bqm}^{-3}$ ,  $53.8 \pm 6.6 \text{ Bqm}^{-3}$ ,  $54.7 \pm 6.7 \text{ Bqm}^{-3}$  and  $68.5 \pm 8.2 \text{ Bqm}^{-3}$ , respectively. The result at 1.5 m was in the same range as the results on the table with a mean of  $46.3 \pm 2.5 \text{ Bqm}^{-3}$ . The results at 3.3 m showed an increased radon concentration since it was close to the ceiling. In this case, the thoron source is presumably the materials in the ceiling.

The results for radon concentration in workplaces (offices and laboratories) is shown in Figure 4.2 and presented in Table 4.2.

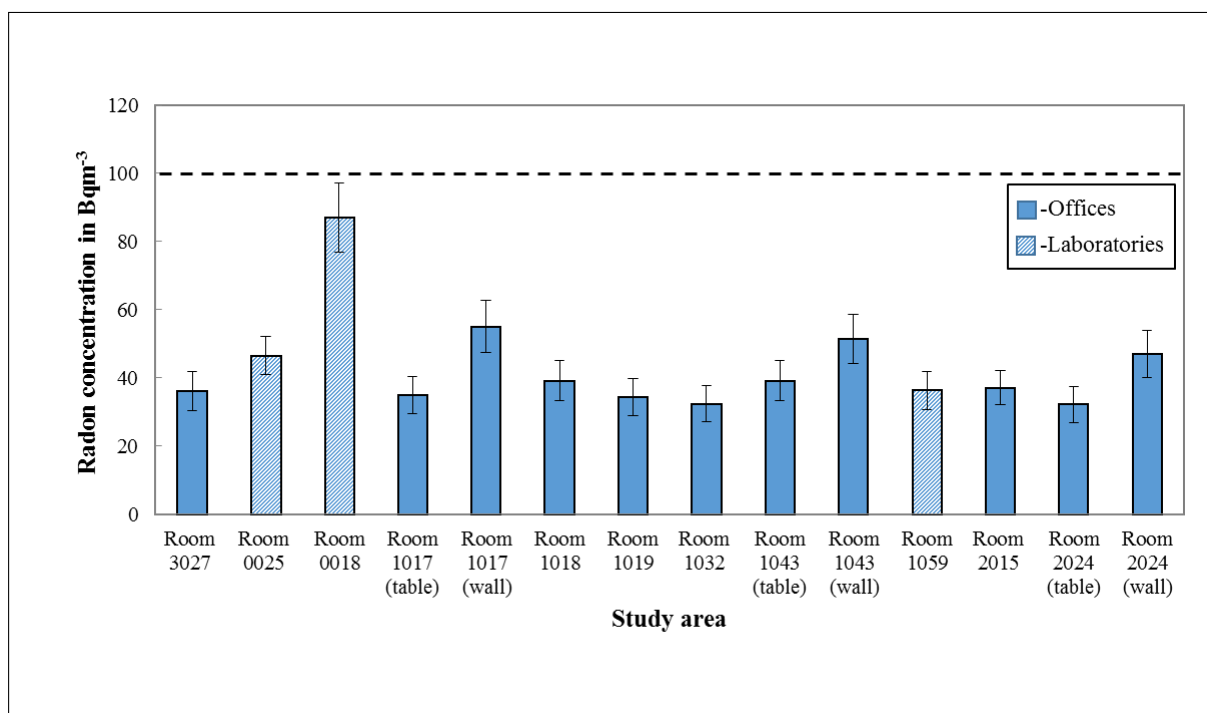


Figure 4.2: Radon levels in offices and laboratories located at Stellenbosch University.

Table 4.2: The radon levels in different locations.

Places	No. of measurements	Radon concentration ( $\text{Bqm}^{-3}$ )		
		Minimum	Average	Maximum
Offices	8	$32.2 \pm 5.2$	$35.7 \pm 2.7$	$39.2 \pm 5.9$
Laboratories	3	$36.3 \pm 5.7$	$56.6 \pm 26.8$	$87.0 \pm 10.1$
Tables	3	$32.2 \pm 5.2$	$35.4 \pm 3.5$	$39.2 \pm 5.9$
Walls	3	$47.1 \pm 6.9$	$51.2 \pm 3.9$	$55.0 \pm 7.7$

All radon levels were below the action level of  $100 \text{ Bqm}^{-3}$ , the highest radon concentration was measured inside the laboratory (room 0018) which is normally kept closed with no ventilation. The value there was  $87.0 \pm 10.1 \text{ Bqm}^{-3}$ . The results of radon levels in offices ranged from  $32.2 \pm 5.2 \text{ Bqm}^{-3}$  to  $35.7 \pm 2.7 \text{ Bqm}^{-3}$  with a mean of  $39.2 \pm 5.9 \text{ Bqm}^{-3}$ . These levels are considered safe because it is below the EU action level of  $100 \text{ Bqm}^{-3}$ . In three offices, two detectors were deployed in each office. One detector was placed close to the wall and one on the table. The results of radon concentration were compared and it was observed that the results from the detectors close to the wall were higher than the results of the detectors on the tables.

#### 4.1.2 Campaign A2: a comparison results between E-PERM and ParcRGM systems

A comparative assessment of several integrating detector types was undertaken during winter (March 2020 - July 2020). The track-etch detectors from ParcRGM were deployed parallel with electret detectors (E-PERM) from RadElec for more than 3 months. Different configurations were used for E-PERM, involving both long-term and short-term electrets. The measurements were conducted at different locations in the same building, and another set of measurements was conducted inside a house. The results for each location are shown from Figure 4.3 to Figure 4.8.

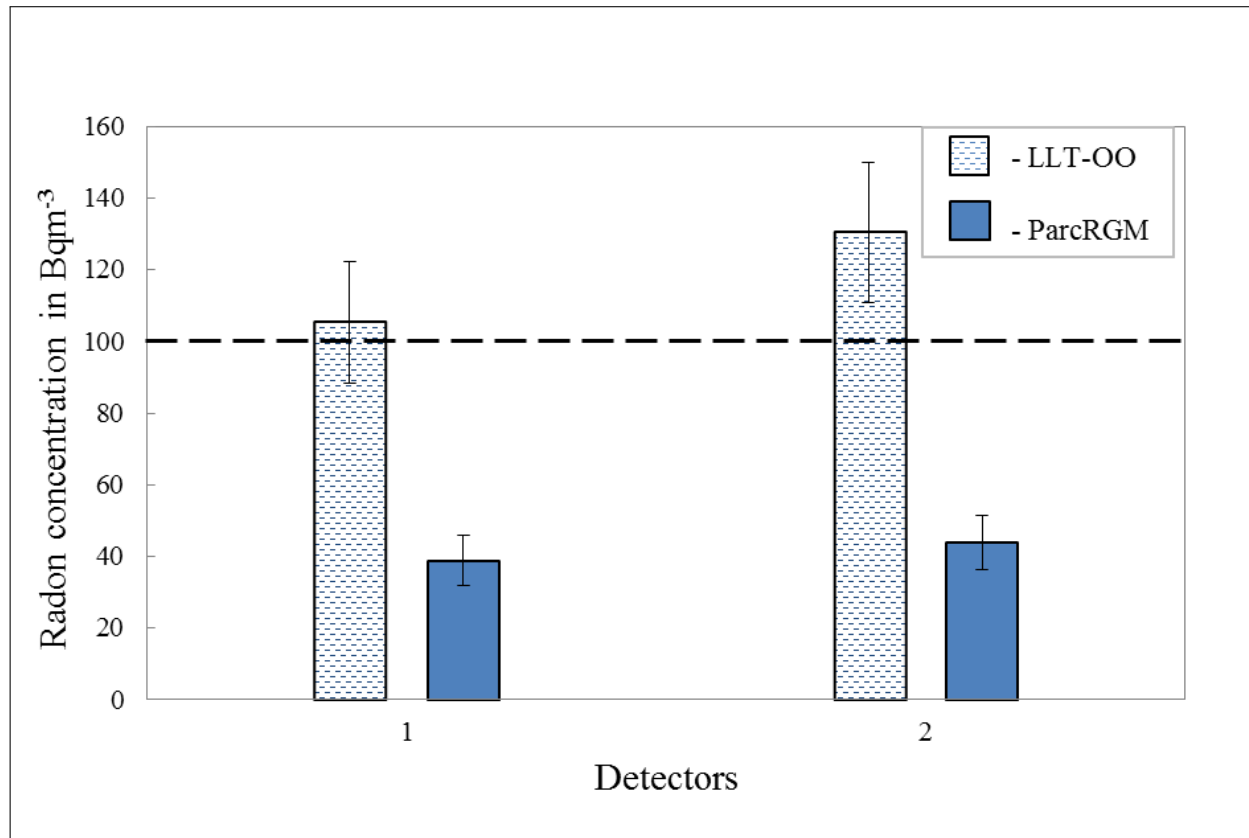
**Location 1: Room 2026 Merensky building, Stellenbosch University.**

Figure 4.3: Results of two sets of LLT-OO and ParcRGM.

A comparison between LLT-OO results and those of ParcRGM showed that the average radon concentration was measured to be  $117.9 \pm 17.7 \text{ Bqm}^{-3}$  and  $41.5 \pm 3.6 \text{ Bqm}^{-3}$ , respectively. The relative difference between the two means was calculated to be 64.8%.

**Location 2: Room 1059 (Health Physics Laboratory) Merensky building, Stellenbosch University.**

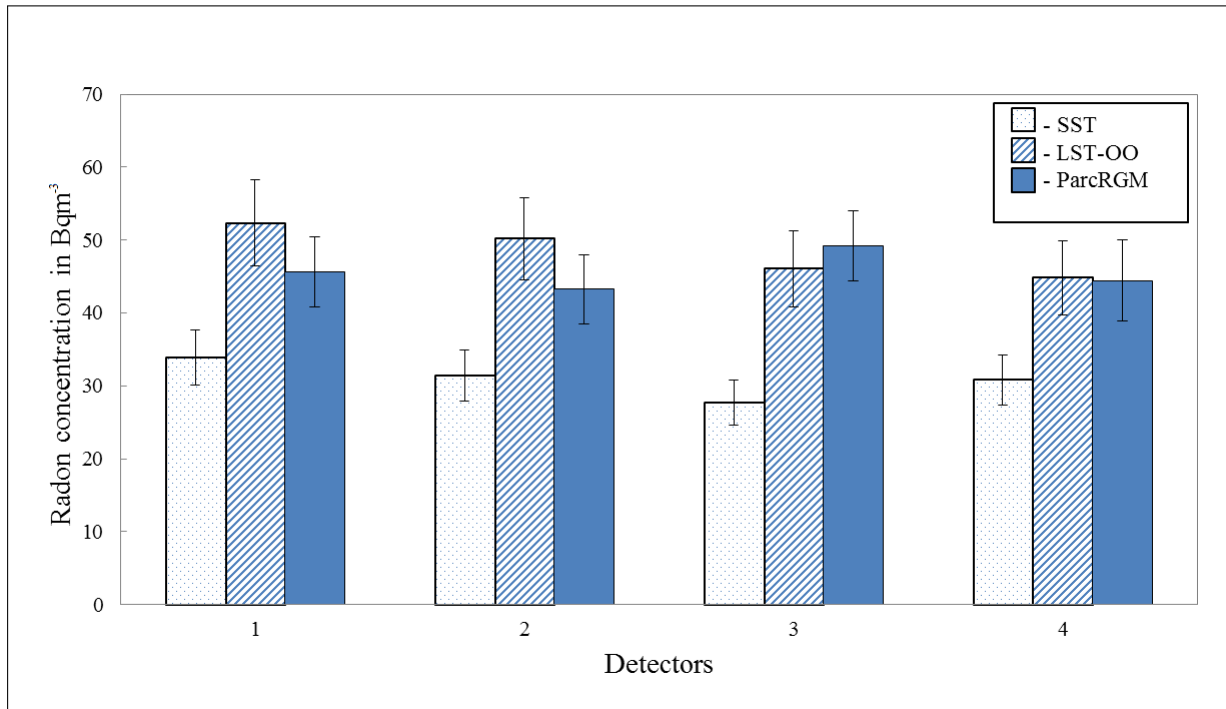


Figure 4.4: Results of SST, LST-OO and ParcRGM.

A comparison between SST, LST-OO and ParcRGM results showed that the average radon concentration was measured to be  $30.9 \pm 2.6 \text{ Bqm}^{-3}$ ,  $48.4 \pm 3.5 \text{ Bqm}^{-3}$  and  $45.6 \pm 2.6 \text{ Bqm}^{-3}$ , respectively. The percentage difference between the three obtained averages are presented in Table 4.3. The lowest percentage difference of 5.6% was recorded between the LST-OO and ParcRGM. The results of indoor radon obtained from LST-OO and ParcRGM detectors were consistent within measurement uncertainties. This is expected since both detectors were designed to measure radon for more than three months.

Table 4.3: The relative percentage difference between the detectors in room 1059.

	SST	LST-OO	ParcRGM
SST	0	-	-
LST-OO	36.1	0	-
ParcRGM	32.2	5.63	0

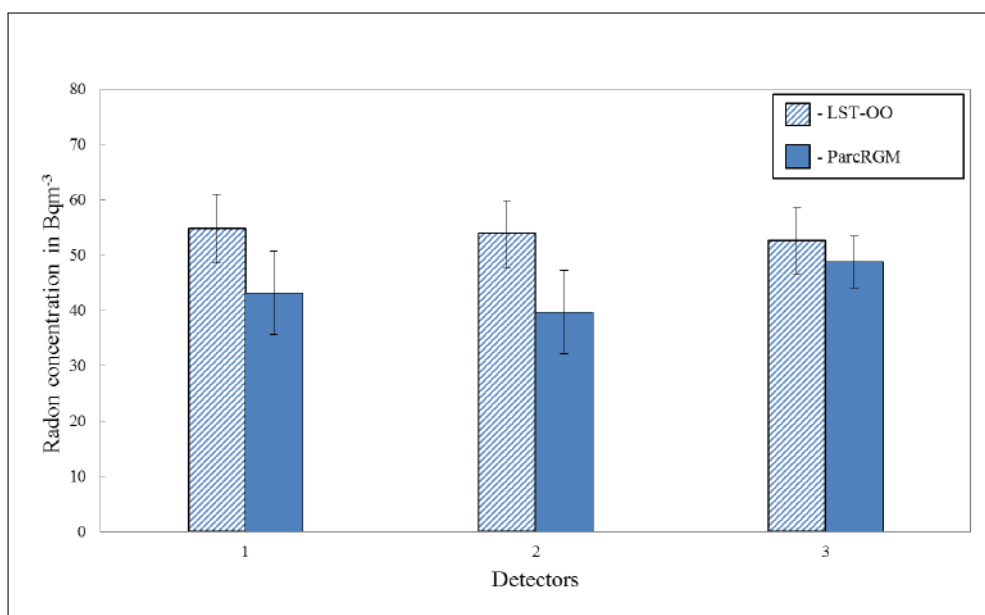


Figure 4.5: Results of LST-OO and ParcRGM deployed in parallel and placed next to the wall (&lt;0.5 m).

Figure 4.5 show the results of indoor radon gas between the LST-OO and ParcRGM, with a mean of  $53.8 \pm 1.1 \text{ Bqm}^{-3}$  and  $43.9 \pm 4.6 \text{ Bqm}^{-3}$ , respectively. The average LST-OO result was 18.3% higher than the average ParcRGM result. The results of LST-OO measurements adjacent to a wall were 10% more than the average results of LST-OO measurements on the table since the thoron from the walls contribute more when the radon detectors are placed close to a wall. Whereas, the average radon concentration of ParcRGM close to a wall was 3.8% less than the average radon concentration of ParcRGM in the table was because the detectors were deployed closer to the wall which prevented enough radon gas and its product from flowing into the detectors.

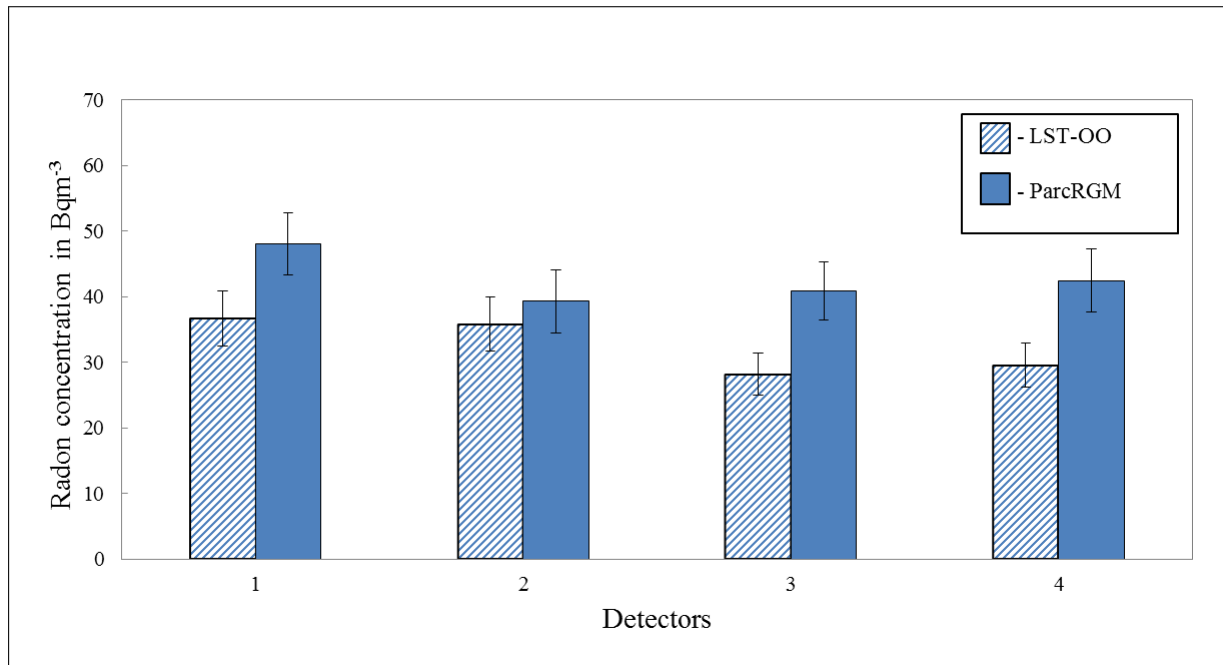
**Location 3: Room 2020 Merensky building, Stellenbosch University**

Figure 4.6: Results of LST-OO and ParcRGM in room 2024.

Figure 4.6 show the results of indoor radon gas between the LST-OO and ParcRGM, with a mean of  $32.6 \pm 4.3 \text{ Bqm}^{-3}$  and  $42.7 \pm 3.8 \text{ Bqm}^{-3}$ , respectively. The average ParcRGM result was 23.6% higher than the average LST-OO result.

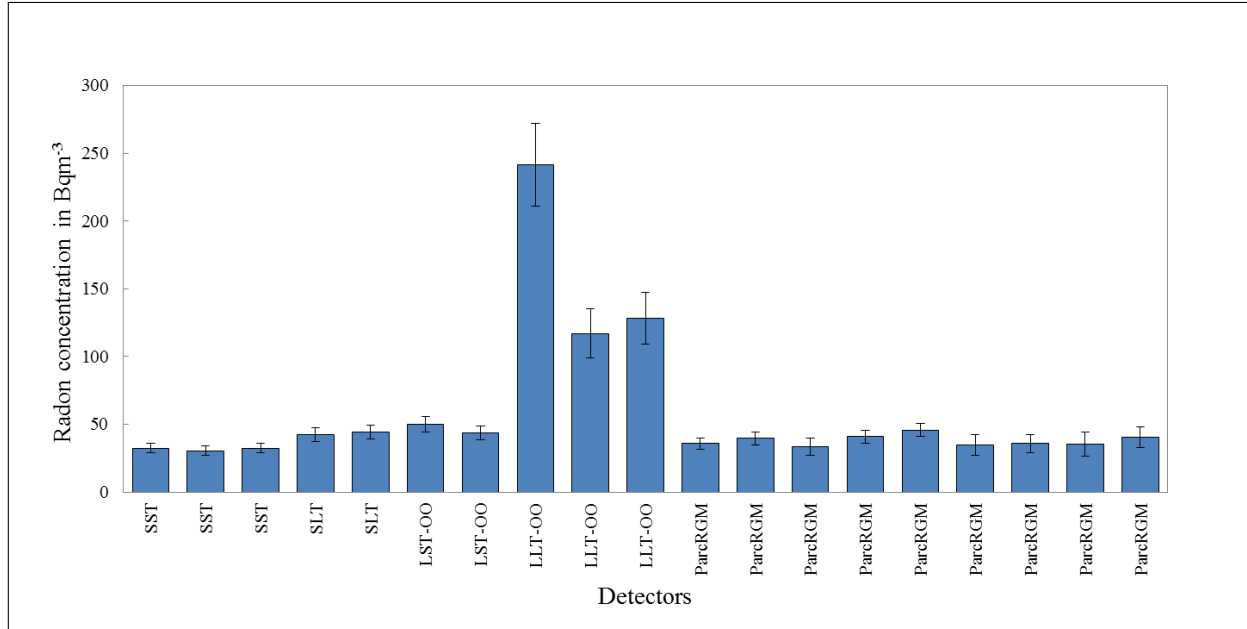
**Location 4: Room 2024 Merensky building, Stellenbosch University.**

Figure 4.7: Results showing of two LST-OO , three LLT-OO, three SST, and two SLT that were deployed along with nine ParcRGM.

Figure 4.7 show the results of indoor radon gas between the SST, SLT, LST-OO, LLT-OO and ParcRGM, with a mean of  $31.9 \pm 1.1 \text{ Bqm}^{-3}$ ,  $43.5 \pm 1.3 \text{ Bqm}^{-3}$ ,  $46.8 \pm 4.2 \text{ Bqm}^{-3}$ ,  $162.4 \pm 68.9 \text{ Bqm}^{-3}$  and  $38.0 \pm 3.9 \text{ Bqm}^{-3}$ , respectively. The relative difference was calculated between the detectors and presented in Table 4.4. When different configurations of E-PERM compared to ParcRGM, the lowest percentage difference for SLT and LLT-OO was 12% and the highest of 76.6%, respectively.

Table 4.4: The relative percentage difference between the detectors in room 2024.

	SST	SLT	LST-OO	LLT-OO	ParcRGM
SST	0.0	-	-	-	-
SLT	26.8	0.0	-	-	-
LST-OO	31.9	7.0	0.0	-	-
LLT-OO	80.4	73.2	71.2	0.0	-
ParcRGM	16.2	12.7	18.8	76.6	0.0

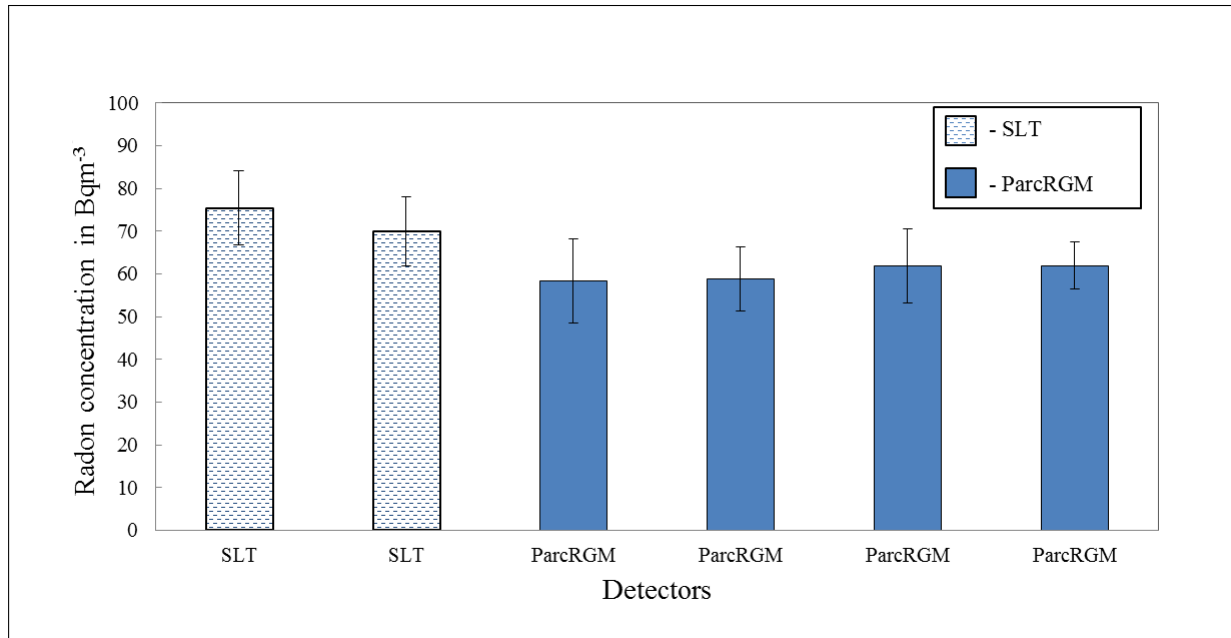
**Location 5: House in Stellenbosch.**

Figure 4.8: Results showing SLT and ParcRGM.

The results of the indoor radon concentration are shown in Figure 4.8. The mean between the SLT and ParcRGM was calculated to be  $72.6 \pm 3.9$  Bqm<sup>-3</sup> and  $60.2 \pm 2.0$  Bqm<sup>-3</sup>, respectively. The average SLT result was 17.1% higher than the average ParcRGM result.



### 4.1.3 Comparison between Airthings Wave and E-PERM

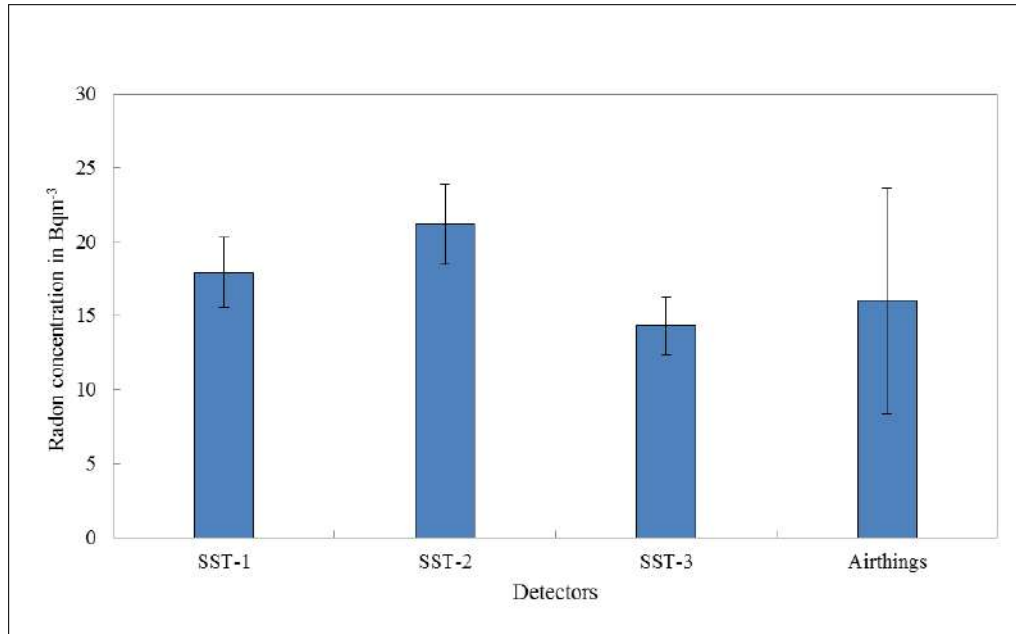


Figure 4.9: Results showing SST and Airthings radon detectors for a week measurement.

The results of indoor radon concentration are shown in Figure 4.9. The mean for the SST and Airthings radon detectors was calculated to be  $17.7 \pm 4.3 \text{ Bqm}^{-3}$  and  $17.3 \pm 7.6 \text{ Bqm}^{-3}$ , respectively. The average SST result was 0.5% higher than the average Airthings result.

### 4.1.4 Seasonal variation of indoor radon using EIC (SST)

The data was extracted from Figure 4.1 and Figure 4.9 to compare the indoor radon concentration for summer and winter, respectively. These measurements were taken in the same location (room 2024 Merensky building, Stellenbosch University) and were deployed for a week. The mean for summer and winter were found to be  $17.8 \pm 3.4 \text{ Bqm}^{-3}$  and  $49.9 \pm 6.0 \text{ Bqm}^{-3}$ , respectively. It was observed that winter radon levels were three times more than the radon concentration in summer. This indicates that radon levels are higher in the winter season since the doors and windows are always kept closed compared to in summer. This can be used to determine the seasonal correction factor. However, calculating seasonal corrective factors requires a large number of measurements; It is, therefore, preferable to perform year long measurements instead of correcting for measurements of shorter duration.

#### 4.1.5 Day and night variation of indoor radon using Airthings Wave

Figure 4.10 show the results of indoor radon concentration taken at home for a week. The hourly radon results were downloaded from the Airthings dashboard and then analysed using the EXCEL program. The results are shown in Figure 4.11 and presented in Table 4.5. The results show that indoor radon gas fluctuates and is not uniformly distributed since detector 1 measured a lower average for indoor radon levels when compared with detectors 2 and 3. The average percentage difference was calculated to be 8%. The results from detectors 2 and 3 were too close to one another. The mean value in detector 2 was 0.3% higher than the mean value in detector 3. The average concentration values for indoor radon measured from detector 1, 2 and 3 were  $28.7 \pm 12.1 \text{ Bqm}^{-3}$ ,  $31.3 \pm 16.5 \text{ Bqm}^{-3}$ , and  $31.2 \pm 12.3 \text{ Bqm}^{-3}$ , respectively.

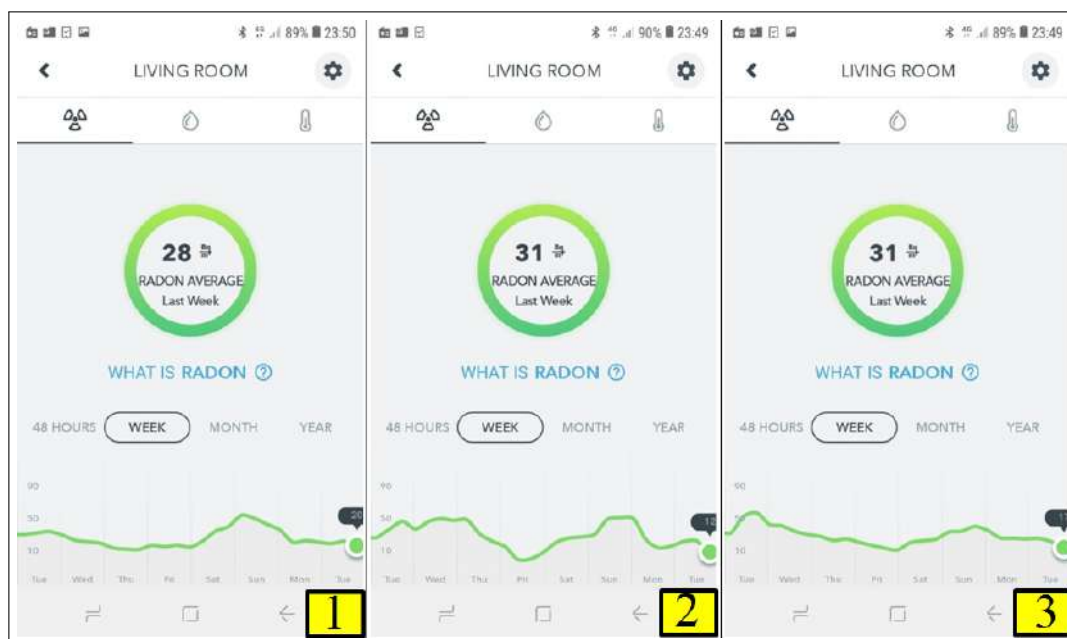


Figure 4.10: Screenshots taken from a smartphone showing weekly radon average levels for each detector.

Table 4.5: Descriptive statistics for each Airthings Wave radon detector.

Descriptive statistics			
	Detector 1	Detector 2	Detector 3
Mean	28.7	31.3	31.2
Standard Error	0.9	1.2	0.9
Median	25.0	29.0	29.0
Mode	22.0	25.0	28.0
Standard Deviation	12.1	16.5	12.3
Sample Variance	145.6	273.1	150.9
Kurtosis	0.4	-1.1	0.5
Skewness	0.9	0.1	0.6
Range	61.0	59.0	59.0
Minimum	7.0	1.0	9.0
Maximum	68.0	60.0	68.0
Sum	5311.0	5786.0	5780.0
Count	185.0	185.0	185.0
Confidence Level(95.0%)	1.8	2.4	1.8

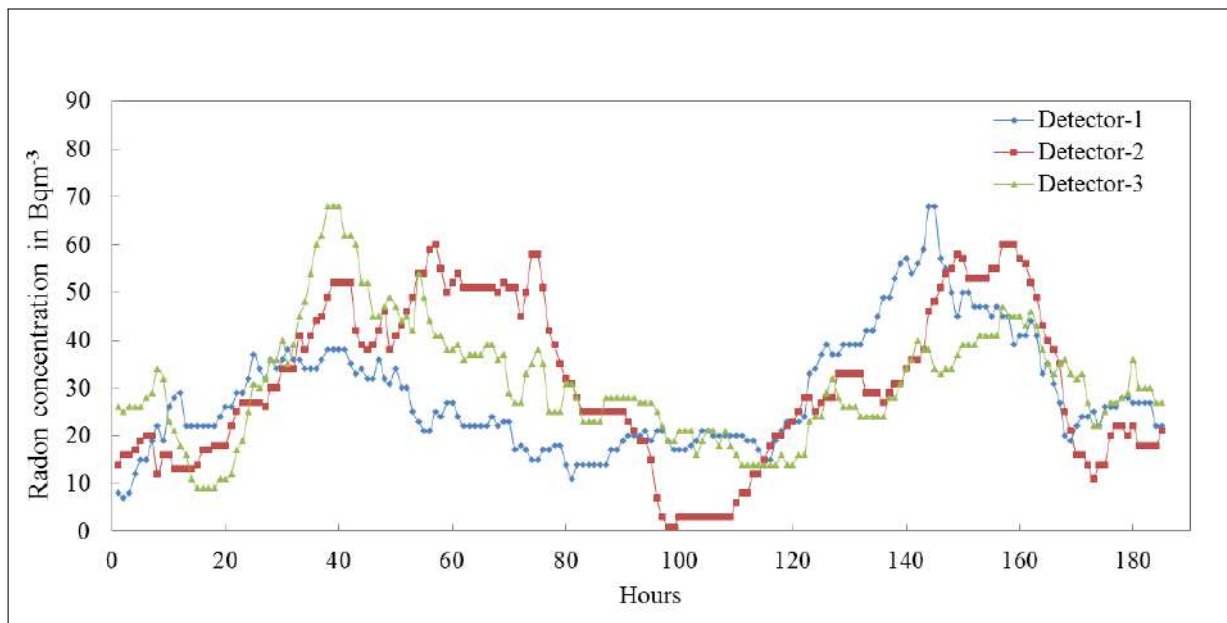


Figure 4.11: The indoor radon data plotted in EXCEL showing hourly measurements for each detector.

Table 4.6: Day and night results of indoor radon levels.

Day	Period	Radon level in Bqm <sup>-3</sup>
1	Day	18.7 ± 6.7
	Night	25.7 ± 7.6
2	Day	42.4 ± 8.9
	Night	43.9 ± 10.8
3	Day	35.2 ± 13.7
	Night	39.4 ± 13.0
4	Day	24.7 ± 9.2
	Night	20.9 ± 6.7
5	Day	13.9 ± 7.9
	Night	17.3 ± 4.7
6	Day	31.2 ± 5.6
	Night	40.3 ± 12.4
7	Day	39.7 ± 10.3
	Night	47.4 ± 7.5

The mean for indoor radon concentration was calculated from three Airthings detectors, and the day and night variation of indoor radon was investigated. The indoor radon concentration results for day and night are presented in Table 4.6. The weekly results indicated that the radon concentration was higher at night compared to during the day time. The increase of radon concentration at night is because of the higher exhalation rate of radon from soil. Another fact is that the radon accumulates indoors more during the night since windows and doors are closed and less radon escapes during the night. The weekly results show that for only 1 day out of 7 the radon concentrations was recorded to be higher during the day than during the night.

## 4.2 Campaign B: Results of $^{222}\text{Rn}$ from homes in Gauteng.

The results of indoor radon levels in Gauteng homes were divided into 10  $\text{Bqm}^{-3}$  bin range and plotted in the Frequency-Concentration plot, as shown in Figure 4.12. All radon levels were below the South African action level of  $300 \text{ Bqm}^{-3}$  recommended by NNR. The radon concentration in homes ranged from  $2.4 \pm 0.3 \text{ Bqm}^{-3}$  to  $102.5 \pm 11.7 \text{ Bqm}^{-3}$  with the mean of  $31.1 \pm 17.3 \text{ Bqm}^{-3}$  as presented in Table B.1 in Appendix B. Comparing the mean indoor radon concentration of this campaign to other studies done across the country reveals that the mean value was lower than the mean values obtained from existing studies in Gauteng [Leu02], and the obtained mean value is lower than the global average of  $40 \text{ Bqm}^{-3}$ .

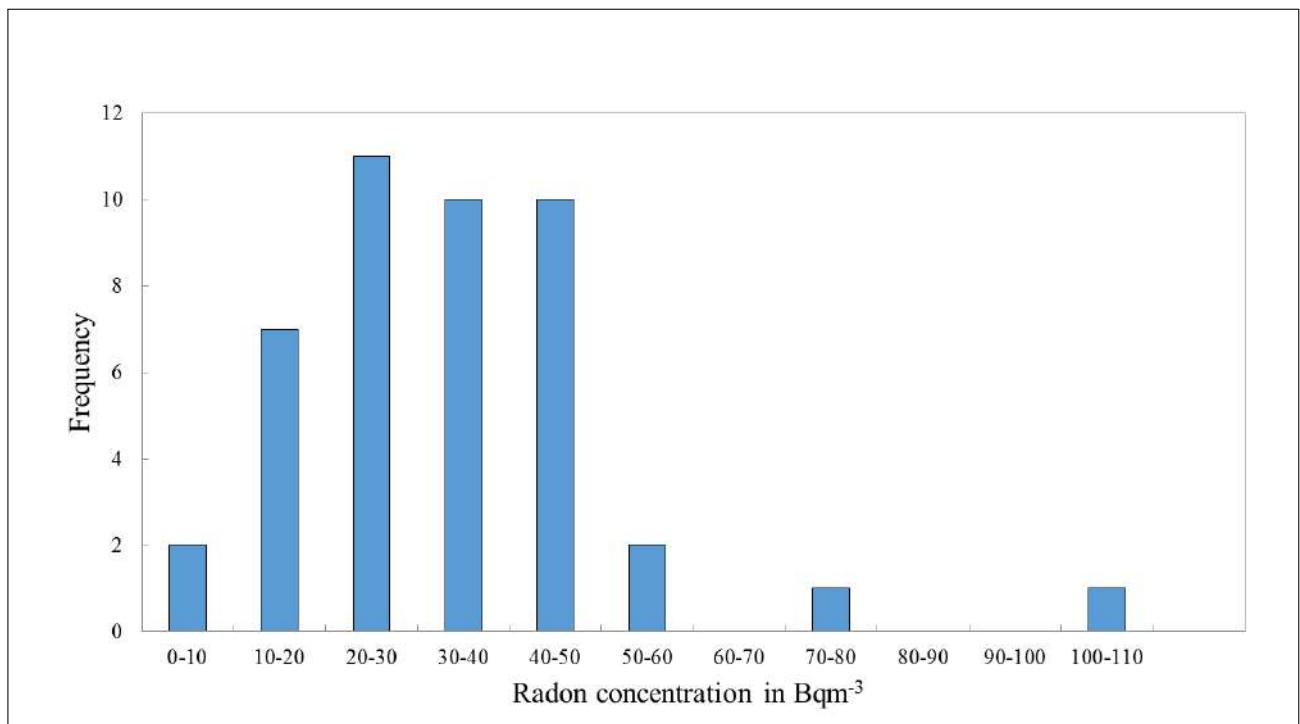


Figure 4.12: Frequency distribution of radon in homes around Gauteng.

Indoor radon concentrations often considered following a log-normal distribution, as shown in Figure 4.12. The distribution showed that 79.5% of data obtained from 44 measurement points have a radon concentration of less than  $40 \text{ Bqm}^{-3}$ . Whereas, only one location reported radon concentration above the action level of  $100 \text{ Bqm}^{-3}$  recommended by WHO, as shown in Figure 4.13.

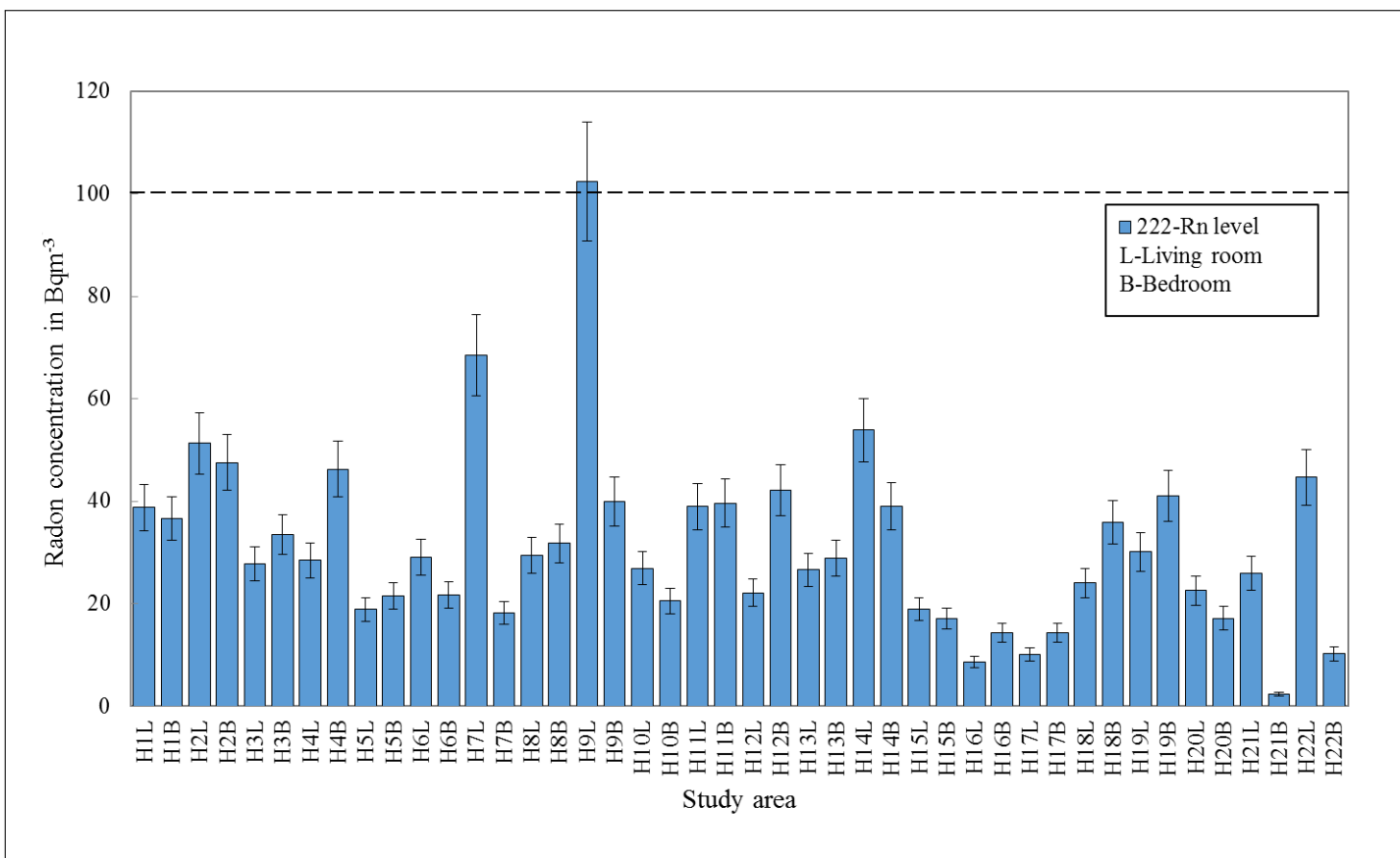


Figure 4.13: Radon concentrations in living rooms and bedrooms.

The minimum and maximum values in the living rooms were measured to be  $8.7 \pm 1.1 \text{ Bqm}^{-3}$  and  $102.5 \pm 11.7 \text{ Bqm}^{-3}$ , respectively. The maximum value was measured in the living room (1<sup>st</sup> floor) of a 16-year old brick house with floor tiles as shown in Table B.1[House9] in Appendix B. The minimum and maximum values in the bedrooms were measured to be  $2.4 \pm 0.3 \text{ Bqm}^{-3}$  and  $47.6 \pm 5.5 \text{ Bqm}^{-3}$ , respectively. The bedrooms and living rooms values are mostly within the error bars. Apart from the levels in [House7] and [House9].

The linear regression analysis for indoor radon concentrations in the living rooms and bedrooms indicated no strong correlation with the coefficient of determination of  $R^2 = 0.18$ , as indicated in Figure 4.14. The results show that indoor radon concentration can vary in the different rooms of the same house. Since indoor radon gas comes from the building materials, and the building materials used for construction are different from one room to another, difference could also be due to different ventilation.

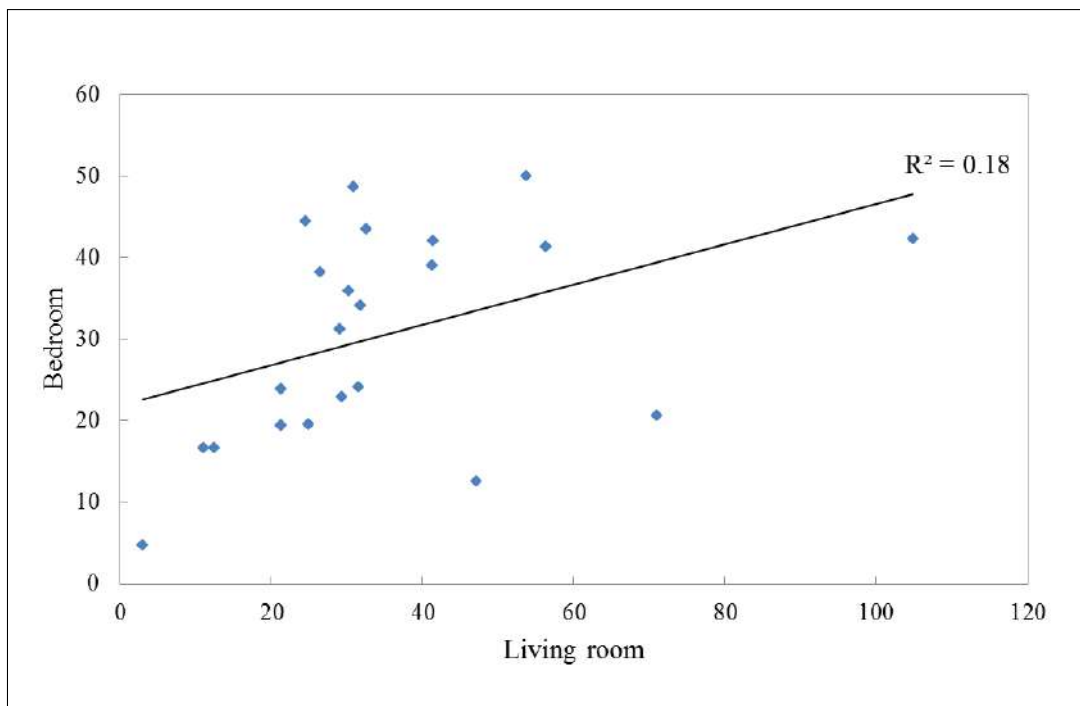


Figure 4.14: Linear regression of the relationship between indoor radon concentration in living rooms and bedrooms for 22 homes.

Figure 4.15 shows a box-plots for indoor radon concentration as a function of floor (left) and house type (right), respectively. The box shows the median (long horizontal line) and values

between the 25 and 75% percentiles. The short horizontal lines describe the values between 10 and 90% percentiles. The dots represent the highest values obtained. The box-plots show that indoor radon gas was higher in brick houses relative to shack houses. The average radon concentration was found to be  $36.9 \pm 13.1 \text{ Bqm}^{-3}$  for brick houses and  $22.2 \pm 15.0 \text{ Bqm}^{-3}$  for shack houses. That is because radon content is mainly present in the sand and cement of the bricks. Moreover, the indoor radon concentration was higher in homes with tiles and concrete floors relative to homes with carpet floors. The average radon concentration was found to be  $37.9 \pm 14.1 \text{ Bqm}^{-3}$  for homes with tile floor and  $25.7 \pm 13.6 \text{ Bqm}^{-3}$  in the homes with concrete floor. However, the radon gas was recorded to be lower in houses with a carpeted floor with an average value of  $14.2 \pm 0.5 \text{ Bqm}^{-3}$ .

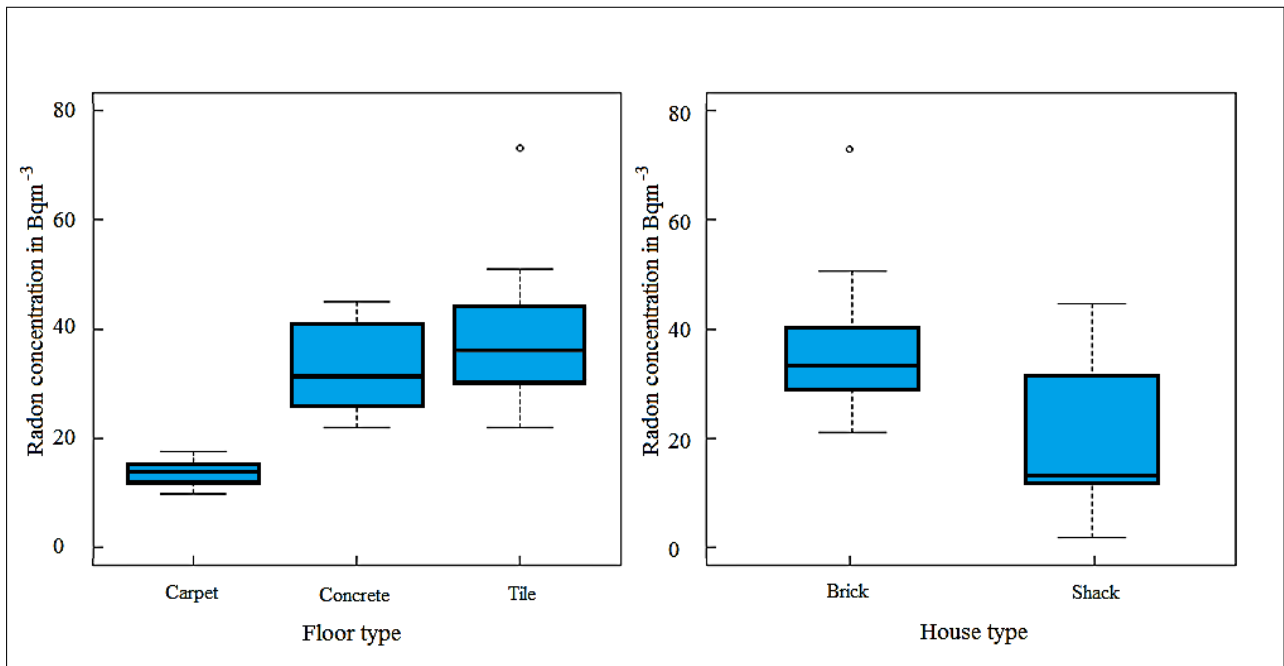


Figure 4.15: Box plots showing indoor radon concentration as a function of the building materials.

Since the value of indoor radon concentration is influenced by the geological conditions of the measurement area, the indoor radon was investigated as a function of the geological features such as soil types and underlying geology. The average of indoor radon concentration was calculated for each study region. For the City of Tshwane, the City of Johannesburg and the City of Ekurhuleni, the corresponding average indoor radon values were calculated to be  $39.4 \pm 15.1 \text{ Bqm}^{-3}$ ,  $23.5 \pm 12.6 \text{ Bqm}^{-3}$  and  $29.6 \pm 14.6 \text{ Bqm}^{-3}$ , respectively.



The 10 km × 10 km grid layer was created using the GIS for each region. Each grid presented all measurement points and the average indoor radon concentrations. The grid layer was overlaid on the geology and the soil type layer, as shown in Figure 4.16 and Figure 4.17. The maximum value was found to be in the City of Tshwane region with the underlying soil type classified as Lithic leptosol and the geology classified as Transvaal. However, the maximum value was below the global average of 40 Bqm<sup>-3</sup> [UNSO0]. The minimum value of indoor radon concentration was found to be in the City of Johannesburg region with the underlying soil type classified as Plinthic Acrisol and the geology classified as Transvaal and Sand river gneiss.

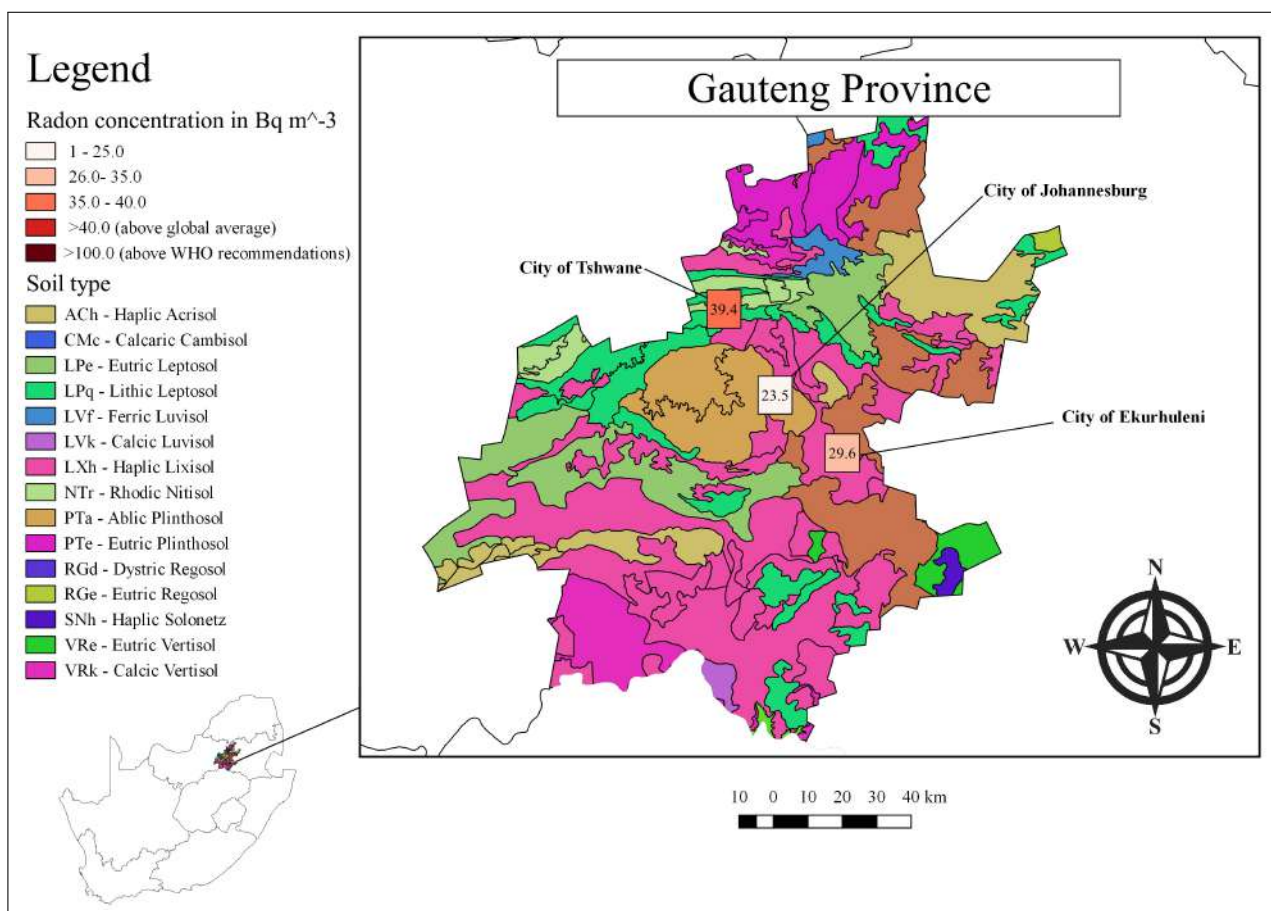


Figure 4.16: Average indoor radon concentration as a function of the surrounding soil type in the selected study areas.

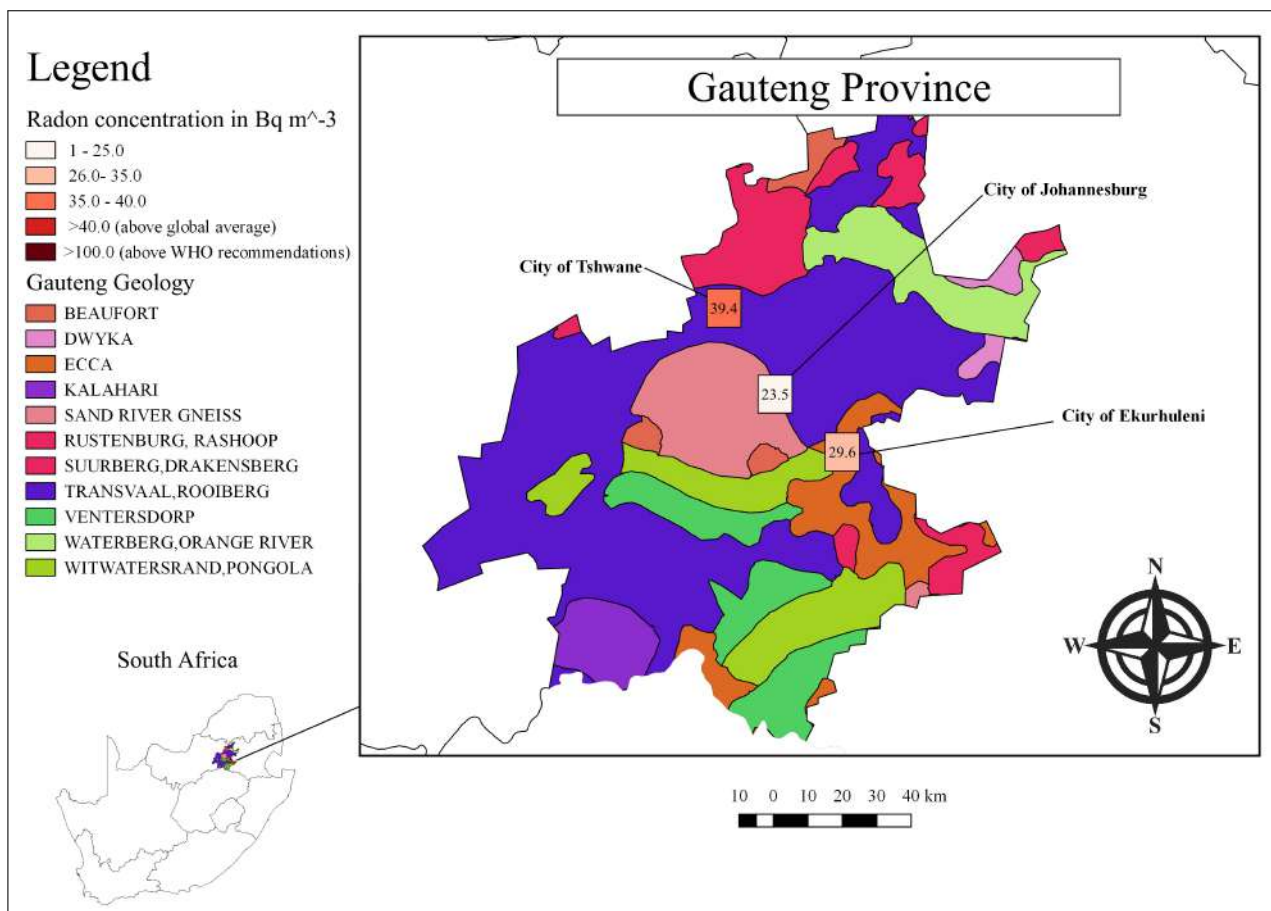


Figure 4.17: Average indoor radon concentration as a function of the surrounding geology in the selected study areas.

Similar geology features were found to be in the homes assessed for maximum [House9] and minimal [House21] indoor radon concentrations. In this case, no contribution to the indoor concentration is indicated by the geological features. It is, therefore, clear that the variation of indoor radon can be attributed to the surrounding soil type and types of construction materials used for the construction of the houses. However, the study conducted in Paarl showed a strong connection between the geology and indoor radon [Lin08]. Indoor radon concentrations were observed to be higher in the houses located less than 2 km away from the Paarl Mountain with granite outcrops, whereas the radon concentrations were observed to be lower in houses located more than 3 km from the Paarl Mountain as shown in Figure 4.18.

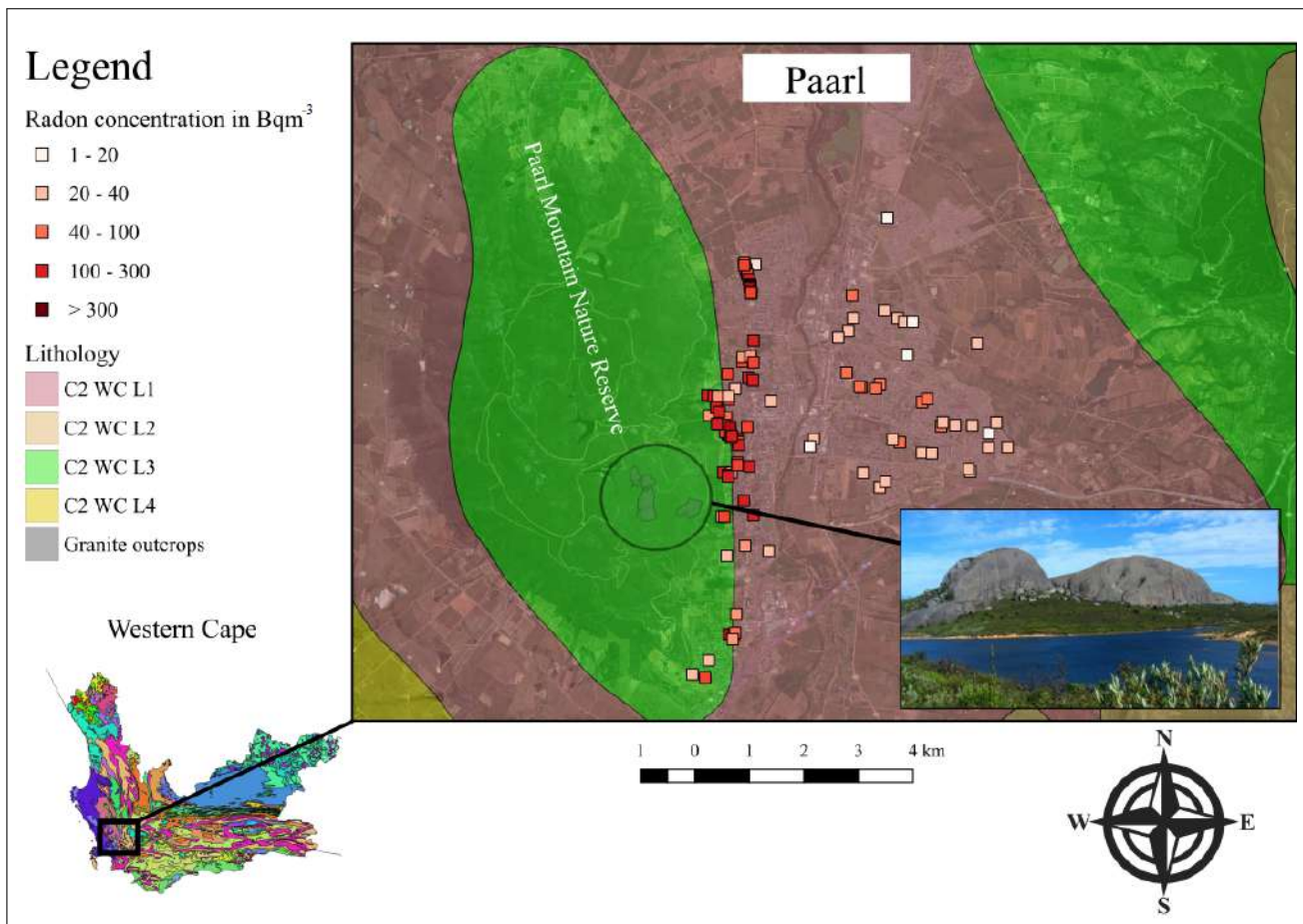


Figure 4.18: Indoor radon concentration as a function of the surrounding geology in Paarl area [Lin08].

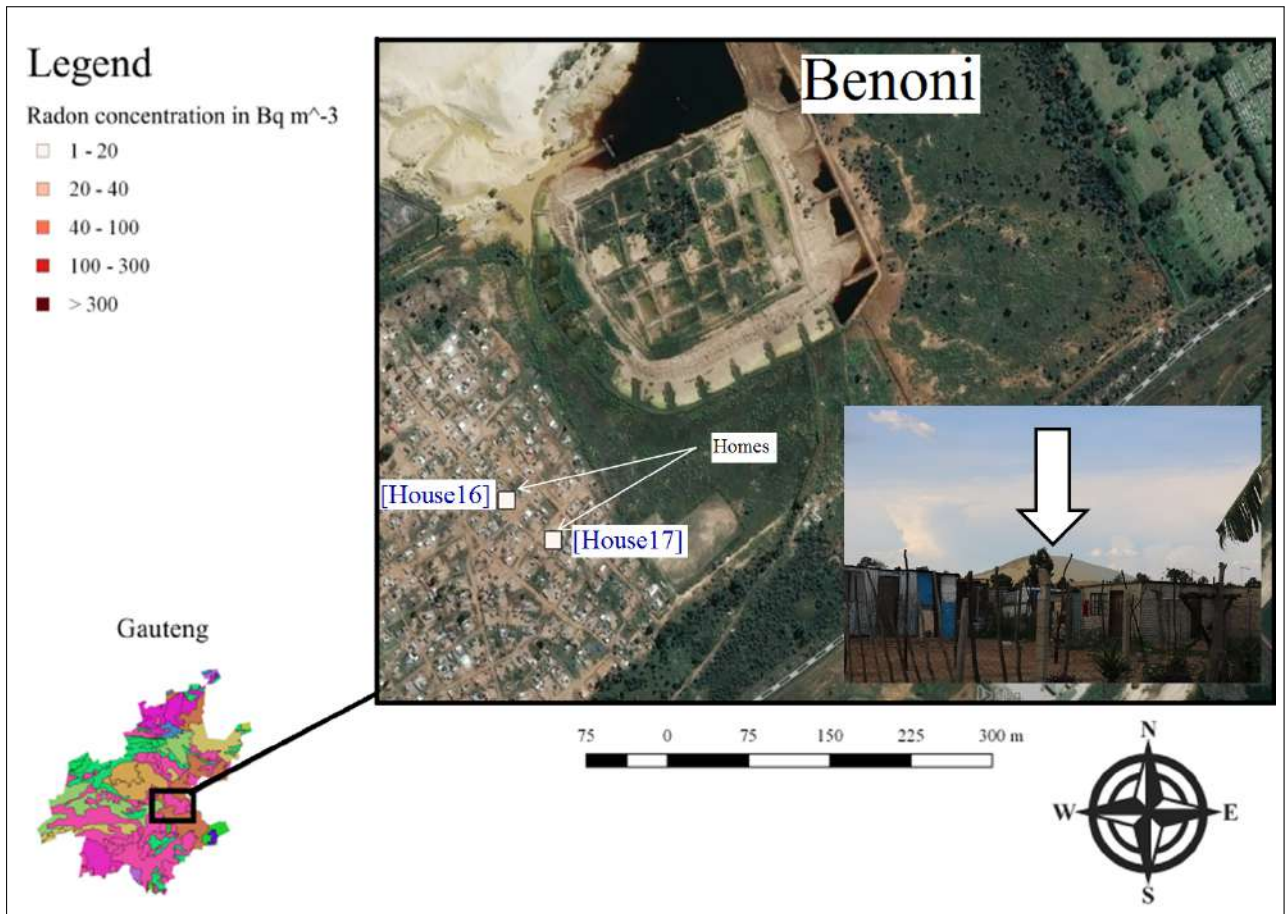


Figure 4.19: Indoor radon concentration in homes located next to mine area.

Figure 4.19 shows a map of homes located next to the mining area where two homes [House16 and House17] were surveyed. The indoor radon concentrations were observed to be relatively lower in both homes with the average values of  $11.5 \pm 4.0 \text{ Bqm}^{-3}$  and  $12.2 \pm 3.0 \text{ Bqm}^{-3}$ , respectively. The radon levels were expected to be higher since the houses are located next to mines. However, both homes were shacks built with corrugated metal and with carpet floors, which in turn may result in lower radon levels in these homes. It could also be due to more ventilation with shacks. This suggests that further measurements in brick homes near mine tailings will be useful.

The effect of gamma-ray background on indoor radon measurements using E-PERM was investigated. Equation 3.1 and equation 3.2 were used to calculate indoor concentration for following cases:

- gamma-ray background was not included;
- default gamma-ray background of  $32 \text{ Bqm}^{-3}$  was used;
- measured gamma-ray background using Graetz dosimeter and;
- elevation factor was taken into consideration.

Figure 4.20 shows the results for different cases using the information obtained from campaign A1 were the average gamma-ray background value was obtained to be  $80 \text{ nGyh}^{-1}$ . Figure 4.21 shows the results from campaign B were the average gamma-ray background value was obtained to be  $120 \text{ nGyh}^{-1}$ .

6	Electret type	Electret no	Location	D [day]	V <sub>i</sub>	V <sub>f</sub>	ΔV	CF	BG (μR/hr)	G	ElevCF	RnC (pCi/L)	RnC (Bq/m <sup>3</sup> )
7	Short term	SGJ 895	Wall	6,50	406	377	29	2,04	9,20	0,087	1	1,39	51,4
8	Short term	SGJ 841	Wall	6,50	382	348	34	2,02	9,20	0,087	1	1,79	66,4
9	Short term	SGJ 885	Wall	6,50	322	287	35	1,97	9,20	0,087	1	1,94	71,8

No background	Default background BG=32 Bqm <sup>-3</sup>	Measured background	Elevation factor
$RnC = 37 \times \left( \frac{V_i - V_f}{CF \times D} \right)$	$RnC = 37 \times \left( \frac{V_i - V_f}{CF \times D} \right) - 32 \text{ Bqm}^{-3}$	$RnC = 37 \times \left( \frac{V_i - V_f}{CF \times D} - (BG \times C_3) \right)$	$RnC = 37 \times \left( \frac{V_i - V_f}{CF \times D} - (BG \times C_3) \times ElevCF \right)$
81.0 Bqm <sup>-3</sup>	49.0 Bqm <sup>-3</sup>	51.4 Bqm <sup>-3</sup>	51.4 Bqm <sup>-3</sup>

Figure 4.20: Indoor radon concentration when using E-PERM system from campaign 1A.

6	Electret type	Electret no	Location	D	V <sub>i</sub>	V <sub>f</sub>	ΔV	CF	BG (μR/hr)	C <sub>3</sub>	ElevCF	RnC (pCi/L)	RnC (Bq/m <sup>3</sup> )
7	Short term	SLF 295	27 Mokwerekwere street	8,89	707	664	43	2,09	13,8	0,087	1,05	1,0	38,8
8	Short term	SLF 344	27 Mokwerekwere street	8,89	656	615	41	2,06	13,8	0,087	1,05	1,0	36,7
9	Short term	SLF 357	38 Mokwerekwere street	8,87	696	647	49	2,08	13,8	0,087	1,05	1,4	51,3

No background	Default background BG=32 Bqm <sup>-3</sup>	Measured background	Elevation factor
$RnC = 37 \times \left( \frac{V_i - V_f}{CF \times D} \right)$	$RnC = 37 \times \left( \frac{V_i - V_f}{CF \times D} \right) - 32 \text{ Bqm}^{-3}$	$RnC = 37 \times \left( \frac{V_i - V_f}{CF \times D} - (BG \times C_3) \right)$	$RnC = 37 \times \left( \frac{V_i - V_f}{CF \times D} - (BG \times C_3) \times ElevCF \right)$
85.6 Bqm <sup>-3</sup>	53.6 Bqm <sup>-3</sup>	41.2 Bqm <sup>-3</sup>	38.8 Bqm <sup>-3</sup>

Figure 4.21: Indoor radon concentration when using E-PERM system from campaign B.

### 4.3 Campaign C: Results of $^{222}\text{Rn}$ from homes and schools in Western Cape.

The indoor radon measurements were performed in 5 schools and 36 homes located mainly in the Cape Flats and the surrounding areas in Western Cape. The distribution of radon concentration is well described by a log-normal distribution as shown in Figure 4.22. Most of the radon concentrations (about 83%) were below the global average of  $40 \text{ Bqm}^{-3}$  and only 4.1% were above the action level of  $100 \text{ Bqm}^{-3}$  recommended by WHO. The maximum value from the data is  $123.8 \pm 14.6 \text{ Bqm}^{-3}$  when using the default gamma-ray background radiation value of  $32 \text{ Bqm}^{-3}$  [Kot90].

It was noted that some values were below zero (negative) due to the overestimation of the gamma-ray background radiation value of  $32 \text{ Bqm}^{-3}$ . One of the disadvantages of using an electret ion-chamber is that the detectors respond to natural gamma-ray background radiation, and correction is required.

To solve this issue, all the values were recalculated using gamma-ray background radiation values of  $15 \text{ Bqm}^{-3}$  and  $12 \text{ Bqm}^{-3}$  and the results are presented in Table D.1 under Appendix D. All values were positive for the gamma-ray background radiation value of  $12 \text{ Bqm}^{-3}$ . From now on, all the results were discussed based on the positive values obtained using the gamma-ray background radiation of  $12 \text{ Bqm}^{-3}$ . Nevertheless, no indoor radon concentration was above the South African action level of  $300 \text{ Bqm}^{-3}$  recommended by NNR. The maximum value was calculated to be  $143.7 \pm 17.0 \text{ Bqm}^{-3}$ .

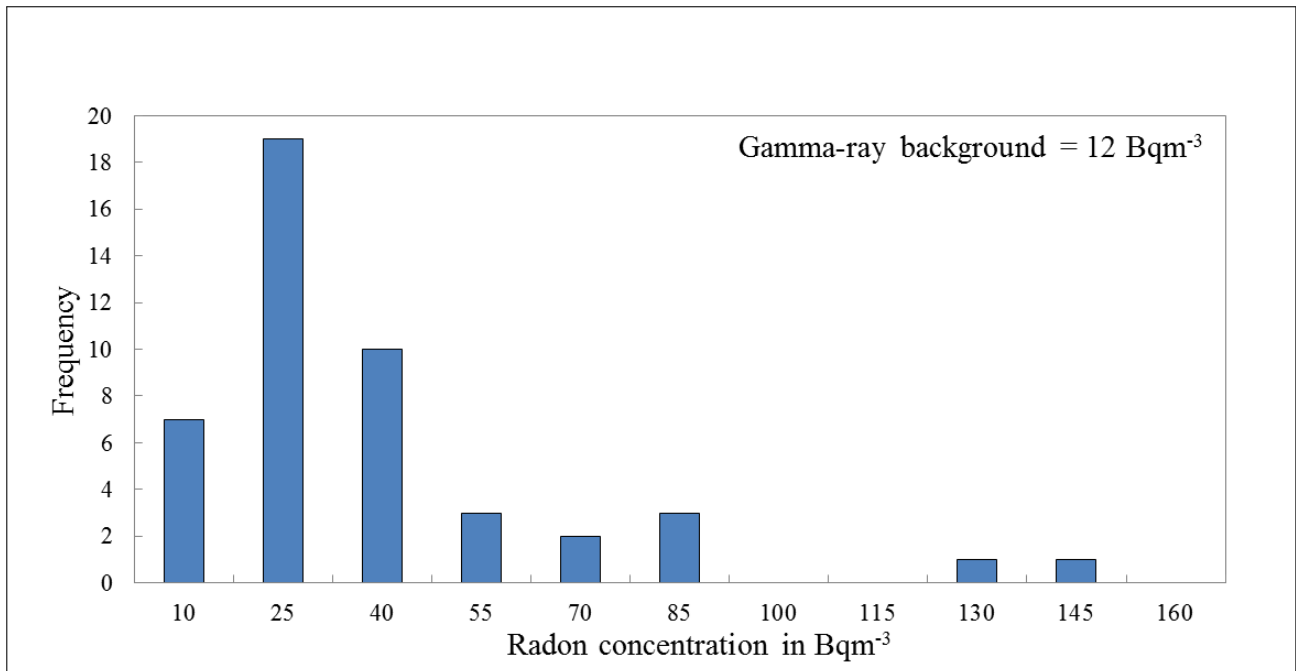


Figure 4.22: Frequency distribution for indoor radon in homes and schools in Western Cape.

Since the idea was to measure the radon gas in the most occupied space, the detectors were either placed in the living rooms or bedrooms in homes. According to Figure 4.23, the results showed that the indoor radon levels in the living rooms were slightly higher than in the bedrooms with a mean of  $35.1 \pm 28.6 \text{ Bqm}^{-3}$  and  $34.6 \pm 23.5 \text{ Bqm}^{-3}$ , respectively. However, there was no direct correlation between the results obtained in the living rooms and bedrooms since only one detector was used for each house.

The results in schools showed that radon levels were higher in staff rooms (offices) than in the classrooms with a mean of  $54.8 \pm 47.3 \text{ Bqm}^{-3}$  and  $31.8 \pm 23.5 \text{ Bqm}^{-3}$ , respectively. The findings are expected since staff rooms are usually smaller and less ventilated than classrooms. Indoor radon concentration in schools cannot be directly compared with the radon in homes, but it is observed that the levels were higher in schools than in homes. The factors influencing higher levels in schools is that South African schools operate mainly from 07h30 to 14h30 or 15h30 and are closed for the rest of the day and on weekends. Therefore, radon gas can build-up due to poor ventilation after working hours and on weekends.

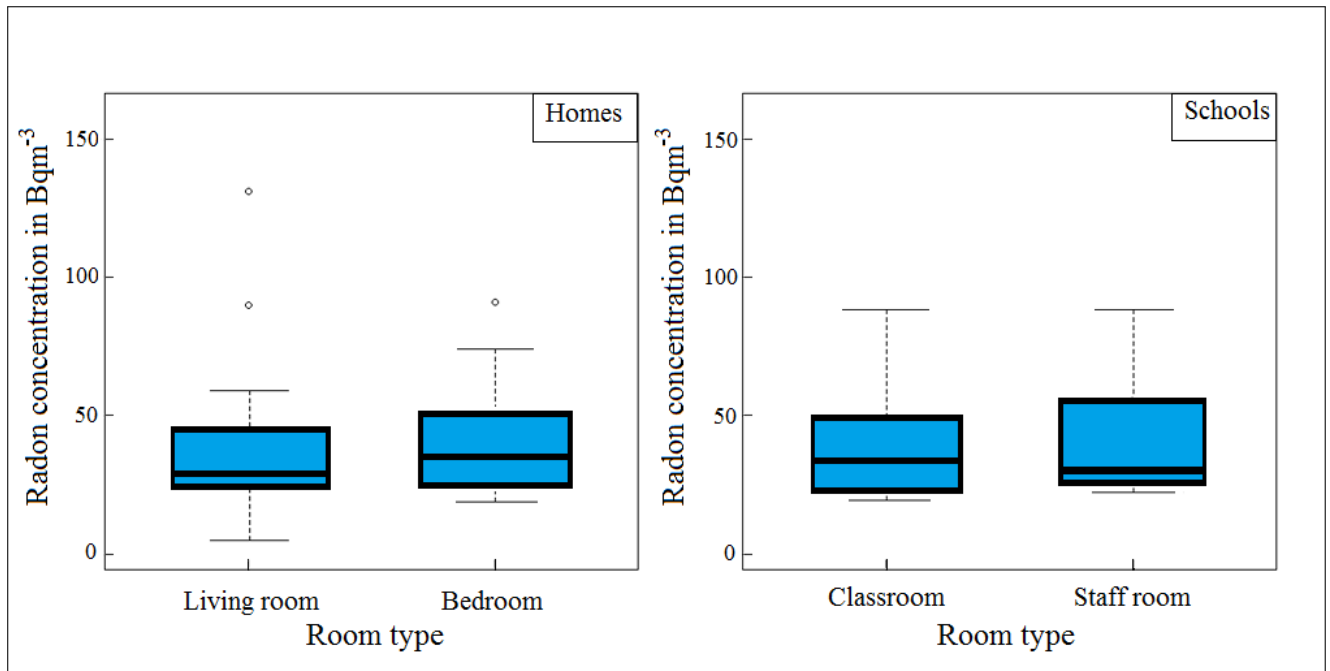


Figure 4.23: Box plots showing indoor radon concentration as a function of the room type.

Tiles, ceramics, marbles, PVCs, and carpets are the most commonly used for flooring in homes and schools in South Africa. Indoor radon concentrations were relatively higher in buildings with tile floors, whereas relatively lower in homes with plastic PVC floor carpets, as shown in Figure 4.24. The mean radon concentration in homes with tile floors was obtained to be  $39.6 \pm 32.8 \text{ Bqm}^{-3}$ , and for plastic PVC floor carpets was  $24.9 \pm 14.8 \text{ Bqm}^{-3}$ . Higher indoor radon concentrations were expected in homes with tiles floors since they are made of ceramic and cement containing radionuclides such as  $^{226}\text{Ra}$ ,  $^{232}\text{Th}$ , and  $^{40}\text{K}$ .



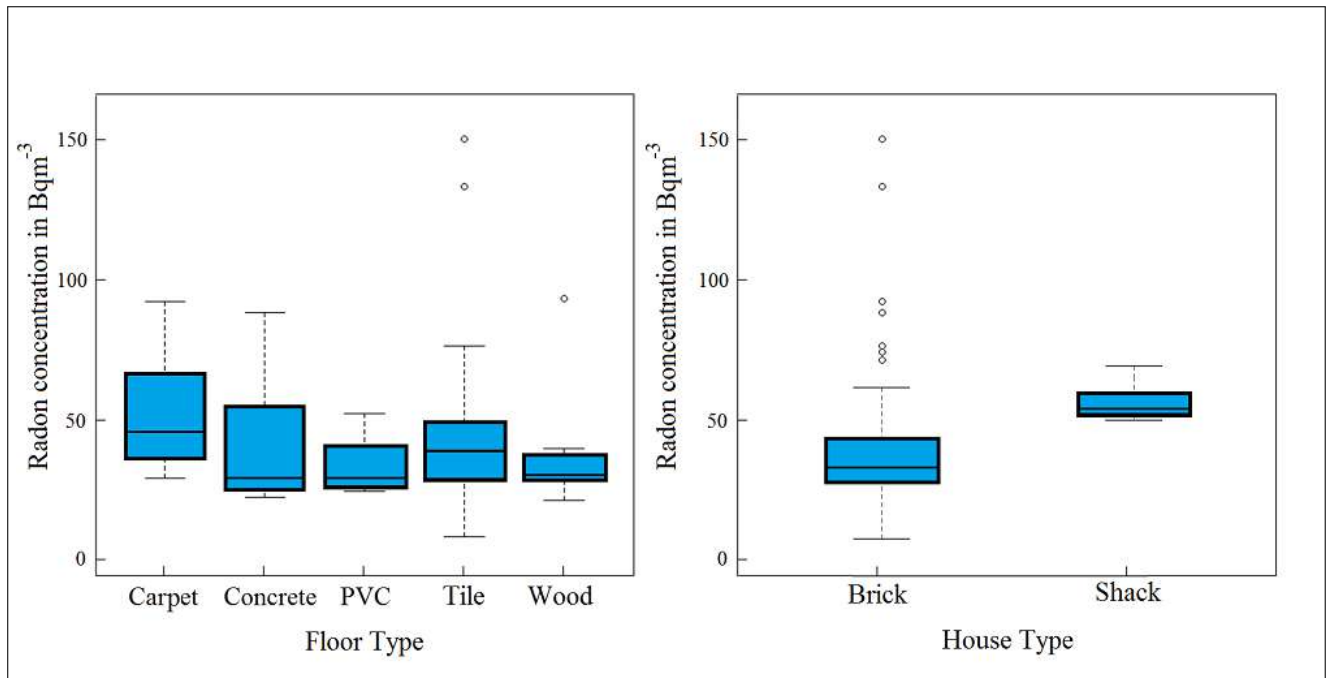


Figure 4.24: Box plots showing indoor radon concentration as a function of the building materials.

The results of indoor radon concentration were compared to the lithology of the measured locations (homes and schools). Figure 4.25 shows the indoor radon location (square boxes) and the lithology of the Cape Flats and the surrounding areas in the Western Cape. About 83.7% of the measurements were carried in the homes and schools located mainly in the C3 WC L5 lithological type described in Table E.2 (Appendix E). The average indoor concentration in this area was  $37.7 \pm 30.4 \text{ Bqm}^{-3}$ . Two buildings [MHS and FHS] measured indoor radon higher above  $100 \text{ Bqm}^{-3}$  and are located in the same lithological type C3 WC L5.

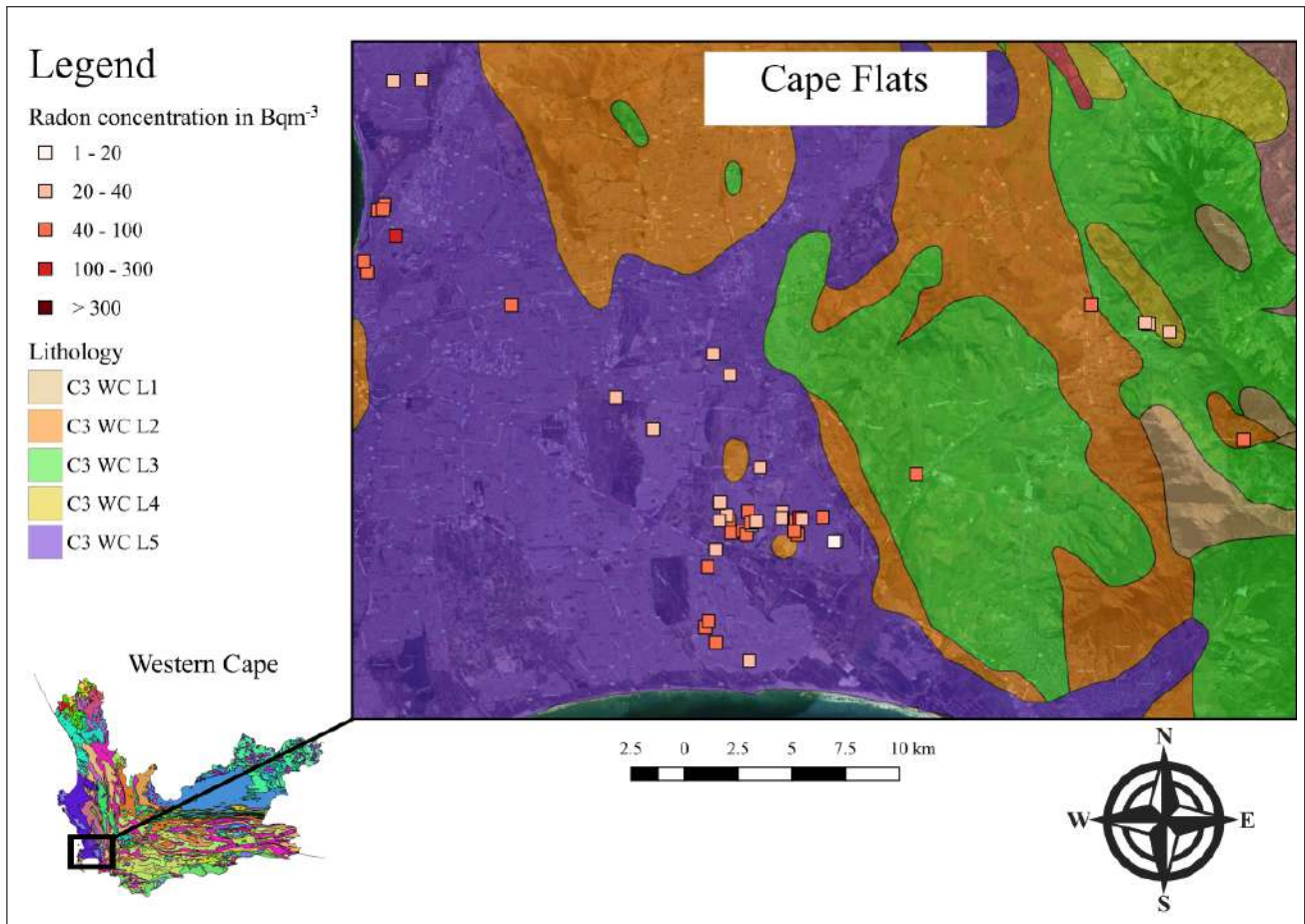


Figure 4.25: Indoor radon concentration as a function of the surrounding geology in Cape Flats area.

When comparing the results in Figure 4.25 and Figure 4.26 [Rou19], it was observed that houses can be in the same geology/lithology area and still be large variation for the indoor radon due to certain variables such as climate parameters, ventilation conditions, and construction materials. For example, all houses are located in an area with the same underlying geology in Figure 4.26 [Rou19], but the home which measured elevated indoor radon was close to a granite outcrop. It is apparent that the underlying geology/lithology is not uniform everywhere therefore indoor radon can vary in homes found in similar geology/lithology areas.

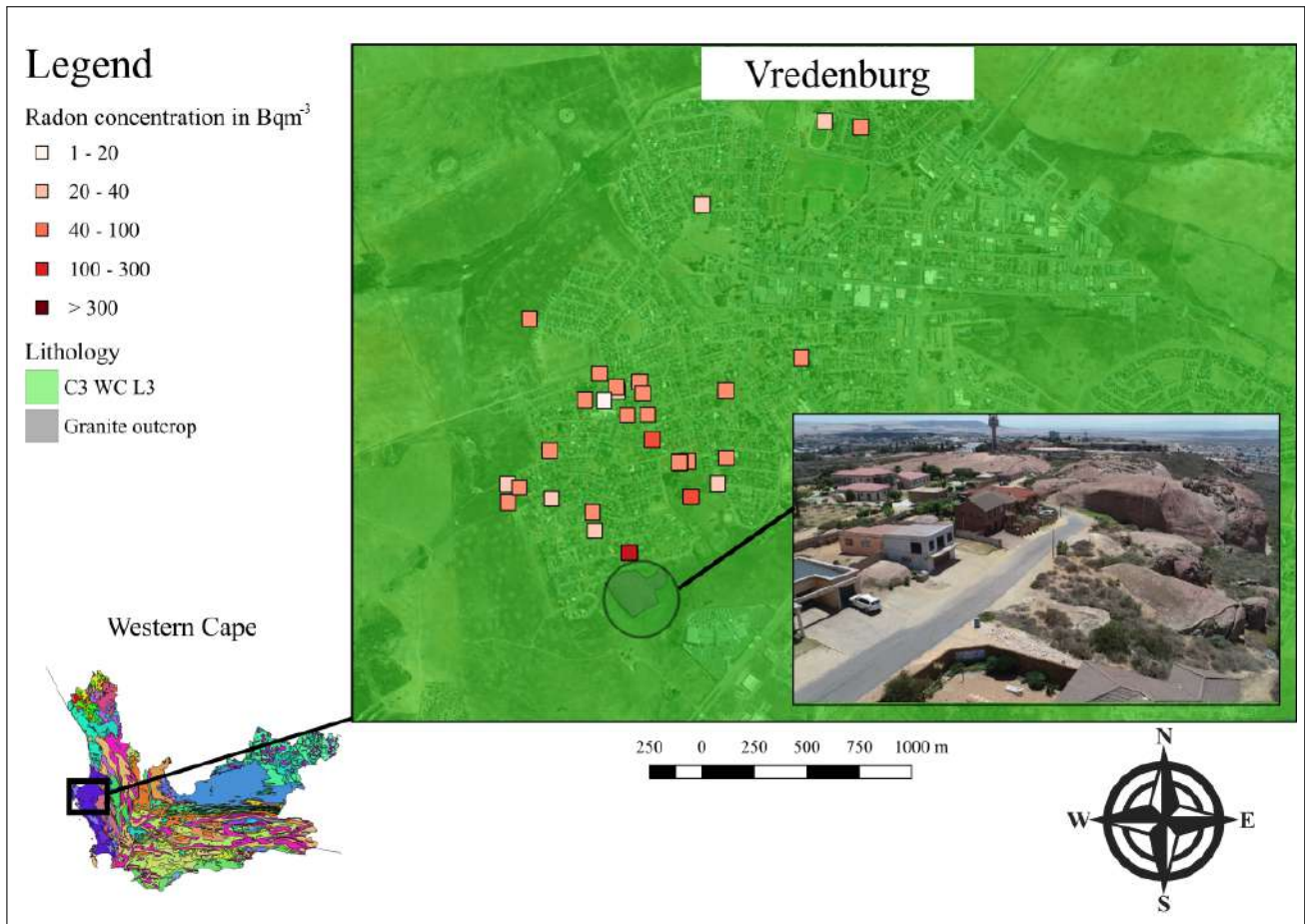


Figure 4.26: Indoor radon concentration as a function of the surrounding geology in Vredenburg, Western Cape [Rou19].

Below are the advantages/disadvantages of the Schools outreach approach to obtain indoor radon data.

Advantages:

- introducing learners to research (applied nuclear physics), environmental science and
- gaining access to homes.

Disadvantages:

- learner results have to be carefully checked (best to independently calculate radon levels),

- consent process more complicated,
- need to have venue to host students,
- need for catering,
- short-term results only,
- scheduling constraints (not during exam time), and
- radon detectors get lost.

#### 4.4 Annual effective dose estimation of indoor $^{222}\text{Rn}$

The annual mean effective dose rate was calculated based on the UNSCEAR (2000) [UNS00] procedure using equation 2.8 described in section 2.4.2 of Chapter 2. The estimated values of the mean effective dose rate ranged from 0.0 to 3.2 mSvy<sup>-1</sup>, with an overall mean of  $0.6 \pm 0.4$  mSvy<sup>-1</sup> (Table 4.7). The estimated values of the annual mean effective dose were calculated based on the short-term measurements ( $\approx 7$  days) which may not accurately indicate annual radon levels. As such, the calculated dose rate in Table 4.7 may be regarded as a rough estimate of indoor radon and its daughters. However, the values of the obtained dose rates were well below the recommended action level of 3 - 10 mSvy<sup>-1</sup> as adopted by ICRP (1993) [ICR93]. The obtained dose rate indicates low indoor levels of radon in dwellings and workplaces.

Table 4.7: Annual mean effective dose (E) and mean lifetime risk for indoor radon exposure in the different campaigns.

Campaign	Place	$^{222}\text{Rn}$ levels (Bqm <sup>-3</sup> )			E (mSvy <sup>-1</sup> )			Risk ( $\times 10^{-3}$ )		
		min	mean	max	min	mean	max	min	mean	max
A	Offices (11)	$32.2 \pm 5.3$	$41.4 \pm 15.6$	$87.0 \pm 10.1$	0.2	0.3	0.6	0.7	0.9	1.9
B	Homes (22)	$2.4 \pm 0.3$	$31.1 \pm 17.3$	$102.5 \pm 11.7$	0.1	0.8	2.6	0.2	2.5	8.3
C	Homes (36)	$0.0 \pm 0.0$	$35.1 \pm 26.3$	$126.9 \pm 14.6$	0.0	0.9	3.2	0.0	2.8	10.2
	Schools (5)	$12.3 \pm 2.8$	$41.3 \pm 36.0$	$143.7 \pm 17.0$	0.1	0.2	0.7	0.2	0.7	2.3

The accumulation of the indoor radon and its daughters emanated from the building materials can have carcinogenic effects [Saa10]. Therefore, the excess lifetime risk was calculated based on the probability of developing lung cancer due to the radon exposure over the average lifetime using the using equation 2.9 described in section 2.4.2 of Chapter 2. The mean risk values are tabulated in Table 4.7 for each campaign, with an overall mean of  $1.7 \pm 1.1 \times 10^{-3}$ , which is below the maximum risk of  $3.5 \times 10^{-3}$  that yields the annual effective dose of 1 mSvy<sup>-1</sup>.

## 5 Conclusion

### 5.1 Summary of main findings

The literature survey has shown that residential indoor radon surveys have been conducted internationally. In some countries, the surveys covered the whole country and in many cases, the surveys were pilot studies. The available data relevant to indoor radon surveys in South Africa were collected up to 2019 and the data was used for mapping and producing databases through the Geographic Information Systems (GIS) software (qGIS 2.18, Free Software Foundation, Inc., 51 Franklin Street, Fifth Floor, Boston, MA 02110-1301 USA, downloaded from: [https://docs.qgis.org/2.18/en/docs/gentle\\_gis\\_introduction/introducing\\_gis.html](https://docs.qgis.org/2.18/en/docs/gentle_gis_introduction/introducing_gis.html)). A map that includes the indoor radon data from more than 20 towns in 7 provinces was produced as presented in Figure 2.7. The minimum and maximum indoor radon levels were found to be 12 Bqm<sup>-3</sup> and 2600 Bqm<sup>-3</sup> in wine cellars and Cango Caves (Western Cape), respectively.

The part of this study also involved the direct measurement of indoor radon in homes and workplaces such as schools and offices. The sampling strategy was based on building characteristics, geographic locations, underlying geology, and soil. The experimental work in this study was divided into three campaigns for different objectives. In the first campaign, a comparative assessment was taken between the track-etch, electrets, and Airthings™ radon detectors. It was concluded that track-etch and electrets are the most applicable and suitable technologies for conducting the national indoor radon surveys.

The EIC results show that radon levels are found to be higher (up to 33%) for measurements close to walls as opposed to measurements where the EIC detectors are placed > 0.5 m away from walls. This is most likely due to thoron from the wall, in addition to radon entering the EIC detectors. The EIC results show that radon levels increase with height. This is most likely due to the thoron effect. In this case the thoron source is the materials in the ceiling. The results showed radon levels to vary significantly in areas with the same underlying geology and soil profile. This indicates that using underlying geology and soil profile alone is not sufficient to develop an indoor radon survey strategy. However, the results of the existing data from Paarl and Vredenburg indicated significant geographical variation in indoor radon concentrations only in the areas located next to granite outcrops. Such areas are classified as high-radon areas, and

should be prioritised during the national radon survey.

No clear correlation between bedroom and living room radon concentrations was found in the Gauteng study. This suggests that one should try to measure in the bedrooms and living rooms. Bedrooms levels are necessary because the occupancy of the room can be up to 8 hours a day (during sleep).

The annual effective dose assessment was performed for all the three campaigns, and the annual mean effective dose rate was calculated to be  $0.6 \pm 0.4 \text{ mSvy}^{-1}$  which was lower than the allowable limit. The lifetime risk was found to have a mean of  $1.7 \pm 1.1 \times 10^{-3}$ . No level of indoor radon is considered safe. Therefore, it is necessary to increase the level of public awareness concerning the risks associated with indoor radon gas. Finally, national indoor radon programs are required in the country to protect the citizens from preventable lung cancer deaths caused by the silent killer, radon.

## 5.2 Recommendations

Some recommendations for future work on national indoor radon survey are:

- All high population density areas and areas more likely to have high levels of radon should be prioritised when conducting a national survey.
- The National Nuclear Regulator (NNR) in South Africa must encourage homeowners to have radon measurements made in their homes to identify the individual dwellings with elevated indoor radon levels.
- The sampling method should be carried in two phases. In phase 1, directed sampling should be considered based on the geology, soil, NORM/TENORM industry. In phase 2, the grid sampling will be based on the district population for the development of a higher resolution national radon map.
- Access to homes and public buildings can be gained through a door-to-door approach, invitation, advertisement, and school outreach.
- Short-term measurements with electret ion-chambers (SST or SLT) or Airthings detectors can be used for screening purposes. Track-etch detectors should be considered for long-

---

term measurements. The cost-effectiveness of the three measuring systems is well outlined in Appendix F.

- The radon results for LLT-OO (long-term electret on LOO-chamber) configuration were found to be inaccurate when compared to other radon detectors, the reason for this will be further investigated.
- The measurements should preferably be conducted during the winter seasons. The higher levels in the winter is attributed to the observation that people normally keep their windows closed during the winter, allowing indoor radon concentrations to rise.
- To continue using qGIS to build on what was created in this study.



## **6 Appendices**

### **A Questionnaire**



UNIVERSITEIT • STELLENBOSCH • UNIVERSITY  
jou kennisvenoot • your knowledge partner

Deployment and household Questionnaire

HOUSE DETAILS

Parents name and surname: \_\_\_\_\_

Physical address: \_\_\_\_\_

City: \_\_\_\_\_

Province: \_\_\_\_\_

DEPLOYMENT INFO

Detector serial number: \_\_\_\_\_ (*indicated under the detector*)

Start Date: \_\_\_\_\_ Start Time: \_\_\_\_\_ Deployed by: \_\_\_\_\_

End Date: \_\_\_\_\_ End Time: \_\_\_\_\_ Retrieved by: \_\_\_\_\_

SECTION A: DWELLING\HOUSE INFORMATION

Dwelling type:

- Shed\Wendy House
- Shack
- Hut
- Concrete\ brick house
- Caravan
- Other (specify below)

\_\_\_\_\_  
\_\_\_\_\_



UNIVERSITEIT • STELLENBOSCH • UNIVERSITY  
jou kennisvenoot • your knowledge partner

Floor type:

- Wood
  - PVC flooring
  - Tiles
  - Mud
  - Concrete
  - Carpet
  - Stone (marble, granite, slate, sandstone, limestone)
  - Other (specify below)
- 
- 

How old is a Dwelling\House?

- 0 – 3years     3 – 8years     9 - 20 years     21- 30 years
- 31 - 40 years     41 – 50 years     More than 50 years     Not sure



UNIVERSITEIT • STELLENBOSCH • UNIVERSITY  
jou kennisvenoot • your knowledge partner

SECTION B: DEPLOYED AREA

Which room did you deployed the detector?

- Bedroom
- Living room
- Other (specify below)

---

---

Which level is the room is located in the house:

- Ground floor
- First floor
- Basement
- The house does not have levels (single storey)
- Other (specify below)

---

---

According to the instructions, the detectors must be deployed 0.5 m away from the wall or open window and 1m above the ground. Did you follow these instruction? Yes  No

If No, Please describe how you deployed the detector

---

---

---

## B Gauteng homes: building materials information

Table B.1: Building characteristics for each home in Gauteng

House N <sup>o</sup>	House characteristics			Dwelling type	Floor type	House age	Photographs	
	Living room (Bqm <sup>-3</sup> )	Bedroom (Bqm <sup>-3</sup> )	Average levels (Bqm <sup>-3</sup> )					
1	[H1L],[H1B]	38.8 ± 4.5	36.7 ± 4.3	37.7 ± 1.5	Brick	Tile	21 - 30	<a href="#">House1</a>
2	[H2L],[H2B]	51.3 ± 5.9	47.6 ± 5.5	49.5 ± 2.6	Brick	Tile	9 - 20	<a href="#">House2</a>
3	[H3L],[H3B]	27.9 ± 3.3	33.5 ± 3.9	30.7 ± 4.0	Brick	Tile	9 - 20	<a href="#">House3</a>
4	[H4L],[H4B]	28.5 ± 3.4	46.3 ± 5.4	37.4 ± 12.6	Brick	Tile	3 - 8	<a href="#">House4</a>
5	[H5L],[H5B]	18.9 ± 2.3	21.5 ± 2.6	20.2 ± 1.8	Shack	Concrete	9 - 20	<a href="#">House5</a>
6	[H6L],[H6B]	29.2 ± 3.5	21.7 ± 2.6	25.4 ± 5.2	Brick	Tile	3 - 8	<a href="#">House6</a>
7	[H7L],[H7B]	68.6 ± 7.9	18.2 ± 2.2	43.4 ± 35.6	Shack	Concrete	0 - 3	<a href="#">House7</a>
8	[H8L],[H8B]	29.4 ± 3.5	31.8 ± 3.8	30.6 ± 1.7	Brick	Concrete	9 - 20	<a href="#">House8</a>
9	[H9L],[H9B]	102.5 ± 11.7	40.0 ± 4.7	71.2 ± 44.1	Brick	Tile	9 - 20	<a href="#">House9</a>
10	[H10L],[H10B]	26.9 ± 3.2	20.5 ± 2.5	23.7 ± 4.5	Brick	Concrete	21 - 30	<a href="#">House10</a>
11	[H11L],[H11B]	39.0 ± 4.6	39.7 ± 4.7	39.3 ± 0.5	Brick	Concrete	3 - 8	<a href="#">House11</a>
12	[H12L],[H12B]	22.1 ± 2.7	42.1 ± 5.0	32.1 ± 14.1	Brick	Tile	9 - 20	<a href="#">House12</a>
13	[H13L],[H13B]	26.6 ± 3.2	28.9 ± 3.4	27.8 ± 1.6	Brick	Concrete	9 - 20	<a href="#">House13</a>
14	[H14L],[H14B]	53.9 ± 6.2	39.0 ± 4.6	46.5 ± 10.5	Brick	Tile	9 - 20	<a href="#">House14</a>
15	[H15L],[H15B]	18.9 ± 2.2	17.1 ± 2.0	18.0 ± 1.3	Brick	Tile	9 - 20	<a href="#">House15</a>
16	[H16L],[H16B]	8.7 ± 1.1	14.4 ± 1.8	11.5 ± 4.0	Shack	Carpet	3 - 8	<a href="#">House16</a>
17	[H17L],[H17B]	10.1 ± 1.3	14.4 ± 1.8	12.2 ± 3.0	Shack	Carpet	3 - 8	<a href="#">House17</a>
18	[H18L],[H18B]	24.1 ± 2.9	35.9 ± 4.2	30.0 ± 8.3	Shack	Tile	3 - 8	<a href="#">House18</a>
19	[H19L],[H19B]	30.1 ± 3.8	41.1 ± 5.0	35.6 ± 7.8	Brick	Tile	3 - 8	<a href="#">House19</a>
20	[H20L],[H20B]	22.6 ± 2.9	17.2 ± 2.2	19.9 ± 3.8	Brick	Tile	9 - 20	<a href="#">House20</a>
21	[H21L],[H21B]	25.9 ± 3.3	2.4 ± 0.3	14.2 ± 16.6	Shack	Concrete	9 - 20	<a href="#">House21</a>
22	[H22L],[H22B]	44.7 ± 5.4	10.2 ± 1.4	27.5 ± 24.4	Brick	Tile	21 - 30	<a href="#">House22</a>

Table B.2: Additional information about homes in Gauteng.

Electret no	Code	Room type	Location	Start date	Finish date	Days	$V_i$	$V_f$	$\Delta V$	CF	Coordinates	
											x	y
SLF 295	H1L	Living room	Atteridgeville	18/12/2019 14:40	27/12/2019 11:55	8.9	707.0	664.0	43.0	0.06	Available on request	
SLF 344	H1B	Bedroom	Atteridgeville	18/12/2019 14:40	27/12/2019 11:55	8.9	656.3	615.0	41.3	0.06		
SLF 357	H2L	Living room	Atteridgeville	18/12/2019 14:50	27/12/2019 11:45	8.9	696.0	647.0	49.0	0.06	Available on request	
SLF 227	H2B	Bedroom	Atteridgeville	18/12/2019 14:50	27/12/2019 11:45	8.9	684.0	637.0	47.0	0.06		
SLF 208	H3L	Living room	Atteridgeville	18/12/2019 15:30	27/12/2019 11:25	8.8	712.3	675.0	37.3	0.06	Available on request	
SLF 267	H3B	Bedroom	Atteridgeville	18/12/2019 15:30	27/12/2019 11:25	8.8	637.3	598.0	39.3	0.06		
SLF 330	H4L	Living room	Atteridgeville	19/12/2019 11:36	27/12/2019 11:15	8.0	707.0	673.0	34.0	0.06	Available on request	
SLF 253	H4B	Bedroom	Atteridgeville	19/12/2019 11:36	27/12/2019 11:15	8.0	705.0	663.0	42.0	0.06		
SLF 333	H5L	Living room	Atteridgeville	19/12/2019 11:45	27/12/2019 11:30	8.0	700.7	671.0	29.7	0.06	Available on request	
SLF 369	H5B	Bedroom	Atteridgeville	19/12/2019 11:45	27/12/2019 11:30	8.0	678.3	647.7	30.7	0.06		
SLF 348	H6L	Living room	Atteridgeville	19/12/2019 11:54	27/12/2019 11:40	8.0	671.0	637.0	34.0	0.06	Available on request	
SLF 309	H6B	Bedroom	Atteridgeville	19/12/2019 11:54	27/12/2019 11:40	8.0	709.0	678.0	31.0	0.06		
SLF 227	H7L	Living room	Lotus Gardens	19/12/2019 12:00	27/12/2019 10:55	8.0	697.7	646.0	51.7	0.06	Available on request	
SLF 525	H7B	Bedroom	Lotus Gardens	19/12/2019 12:00	27/12/2019 10:55	8.0	672.0	643.0	29.0	0.06		
SLF 340	H8L	Living room	Lotus Gardens	19/12/2019 14:00	27/12/2019 12:30	7.9	682.0	648.0	34.0	0.06	Available on request	
SLF 225	H8B	Bedroom	Lotus Gardens	19/12/2019 14:00	27/12/2019 12:30	7.9	712.3	677.0	35.3	0.06		
SLF 302	H9L	Living room	Lotus Gardens	19/12/2019 14:10	27/12/2019 12:35	7.9	686.3	620.0	66.3	0.06	Available on request	
SLF 246	H9B	Bedroom	Lotus Gardens	19/12/2019 14:10	27/12/2019 12:35	7.9	651.3	613.0	38.3	0.06		
SLF 356	H10L	Living room	Lotus Gardens	19/12/2019 14:25	27/12/2019 12:35	7.9	702.0	669.0	33.0	0.06	Available on request	
SLF 307	H10B	Bedroom	Lotus Gardens	19/12/2019 14:25	27/12/2019 12:35	7.9	683.0	653.0	30.0	0.06		
SLF 511	H11L	Living room	Benoni	20/12/2019 12:50	28/12/2019 18:37	8.2	711.0	671.0	40.0	0.06	Available on request	
SLF 346	H11B	Bedroom	Benoni	20/12/2019 12:50	28/12/2019 18:37	8.2	681.0	641.0	40.0	0.06		
SLF 373	H12L	Living room	Benoni	20/12/2019 13:30	28/12/2019 18:21	8.2	707.0	675.0	32.0	0.06	Available on request	
SGJ 855	H12B	Bedroom	Benoni	20/12/2019 13:30	28/12/2019 18:21	8.2	332.0	295.0	37.0	0.05		
SLF 323	H13L	Living room	Benoni	20/12/2019 13:50	28/12/2019 18:15	8.2	707.0	673.0	34.0	0.06	Available on request	
SLF 285	H13B	Bedroom	Benoni	20/12/2019 13:50	28/12/2019 18:15	8.2	702.0	667.0	35.0	0.06		
SLF 430	H14L	Living room	Daveyton	20/12/2019 14:55	28/12/2019 17:30	8.1	698.0	652.0	46.0	0.06	Available on request	
SLF 212	H14B	Bedroom	Daveyton	20/12/2019 14:55	28/12/2019 17:30	8.1	675.0	636.0	39.0	0.06		
SLF 465	H15L	Living room	Daveyton	20/12/2019 15:35	30/12/2019 14:30	10.0	707.0	670.0	37.0	0.06	Available on request	
SLF 372	H15B	Bedroom	Daveyton	20/12/2019 15:35	30/12/2019 14:30	10.0	709.0	673.0	36.0	0.06		
SLF 291	H16L	Living room	Benoni	20/12/2019 16:45	28/12/2019 19:05	8.1	211.0	189.0	22.0	0.05	Available on request	
SLF 287	H16B	Bedroom	Benoni	20/12/2019 16:45	28/12/2019 19:05	8.1	702.0	674.0	28.0	0.06		
SLF 362	H17L	Living room	Benoni	20/12/2019 17:05	28/12/2019 19:35	8.1	693.0	667.0	26.0	0.06	Available on request	
SLF 274	H17B	Bedroom	Benoni	20/12/2019 17:05	28/12/2019 19:35	8.1	699.0	671.0	28.0	0.06		
SLF 313	H18L	Living room	Benoni	20/12/2019 18:18	28/12/2019 17:15	8.0	717.0	685.0	32.0	0.06	Available on request	
SLF 263	H18B	Bedroom	Benoni	20/12/2019 18:18	28/12/2019 17:15	8.0	687.0	650.0	37.0	0.06		
SGJ 859	H19L	Living room	Midrand	23/12/2019 14:40	30/12/2019 09:15	6.8	148.0	123.0	25.0	0.05	Available on request	
SGJ 802	H19B	Bedroom	Midrand	23/12/2019 14:40	30/12/2019 09:15	6.8	196.0	167.0	29.0	0.05		

Table B.3: Additional information about homes in Gauteng (continued).









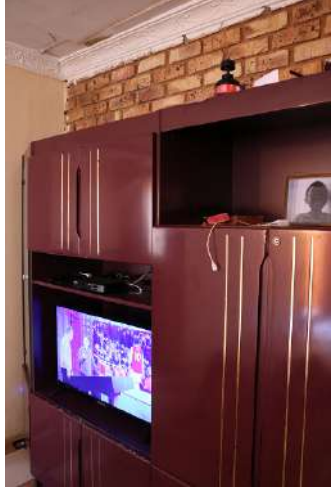
Electret no	Code	Room type	Location	Start date	Finish date	Days	$V_i$	$V_f$	$\Delta V$	CF	Coordinates	
											x	y
SGJ 788	H20L	Living room	Midrand	23/12/2019 15:35	30/12/2019 09:30	6.7	361.0	337.0	24.0	0.05	Available on request	
SGJ 774	H20B	Bedroom	Midrand	23/12/2019 15:35	30/12/2019 09:30	6.7	189.0	168.0	21.0	0.05		
SGJ 817	H21L	Living room	Midrand	23/12/2019 20:05	30/12/2019 08:56	6.5	173.0	158.0	15.0	0.05	Available on request	
SGJ 841	H21B	Bedroom	Midrand	23/12/2019 20:05	30/12/2019 08:56	6.5	258.0	242.0	16.0	0.05		
SGJ 795	H22L	Living room	Midrand	23/12/2019 18:15	30/12/2019 13:56	6.8	156.0	126.0	30.0	0.05	Available on request	
SGJ 885	H22B	Bedroom	Midrand	23/12/2019 18:15	30/12/2019 13:56	6.8	201.0	182.0	19.0	0.05		







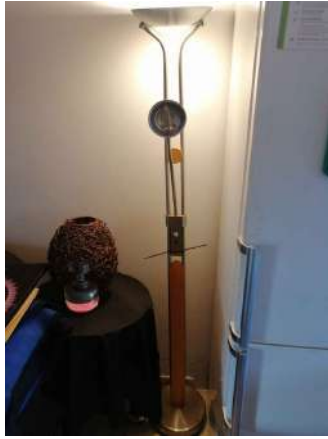

















## C Gauteng homes: photographs showing the building materials

Table C.1: The photographs taken from each home in Gauteng showing the building materials of the house (outside), living room and bedroom.









House N°	Outside	Living room	Bedroom
1			
2			
3			


House N°	Outside	Living room	Bedroom
4			
5			<p data-bbox="1137 1137 1345 1193">no image</p>
6			





House N°	Outside	Living room	Bedroom
7			<p>no image</p>
8			<p>no image</p>
9			

House N°	Outside	Living room	Bedroom
10			<p>no image</p>
11			
12			<p>no image</p>

House N°	Outside	Living room	Bedroom
13			<p data-bbox="1139 577 1340 631">no image</p>
14			

House N°	Outside	Living room	Bedroom
15			
16			
17			<p data-bbox="1136 1639 1337 1693">no image</p>

House N°	Outside	Living room	Bedroom
18			
19			
20			

House N°	Outside	Living room	Bedroom
21			<p>no image</p>
22			<p>no image</p>



## **D Western Cape schools and homes: building materials information**

Table D.1: The information about the building materials of schools and homes in Western Cape.

Code	Building characteristics					Rn level (Bqm <sup>-3</sup> )		
	Dwelling type	Floor type	House age	Room type	Room level	BG = 32	BG = 15	BG = 12
LHS1	Brick	PVC	41 - 50	Classroom	First	-7.6 ± 1.8	9.4 ± 2.2	12.3 ± 2.8
LHS2	Brick	PVC	41 - 50	Staff room	First	2.6 ± 0.5	19.6 ± 4.0	22.5 ± 4.6
LHS3	Brick	PVC	0 - 3	Classroom	First	-1.8 ± 0.4	15.2 ± 3.3	18.1 ± 3.9
LH4	Brick	Tiles	21 - 30	Bedroom	First	1.7 ± 0.3	18.7 ± 3.4	21.6 ± 3.9
LH5	Shack	Concrete	3 - 8	Bedroom	First	39.8 ± 5.1	56.8 ± 7.3	59.7 ± 7.6
LH6	Brick	Tiles	Not sure	Bedroom	First	11.5 ± 1.8	28.5 ± 4.5	31.4 ± 5.0
MHS1	Brick	Tiles	Over 50	Secretary Office	First	8.9 ± 1.6	25.9 ± 4.7	28.8 ± 5.2
MHS2	Brick	Tiles	Over 50	Staff room	First	22.4 ± 3.5	39.4 ± 6.1	42.3 ± 6.5
MHS3	Brick	Concrete	9 - 20	Classroom	First	61.8 ± 7.9	78.8 ± 10.1	81.7 ± 10.5
MH4	Concrete	Tiles	21 - 30	Dining room	First	-4.4 ± 0.8	12.6 ± 2.2	15.5 ± 2.7
MH5	Brick	Tiles	21 - 30	Living room	First	107.0 ± 12.3	124.0 ± 14.3	126.9 ± 14.6
MH6	Brick	Tiles	Not sure	Bedroom	First	49.6 ± 6.3	66.6 ± 8.4	69.5 ± 8.8
MH7	Brick	Tiles	Over 50	Living room	First	9.4 ± 1.4	26.4 ± 3.8	29.3 ± 4.2
MH8	Brick	Tiles	21 - 30	Living room	First	3.3 ± 0.5	20.3 ± 3.1	23.2 ± 3.6
MYH1	Brick	Concrete	3 - 8	Bedroom	First	-5.4 ± 1.0	11.6 ± 2.1	14.5 ± 2.6
MYH2	Brick	Carpet	9 - 20	Living room	First	66.4 ± 8.0	83.4 ± 10.1	86.3 ± 10.4
MYH3	Wood	Wood	3 - 8	Bedroom	First	67.5 ± 8.0	84.5 ± 10.0	87.4 ± 10.4
MYH4	Brick	Wood	3 - 8	Living room	First	11.4 ± 1.6	28.4 ± 4.0	31.3 ± 4.4
MYH5	Brick	Carpet	Not sure	Bedroom	First	9.6 ± 1.4	26.6 ± 3.8	29.5 ± 4.2
FHS1	Brick	Tiles	21 - 30	Classroom	First	23.3 ± 3.7	40.3 ± 6.4	43.2 ± 6.8
FHS2	Brick	Tiles	21 - 30	Staff room	First	123.8 ± 14.6	140.8 ± 16.7	143.7 ± 17.0
FHS3	Brick	Tiles	21 - 30	Classroom	Second	-6.6 ± 1.7	10.4 ± 2.7	13.3 ± 3.5
FH4	Brick	Tiles	21 - 30	Living room	Third	16.4 ± 2.2	33.4 ± 4.6	36.3 ± 5.0
FH5	Brick	Tiles	Not sure	Bedroom	First	13.4 ± 2.0	30.4 ± 4.5	33.3 ± 4.9
FH6	Brick	Tiles	9 - 20	Living room	First	6.4 ± 1.0	23.4 ± 3.5	26.3 ± 3.9
FH7	Brick	Tiles	31 - 40	Living room	First	18.0 ± 2.4	35.0 ± 4.7	37.9 ± 5.1
FH8	Brick	Tiles	21 - 30	Bedroom	First	14.3 ± 2.0	31.3 ± 4.3	34.2 ± 4.7
BDH1	Brick	Tiles	0 - 3	Living room	First	35.7 ± 4.5	52.7 ± 6.6	55.6 ± 7.0
BDH2	Brick	Concrete	9 - 20	Bedroom	First	-0.7 ± 0.1	16.3 ± 2.9	19.2 ± 3.5
BDH3	Brick	Tiles	9 - 20	Living room	First	1.7 ± 0.3	18.7 ± 3.0	21.6 ± 3.5
BDH4	Shack	PVC	0 - 3	Living room	First	26.2 ± 3.5	43.2 ± 5.8	46.1 ± 6.2
BDH5	Brick	Tiles	9 - 20	Living room	First	2.6 ± 0.4	19.6 ± 3.1	22.5 ± 3.5
TGS5	Brick	Concrete	9 - 20	Classroom	First	-3.6 ± 1.0	13.4 ± 3.8	16.3 ± 4.7
TGS7	Brick	Concrete	9 - 20	Classroom	First	17.3 ± 3.3	34.3 ± 3.8	37.2 ± 7.2
TGH1	Brick	Tiles	3 - 8	Living room	First	-19.9 ± 6.9	-2.9 ± 1.0	0.0 ± 0.0
TGH2	Brick	Wood	31 - 40	Living room	First	-5.4 ± 1.0	11.6 ± 2.1	14.5 ± 2.6
TGH3	Brick	Concrete	9 - 20	Bedroom	First	2.9 ± 0.5	19.9 ± 3.1	22.8 ± 3.6
TGH4	Shack	Concrete	3 - 8	Bedroom	First	-0.7 ± 0.1	16.3 ± 2.6	19.2 ± 3.0
TGH6	Brick	Tiles	9 - 20	Living room	First	-17.9 ± 6.6	-0.9 ± 0.3	2.0 ± 0.7
MZS1	Brick	Tiles	21-30	Staff room	First	15.8 ± 2.1	32.8 ± 4.4	15.5 ± 2.6
MZS2	Brick	Tiles	21-30	Staff room	First	-4.4 ± 0.7	12.6 ± 2.2	68.2 ± 8.2
MZS3	Brick	Tiles	21-30	Staff room	First	48.3 ± 5.8	65.3 ± 7.8	35.7 ± 4.8

Table D.2: The information about the building materials of schools and homes in Western Cape (continued).

Code	Building characteristics					Rn level (Bqm <sup>-3</sup> )		
	Dwelling type	Floor type	House age	Room type	Room level	BG = 32	BG = 15	BG = 12
MZH1	Brick	Wood	31 - 40	Bedroom	First	-13.2 ± 3.3	3.8 ± 0.9	6.7 ± 1.7
MZH2	Shack	Carpet	3 - 8	Living room	First	24.9 ± 3.2	41.9 ± 5.4	44.8 ± 5.8
MZH3	Brick	Carpet	Not sure	Living room	First	2.7 ± 0.4	19.7 ± 3.1	22.6 ± 3.5
SKH1	Brick	Tiles	9 - 20	Other (Kitchen)	First	45.3 ± 5.5	62.3 ± 7.6	65.2 ± 8.0
SKH2	Brick	Wood	Not sure	Living room	First	4.4 ± 0.7	21.4 ± 3.3	24.3 ± 3.7
SKH3	Brick	Tiles	31 - 40	Living room	First	4.3 ± 0.7	21.3 ± 3.2	24.2 ± 3.7
SKH4	Brick	Wood	41 - 50	Living room	First	4.3 ± 0.7	21.3 ± 3.5	24.2 ± 3.9

Table D.3: Additional information of schools and homes in Western Cape.

Electret type	Serial number	Code	Location	Start date	Finish date	Days	$V_i$	$V_j$	$\Delta V$	CF	G	Coordinates	
												x	y
Short term	SLF 242	LHS	Lückhoff High School	01/09/2019 12:24	06/09/2019 13:24	5.0	716.7	709.7	7.0	2.1	0.087	Available on request	
Short term	SLF 351	LHS	Lückhoff High School	02/09/2019 08:10	06/09/2019 13:10	4.2	730.0	721.7	8.3	2.1	0.087	Available on request	
Short term	SLF 229	LHS	Lückhoff High School	02/09/2019 02:45	06/09/2019 13:15	4.4	731.3	723.7	7.7	2.1	0.087	Available on request	
Short term	SLF 291	LH4	Stellenbosch (Home)	02/09/2019 03:05	07/09/2019 07:45	5.2	726.0	716.0	10.0	2.1	0.087	Available on request	
Short term	SLF 427	LH5	Stellenbosch (Home)	31/08/2019 17:53	06/09/2019 06:47	5.5	728.7	706.0	22.7	2.1	0.087	Available on request	
Short term	SLF 301	LH6	Stellenbosch (Home)	01/09/2019 12:24	06/09/2019 15:06	5.1	716.7	704.0	12.7	2.1	0.087	Available on request	
Short term	SLF 277	MHS	Milnerton High School	02/09/2019 07:19	06/09/2019 14:24	4.3	716.0	706.0	10.0	2.1	0.087	Available on request	
Short term	SLF 313	MHS	Milnerton High School	02/09/2019 07:22	06/09/2019 14:14	4.3	734.3	721.0	13.3	2.1	0.087	Available on request	
Short term	SLF 344	MHS	Milnerton High School	02/09/2019 07:19	06/09/2019 13:58	4.3	695.0	672.3	22.7	2.1	0.087	Available on request	
Short term	SLF 369	MH4	Milnerton (Home)	31/08/2019 16:44	07/09/2019 07:32	6.6	699.0	688.7	10.3	2.1	0.087	Available on request	
Short term	SLF 246	MH5	Milnerton (Home)	31/08/2019 16:41	07/09/2019 07:14	6.6	717.7	665.7	52.0	2.1	0.087	Available on request	
Short term	SLF 340	MH6	Milnerton (Home)	31/08/2019 17:30	05/09/2019 23:30	5.3	713.3	689.0	24.3	2.1	0.087	Available on request	
Short term	SLF 356	MH7	Milnerton (Home)	31/08/2019 16:30	07/09/2019 07:38	6.6	724.7	709.0	15.7	2.1	0.087	Available on request	
Short term	SLF 274	MH8	Milnerton (Home)	31/08/2019 17:10	07/09/2019 07:42	6.6	732.0	718.7	13.3	2.1	0.087	Available on request	
Short term	SLF 323	MYH1	Khayelitsha (Home)	31/08/2019 17:11	07/09/2019 07:10	6.6	729.3	719.3	10.0	2.1	0.087	Available on request	
Short term	SLF 270	MYH2	Khayelitsha (Home)	01/09/2019 17:15	07/09/2019 06:15	5.5	722.0	691.0	31.0	2.1	0.087	Available on request	
Short term	SLF 371	MYH3	Khayelitsha (Home)	31/08/2019 21:50	07/09/2019 06:46	6.4	721.0	685.0	36.0	2.1	0.087	Available on request	
Short term	SLF 362	MYH4	Khayelitsha (Home)	31/08/2019 16:30	07/09/2019 07:10	6.6	721.7	705.3	16.3	2.1	0.087	Available on request	
Short term	SLF 511	MYH5	Khayelitsha (Home)	31/08/2019 16:50	07/09/2019 06:50	6.6	736.3	720.7	15.7	2.1	0.087	Available on request	
Short term	SLF 263	FHS	Forest Height High School	02/09/2019 11:55	06/09/2019 12:33	4.0	715.0	702.3	12.7	2.1	0.087	Available on request	
Short term	SLF 525	FHS	Forest Height High School	02/09/2019 09:20	06/09/2019 12:36	4.1	727.7	691.0	36.7	2.1	0.087	Available on request	
Short term	SLF 357	FHS	Forest Height High School	02/09/2019 08:48	06/09/2019 12:28	4.2	716.0	710.0	6.0	2.1	0.087	Available on request	
Short term	SLF 302	FH4	Blue Downs (Home)	31/08/2019 17:35	07/09/2019 06:16	6.5	722.7	704.7	18.0	2.1	0.087	Available on request	
Short term	SLF 287	FH5	Blue Downs (Home)	01/09/2019 15:23	07/09/2019 07:19	5.7	723.0	708.3	14.7	2.1	0.087	Available on request	
Short term	SLF 329	FH6	Blue Downs (Home)	31/08/2019 17:20	07/09/2019 07:05	6.6	709.7	695.3	14.3	2.1	0.087	Available on request	
Short term	SLF 219	FH7	Blue Downs (Home)	31/08/2019 15:54	07/09/2019 07:30	6.7	735.7	716.7	19.0	2.1	0.087	Available on request	
Short term	SLF 208	FH8	Blue Downs (Home)	31/08/2019 18:05	07/09/2019 07:25	6.6	735.3	718.0	17.3	2.1	0.087	Available on request	
Short term	SLF 808	BDH1	Blue Downs (Home)	31/08/2019 22:15	07/09/2019 07:10	6.4	738.7	714.0	24.7	2.1	0.087	Available on request	
Short term	SLF 225	BDH2	Blue Downs (Home)	01/09/2019 17:15	07/09/2019 07:15	5.6	737.0	727.0	10.0	2.1	0.087	Available on request	
Short term	SLF 608	BDH3	Blue Downs (Home)	31/08/2019 21:45	07/09/2019 07:25	6.4	733.0	720.7	12.3	2.1	0.087	Available on request	
Short term	SLF 526	BDH4	Blue Downs (Home)	01/09/2019 13:52	07/09/2019 07:29	5.7	723.0	704.0	19.0	2.1	0.087	Available on request	
Short term	SLF 319	BDH5	Blue Downs (Home)	31/08/2019 16:07	07/09/2019 07:26	6.6	695.0	682.0	13.0	2.1	0.087	Available on request	
Short term	SLF 259	TGS5	Tuscany Glen High School	03/09/2019 08:00	06/09/2019 15:00	3.3	726.0	720.7	5.3	2.1	0.087	Available on request	
Short term	SLF 503	TGS7	Tuscany Glen High School	03/09/2019 08:31	06/09/2019 13:21	3.2	723.7	714.7	9.0	2.1	0.087	Available on request	
Short term	SLF 267	TGH1	Blue Downs (Home)	31/08/2019 22:18	07/09/2019 07:00	6.4	665.3	661.0	4.3	2.1	0.087	Available on request	
Short term	SLF 348	TGH2	Blue Downs (Home)	31/08/2019 17:03	07/09/2019 07:33	6.6	712.0	702.0	10.0	2.1	0.087	Available on request	
Short term	SLF 285	TGH3	Blue Downs (Home)	31/08/2019 18:06	07/09/2019 06:39	6.5	727.0	714.0	13.0	2.1	0.087	Available on request	

Table D.4: Additional information of schools and homes in Western Cape (continued).

Electret type	Serial number	Code	Location	Start date	Finish date	Days	$V_i$	$V_j$	$\Delta V$	CF	G	Coordinates	
												x	y
Short term	SLF 235	TGH4	Blue Downs (Home)	31/08/2019 20:15	07/09/2019 22:25	7,1	723,0	710,3	12,7	2,1	0,087	Available on request	
Short term	SLF 330	TGH6	Blue Downs (Home)	02/09/2019 07:05	07/09/2019 06:06	5,0	733,7	729,7	4,0	2,1	0,087	Available on request	
Short term	SLF 332	MZS1	Manzomthombo Secondary School	02/09/2019 00:00	09/09/2019 00:00	7,0	713,0	702,0	11,0	2,1	0,087	Available on request	
Short term	SLF 458	MZS2	Manzomthombo Secondary School	02/09/2019 00:00	09/09/2019 00:00	7,0	728,0	696,0	32,0	2,1	0,087	Available on request	
Short term	SLF 209	MZS3	Manzomthombo Secondary School	02/09/2019 00:00	09/09/2019 00:00	7,0	712,0	693,0	19,0	2,1	0,087	Available on request	
Short term	SLF 355	MZH1	Mfuleni (Home)	01/09/2019 09:09	07/09/2019 07:36	5,9	711,7	705,3	6,3	2,1	0,087	Available on request	
Short term	SLF 214	MZH2	Mfuleni (Home)	31/08/2019 16:24	07/09/2019 07:20	6,6	759,7	738,0	21,7	2,1	0,087	Available on request	
Short term	SLF 253	MZH3	Mfuleni (Home)	31/08/2019 18:08	07/09/2019 07:41	6,6	729,0	716,0	13,0	2,1	0,087	Available on request	
Short term	SLF 307	SKH1	Kuils River (Home)	31/08/2019 18:56	07/09/2019 07:26	6,5	724,0	695,3	28,7	2,1	0,087	Available on request	
Short term	SLF 333	SKH2	Kuils River (Home)	31/08/2019 19:59	07/09/2019 06:15	6,4	720,7	707,3	13,3	2,1	0,087	Available on request	
Short term	SLF 212	SKH3	Kuils River (Home)	31/08/2019 16:20	07/09/2019 07:56	6,7	696,0	682,3	13,7	2,1	0,087	Available on request	
Short term	SLF 360	SKH4	Kuils River (Home)	01/09/2019 12:58	07/09/2019 07:55	5,8	731,0	719,0	12,0	2,1	0,087	Available on request	

## E Western Cape lithology information

Table E.1: Lithology description in Western Cape (Paarl)

Code	Lithology
C2 WC L1	Greywacke, phyllite, schist, limestone
C2 WC L2	Pebbly quartz arenite, diamictite, minor conglomerate, mudrock, siltstone and shale
C2 WC L3	Porphyritic, medium or fine-grained granite and granodiorite, with subordinate syenite, gabbro, diorite and quartz porphyry

Table E.2: Lithology description in Western Cape (Cape Flats)

Code	Lithology
C3 WC L1	Pebbly quartz arenite, diamictite, minor conglomerate, mudrock, siltstone and shale
C3 WC L2	Phyllite, metagreywacke, quartzite, minor volcanic rocks
C3 WC L3	Porphyritic, medium or fine-grained granite and granodiorite, with subordinate syenite, gabbro, diorite and quartz porphyry
C3 WC L4	Quartzite, conglomerate, slate
C3 WC L5	Quartzose sand, pelletal phosphorite, gravel, sandy silt, grey-black carbonaceous kaolinitic clay, peat, shelly limestone and sandstone, shelly sand and (aeolian) calcarenite, coquinite, light grey to reddish sandy soil, loamy sand

## F Cost-Effectiveness of radon detectors

When conducting a radon test is important to take costs into considerations. Here we outline the cost-effectiveness of radon detectors used in this study and roughly estimate how much each radon test can cost.

Short term test (7 days)

Unit	Price
Short term electrets	R 320
S-chamber	R 800

A new electret comes with a potential voltage of 700 volts, and the manufacturer does not recommend using an electret with less than 100 volts.

Checking how many tests can one short-term electret perform the average indoor levels can be assumed to be  $40 \text{ Bqm}^{-3}$  (the global average).

The information above is sufficient to estimate the voltage drop if the measurements are conducted for seven days, with the help of the equation below (F.1) and the results obtained in [House9](#) (bedroom).

$$40 = \frac{\Delta V}{CF \cdot T} - B_{\gamma c} \quad (\text{F.1})$$

$$\Delta V = V_i - V_f \approx 38V$$

Therefore for an electret to get depleted from 700 V to 100 V i.e.  $\frac{700V-100V}{38V} \approx 15$ , then the electret detectors may be reused about 15 times before requiring a recharge. On average, it would cost roughly R25.00 per radon test (excluding the price of S-Chamber).

Now we can compare the cost of long-term (3 months) radon test between the electret ion-chamber (Rad Elec), track-etch (ParcRGM) and Airthings™ radon detectors.

Long term test (91 days)

Unit	Price	Description
Short term electrets	R 325	
Track-etch (ParcRGM)	R 162	The total cost including the delivery and reading/analysis costs.
Airthings™	R 3000	A cost of 1 Airthings radon detector.

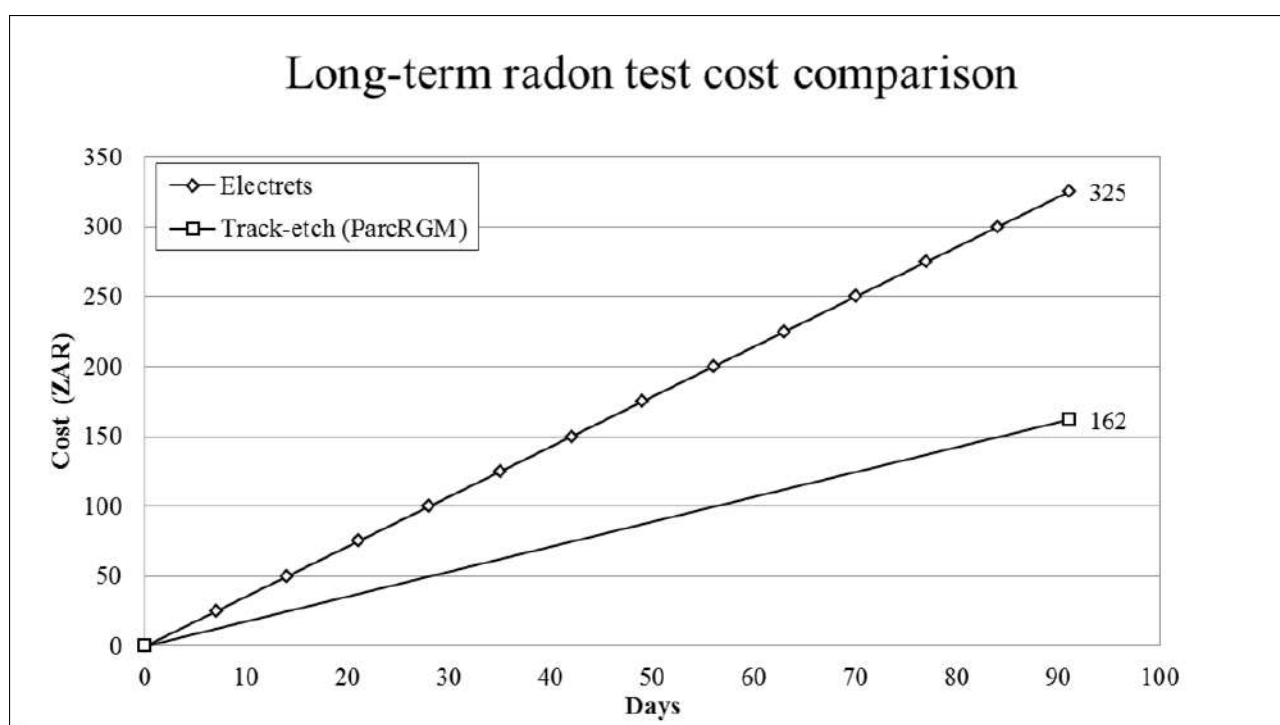


Figure F.1: Cost comparison between the electret detector and track etch detector for long-term measurements (3-months).

Remark 1: The use of electrets for short-term measurements could effectively reduce the cost of radon test.

Remark 2: Track etch radon monitors could be cost-effective for long-term radon measurements.



## References

## References

- [Abd06] Abdelouas, A. 2006. Uranium Mill Tailings: Geochemistry, Mineralogy, and Environmental Impact. *Elements* 2, 335.
- [Air18] Airthings Wave. 2018. Smart Radon Detector user's manual, Revision 2018, access 3 November 2020. URL: <http://www.airthings.com/hubfs/Website/Manuals/Wave/Wave%20Manual.pdf>.
- [Alg14] Alghamdi, A.S. & Aleissa, K.A. 2014. Influences on indoor radon concentrations in Riyadh, Saudi Arabia. *Radiation Measurements* 62 35 - 40.
- [All08] Allègre, C. J. 2008. *Isotope geology*. Cambridge University Press
- [Alp20] AlphaGUARD. 2020. User's manual, Revision 2020-10-20, access 3 November 2020. URL: <http://www.durridge.com/support/product-manuals/>
- [Ana03] Anastasiou, T., Tsertos, H., Christofides, S. & Christodoulides, G. 2003. Indoor radon ( $^{222}\text{Rn}$ ) concentration measurements in Cyprus using high-sensitivity portable detectors. *J. Environ. Radioact.* 68, 159–169. URL: [https://doi.org/10.1016/S0265-931X\(03\)00052-3](https://doi.org/10.1016/S0265-931X(03)00052-3).
- [Bal20] Ballance, L. 2020. Radon: how is radon measured? How does an Airthings device measure radon? URL: <https://help.airthings.com/en/articles/3119759-radon-how-is-radon-measured-how-does-an-airthings-device-measure-radon>.
- [Bau97] Bauser, H. & Range, W. 1997. The electret ionization chamber: a dosimeter for long-term personnel monitoring. *Health Physics* 34, 97.
- [Bát15] Bátor, G., Csordás, A., Horváth, D., Somlai, J. & Kovács, T. 2015. A comparison of a track shape analysis-based automated slide scanner system with traditional methods. *J Radioanal Nucl Chem* 306:333–339.
- [Bay04] Baysson, H., Tirmarche, M., Tymen, G., Gouva, S., Caillaud, D., Artus, J.C., Vergnenegre, A., Ducloy, F. & Laurier, D. 2013. Indoor radon and lung cancer in France. Vol. 15, No. 6, pp. 709-716 (8 pages) URL: <https://www.jstor.org/stable/20485979>
- [Bos03] Bossew, P. 2003. The radon emanation power of building materials, soils and rocks. *Applied Radiation and Isotopes* 59(5-6):389-92
- [Bos19] Bossew, P. 2015. Radon priority areas and radon extremes - initial statistics considerations. *Radiation Environment and Medicine*, vol.8 No.2 94-104.
- [Bot19] Botha, R., Labuschagne, C., Williams, A.G., Bosman, G., Brunke, E.-Eg., Rossouw, A. & Lindsay, R. 2018. Radon-222 measurements at Cape Point: a characterization of a 15 year time series. *Clean Air J.* 28(2). URL: <http://dx.doi.org/10.17159/2410-972x/2018/v28n2a11>.
- [Bot17] Botha, R., Newman, R.T., Lindsay, R. & Maleka, P.P. 2017. Radon and thoron in-air occupational exposure study within selected wine cellars of the Western Cape (South Africa) and associated annual effective doses, *Health Physics Society* 11 2(1):98-107.

## References

- [Bot16] Botha, R., Newman, R.T. & Maleka, P.P. 2016. Radon levels measured at a touristic thermal spa resort in Montagu (South Africa) and associated effective doses. *Health Health Physics Society* 111:281289.
- [Bus11] Bushberg, J.T. & Boone, J.M. 2011. *The essential physics of medical imaging*. Lippincott Williams & Wilkins.
- [Car19] Carelli, V., Bianco, V., Cordedda, C., Ferrigno, G., Carpentieri, C & Bochicchio, F. 2009. A national survey on radon concentration in underground inspection rooms and in buildings of a telephone company: methods and first results. *Radiat. Meas.* 44,1058–1063. URL: <https://doi.org/10.1016/j.radmeas.2009.10.085>.
- [Cin15] Cinelli, G. & Tondeur, F. 2015. Log-normality of indoor radon data in the Walloon region of Belgium. *Journal of Environmental Radioactivity*, 143 (2015) 100-109. URL: <https://doi.org/10.1016/j.jenvrad.2015.02.014>.
- [Dar05] Darby, S., Hill, D., Auvinen, A., Barros-Dios, J.M., Baysson, H., Bochicchio, H., Deo, H., Falk, R., Forastiere, F., Hakama, M., Heid, I., Kreienbrock, L., Kreuzer, M., Lagarde, F., Mäkeläinen, I., Muirhead, C., Oberaigner, W., Pershagen, G., Ruano-Ravina, A., Ruosteenoja, E., Schaffrath Rosario, A., Tirmarche, M., Tomásek, L., Whitley, E., Wichmann, H.E. & Doll, R. 2005. Radon in homes and risk of lung cancer: collaborative analysis of individual data from 13 European case-control studies, *British Medical Journal*.330:223–227.
- [Dar14] Daraktchieva, Z., Miles, J. C. H. & McColl, N. 2014. Radon, the lognormal distribution and deviation from it *Journal of Radiological Protection*, IOP Publishing, 2014, 34, 183-190.
- [Deh12] Dehkordi, A.N. 2012. Assessment of radiation doses to the West Rand public due to inhalation of  $^{222}\text{Rn}$  and its daughter products. Master's thesis, University of Witwatersrand.
- [Dow17] Dowdall, A., Murphy, P., Pollard, D. & Fenton, D. 2017. Update of Ireland's national average indoor radon concentration – application of a new survey protocol. *J. Environ. Radioact.* 169 (170), 1–8. URL: <https://doi.org/10.1016/j.jenvrad.2016.11.034>.
- [Dur20] DURRIDGE. 2020. RAD7 user's manual, revision 2020-10-20, access 3 November 2020. URL: <http://www.durridge.com/support/product-manuals/>
- [Eli98] Ellis, J.F. 1998. The assessment of potential radiation hazards from gold mines in the free state goldfields to members of the public, Master's thesis, Department of Physics, University of Free State.
- [EPA03] United States Environmental Protection Agency. 2003. EPA assessment of risks from radon in homes. Washington, DC.
- [Fil19] Filip, S., Jan Š. & Jan Š. 2019. Low-Cost Radon Detector with Low-Voltage Air-Ionization Chamber. *Sensors*, 19, 3721; doi:10.3390/s19173721
- [Fri05] Friedmann, H., 2005. Final results of the Austrian radon project. *Health Phys.* 89,339–348. URL: <https://doi.org/10.1097/01.HP.0000167228.18113.27>.

## References

---

- [Gra09] Gray, A., Read, S., McGale, P. & Darby, S. 2009. Lung cancer deaths from indoor radon and the cost effectiveness and potential of policies to reduce them. *BMJ*; 338 doi: <https://doi.org/10.1136/bmj.a3110>.
- [Ham71] Hamilton, E.I. 1971. The Relative Radioactivity of Building Materials, *American Industrial Hygiene Association Journal*, p 398-403.
- [How07] Howarth, C.B. & Miles, J.C.H. 2007. Results of the 2003 NRPB Intercomparison of Passive Radon Detectors.
- [IAE04] International Atomic Energy Agency. 2004. The Long Term Stabilization of Uranium Mill Tailings, IAEA-TECDOC-1403.
- [IAE19] International Atomic Energy Agency. 2019. Radon Survey Design, IAEA-PUB1848.
- [ICR93] ICRP (International Commission on Radiological Protection). 1993. Protection against radon 222 at Homes and at Work. ICRP publication 65. Pergamon Press. Oxford.
- [ICR08] ICRP (International Commission on Radiological Protection). 2008. Radiation Dose to Patients from Radiopharmaceuticals - Addendum 3 to ICRP Publication 53. ICRP Publication 106. *Ann. ICRP* 38 (1-2).
- [Iva13] Ivanova, K., Stojanovska, Z., Badulin, V. & Kunovska, B. 2013. Pilot Survey of Indoor Radon in the Dwellings of Bulgaria. *Radiation protection Dosimetry*, 157 (4), 594-599.
- [Jen02] Jensen, C. L., Strand, T., Ramberg, G., Ruden, L. & Ånestad, K. 2002. The Norwegian Radon Mapping and Remediation Program, Norwegian Radiation Protection Authorities, P.O. Box 55, N-1332 Osteraas, Norway.
- [Joj09] Jo, J.H., Seok, H.T., Yeo, M.S. & Kim, K.W. 2009. Simplified prediction method of stack-induced pressure distribution in high-rise residential buildings, *Journal of Asian Architecture and Building Engineering*, 8:1, 283-290, DOI: 10.3130/jaabe.8.283
- [Jón15] Jónsson, G., Theodórsson, Ó.H.P., Karlsson, S.M.M.R.K. 2015. Indoor and outdoor radon levels in Iceland. URL: <https://gr.is/wp-content/uploads/2016/09/Indoor-and-outdoor-radon-levels-in-Iceland>
- [Kam17] Kamunda, C., Mathuthu, M. & Madhuku, M. 2017. Determination of Radon in Mine Dwellings of Gauteng Province of South Africa using AlphaGUARD Radon Professional Monitor. *J Environ Toxicol Stud* 1(1).
- [Kel01] Keller, G., Hoffmann, B., Feigenspan, T. 2001. Radon permeability and radon exhalation of building materials. *Science of the Total Environment*.272:85–89.
- [Kel15] Kelly, R.I. & Bobrowsky P.T. 2015. Aggregate potential mapping. URL: <https://www.researchgate.net/publication/276206887>.
- [Kha13] Khalid, N., Majid, A.A, Ismail, A.F., Yasir, M.S., Yahaya, R., Mustafa, I.A. 2013. Variation of radon emanation in workplaces as a function of room parameters, *The Malaysian Journal of Analytical Sciences*, Vol 17 No 1: 59 - 70.

References

---

- [Kha19] Khalil, M.T., Walid, M.K., Anwar, M.J. 2019. Measurements of Indoor Radon Concentrations in Selected Educational Institutions and Homes in Jericho City - Palestine. *Hebron University Research Journal( A)*, Vol.(8), pp.(40 -51)
- [Kie97] Kies, A., Biell, A., Rowlinson, L., Feider, M.1997. Radon survey in the grand-duchy of Luxembourg - indoor measurements related to house features, soil, geology, and environment. *Environ. Int.* 22, 805–808. URL: [https://doi.org/10.1016/S0160-4120\(96\)00187-0](https://doi.org/10.1016/S0160-4120(96)00187-0).
- [Kno00] Knoll, G.F. 2000. *Radiation detection and measurement*. John Wiley & Sons.
- [Kim03] Kim, C.K., Lee, S.C., Lee, D.M. 2003. Nationwide survey of radon levels in Korea. *Health Physics*. 84(3):354-360.
- [Kot90] Kotrappa, P., Dempsey, J.C., Ramsey, R.W., Stieff, L.R. 1990. A practical EPERMTM (electret passive environmental radon monitor) system for indoor <sup>222</sup>Rn measurement. *Health Phys.* 58, 461-467.
- [Kra88] Krane, K.S. 1988. *Introductory nuclear physics*. John Wiley & Sons.
- [Kre05] Krewski, D., Lubin, J.H., Zielinski, J.M., Alavanja, M., Catalan, V.S., Field, R.W., Klotz, J.B., Létourneau, E.G., Lynch, C.F., Lyon, J.I., Sandler, D.P., Schoenberg, J.B., Steck, D.J., Stolwijk, J.A., Weinberg, C. & Wilcox, H.B. 2005. Residential radon and risk of lung cancer: a combined analysis of 7 North American case-control studies. *Epidemiology*.16:137–145.
- [Kri17] Kristiansen, C. 2017. Charcoal Versus Airthings – Accuracy. *Airthings.com*. Accessed from: [www.airthings.com](http://www.airthings.com). Retrieved 13 December 2020.
- [Lem01] Lembrechts, J., Janssen, M., Stoop, P., 2001. Ventilation and radon transport in Dutch dwellings: computer modelling and field measurements. *Sci. Total Environ.* 272, 73–78. URL: [https://doi.org/10.1016/S0048-9697\(01\)00667-2](https://doi.org/10.1016/S0048-9697(01)00667-2).
- [Leu02] Leuschner, A.H., Steyn, A., Strydom, R. & de Beer, G.P. 2002. Indoor radon concentrations in South African Homes. Atomic Energy Corporation of South Africa Limited.
- [Lin08] Lindsay, R., Newman, R.T. & Speelman, W.J. 2008. A study of airborne radon levels in Paarl houses (South Africa) and associated source terms, using electret ion chambers and gamma-ray spectrometry, *Applied Radiation and Isotopes*, Vol.66(11), pp.1611-1614.
- [Lub04] Lubin, J.H., Tomásek, L., Edling, C., Hornung, R.W., Howe, G., Kunz, E., Kusiak, R.A., Morrison, H.I., Radford, E.P., Samet, J.M., Tirmarche, M., Woodward, A., Yao, S.X. 2004. Risk of lung cancer and residential radon in China: pooled results of two studies. *International Journal of Cancer*. 109:132–137.
- [Mar15] Mar, Y., Abbas, S., Mohammad, H. M., Narges, S., Noushin, R. & Majid, K. 2016. Estimation of the residential radon levels and the annual effective dose in dwellings of Shiraz, Iran, in 2015, *Electronic Physician* (ISSN: 2008-5842), Volume: 8, Issue: 6, Pages: 2497-2505, DOI: <http://dx.doi.org/10.19082/2497>
- [Mil90] Miles, J.C.H., Green, B.M.R., Lomas, P.R. & Cliff, K.D. 1990. Radon Affected Areas: Cornwall and Devon. *Documents of the NRPB I*, (4), p 37-43.

## References

---

- [Moe80] Moeller, T., Kleinberg, J. & Castellion, M.E. 1980. Chemistry with Inorganic Qualitative Analysis. Elsevier Inc. DOI: <https://doi.org/10.1016/B978-0-12-503350-3.X5001-X>.
- [Mor99] Morkunas, I., Akelbrom, G. 1999. The results of the Lithuanian radon survey. Radon in the Living Environment.
- [Mos19] Moshupya, P., Abiye, T., Mouri, H., Levin, M., Strauss, M. & Strydom, R. 2019. Assessment of Radon Concentration and Impact on Human Health in a Region Dominated by Abandoned Gold Mine Tailings Dams: A Case from the West Rand Region, South Africa, *Geosciences* 9(11), 466.
- [Nad19] Nader, A.F. 2019. The determination of equilibrium factor of radon and thoron using LR-115 type II detector in a selected area from Basra Governorate, Iraq, *IOP Conf. Series: Journal of Physics: Conf. Series* 1258 (2019) 012032
- [Nem05] Nemangwele, F. 2005. Radon in the Cango Caves, Master's thesis, Department of Physics, University of the Western Cape.
- [Nik02] Nikolopoulos, D., Louizi, A., Koukoulidou, V., Serefoglou, A., Georgiou, E., Ntalles, K., Proukakis, C. 2002. Radon survey in Greece - risk assesment. *J. Environ. Radioact.* 63, 173–186. [https://doi.org/10.1016/S0265-931X\(02\)00026-7](https://doi.org/10.1016/S0265-931X(02)00026-7)
- [Ott92] Otton, J.K. 1992. The geology of radon, Report, URL: <https://pubs.usgs.gov/gip/7000018/report.pdf>
- [Pan14] Pantelić, G., Eremic Savković, M., Živanović, M., Nikolić, J., Rajačić, M. & Todorović, D. 2014. Uncertainty evaluation in radon concentration measurement using charcoal canister. *Applied Radiation and Isotopes* 87 452–455.
- [Pan19] Pantelić, G., Čeliković, I., Živanović, M., Vukanac, I., Nikolić, J.K., Cinelli, G., Gruber, V. 2019. Qualitative overview of indoor radon surveys in Europe, *Journal of Environmental Radioactivity* 204 163174.
- [Par20] Parc RGM (Radon gas monitoring) (pty) Ltd, ([www.parcrgm.co.za](http://www.parcrgm.co.za)), 2020
- [Par18] Park, T.H., Kang, D.R., Park, S.H., Yoon, D.K. & Lee, C.M. 2018. Indoor radon concentration in Korea residential environments, *Environmental Science and Pollution Research* 25:12678–12685.
- [Phe20] Phefo, L. 2020. Determining the Radon Emanation Coefficient for Soil Samples. MSc thesis. University of Zululand.
- [Rad15] Rad-Elec. 2015. Quick Start Manual, Version 2.321i.
- [Rim18] Rima, R.H., Rida, Y.N., Zena, H., Ibrahim, A., Gabriel, K. 2018. Indoor and Outdoor Radon Concentration Levels in Lebanon, *Health Physics* 115(3):344-353
- [Rob13] Robertson, A., Allen, J., Laney, R. & Curnow, A. 2013. The cellular and molecular carcinogenic effects of radon exposure: a review, *International Journal of Molecular Sciences* 14(7):14024-63
- [Rou19] Roux, R.R., Bezuidenhout, J. & Smit, H.A.P. 2019. The influence of different types of granite on indoor radon concentrations of dwellings in the South African West Coast Peninsula. *Journal Of Radiation Research And Applied Sciences*, Vol. 12, No. 1, 375382.

## References

- [Saa10] Saad, A.F., Abdalla, Y.K., Hussein, N.A., Elyaseery, I.S. 2010. Radon exhalation rate from building materials used on the Garyounis University campus, Benghazi, Libya. *Turkish J. Eng. Env. Sci.* 34 (2010) , 67 – 74.
- [Saa18] Saadi, R., Marah, H., Hakam, O.K. 2018. Setting up a continuous monitor for the control of temporal variability of  $^{222}\text{Rn}$  in groundwater: Application to samples from Tadla Basin, Morocco, *J. Mater. Environ. Sci.*, Volume 9, Issue 5, Page 1439-1445.
- [Sah10] Sahooa, B.K., Mayyaac, Y.S., Sapraa, B.K., Gawarea, J.J., Banerjeeb, K.S. & Kushwahaa, H.S. 2010. Radon exhalation studies in an Indian uranium tailings pile, *Radiation Measurements*, Volume 45, Issue 2 Pages 237-241.
- [Sap12] Saphymo GmbH. 2012. AlphaGUARD user's manual, Revision 2012-18, access 3 November 2020. URL:<http://www.saphymo.de>.
- [Spe04] Speelman, W.C. 2004. Modelling and measurement of radon diffusion through soil for application on mine tailings dam. MSc thesis. University of the Western Cape.
- [Suz10] Suzuki, G., Yamaguchi, I., Ogata, H., Sugiyama, H., Yonehara, H., Kasagi, F., Fujiwara, S., Tatsukawa, Y., Mori, I. & Kimura, S. 2010. A nation-wide survey on indoor radon from 2007 to 2010 in Japan. *J. Radiat. Res.*, 51 683689.
- [Syn06] Synnott, V., Hanley, O., Fenton, D. & Colgan, P.A. 2006. Radon in Irish schools: the results of a national survey, *J. Radiol. Prot.* 26 8596.
- [Tas15] TASLIMAGE Radon and Neutron dosimetry system. 2015. Manual, Track Analysis Systems Ltd, Bristol, UK.
- [Tho02] Thomas, J., Hulka, J., Tomasek, L., Fojtikova, I. & Barnet, I. 2002. Determination of radon prone areas by probabilistic analysis of indoor survey results and geological prognostic maps in the Czech Republic International Congress Series 1225 49 54.
- [Tre08] Tretkoff, E. 2008. American Physics Society. URL:<https://www.aps.org/publications/apsnews/200803/physicshistory.cfm>.
- [Tre18] Trevisi, R., Leonardi, F., Risica, S., Nuccetelli, C. 2018. Updated database on natural radioactivity in building materials in Europe, *Journal of Environmental Radioactivity*, Volume 187, Pages 90-105.
- [UNS00] United Nations Scientific Committee on the Effects of Ionizing Radiation. 2000. New York, p. 453-87.
- [UNS08] United Nations Scientific Committee on the Effects of Atomic Radiation. 2008. UNSCEAR Report on Sources And Effects of Ionizing Radiation. Vol.I.
- [Vuk18] Vukotic, P., Antovic, N., Djurovic, A., Zekic, R., Svrkota, N., Andjelic, T., Svrkota, R., Mrdak, R., Bjelica, N., Djurovic, T., Dlabac, A., Bogicevic, M. 2018. Radon survey in Montenegro - a base to set national radon reference and "urgent action" level. *J. Environ. Radioact.* 1–8. URL: <https://doi.org/10.1016/j.jenvrad.2018.02.009>.
- [WHO09] World Health Organization. 2009. WHO Handbook on Indoor Radon. Geneva: WHO.

## References

---

- [WHO17] World Health Organization. 2017. WHO report on the global tobacco epidemic: country profile Austria. Geneva: WHO.
- [Wil16] Williams, J.M. 2016. Biological Effects of Microwaves: Thermal and Non-thermal Mechanisms. A Report by an Independent Investigator. v. 4.7 URL:<http://www.scribd.com/jmmwill/documents>.
- [Yar12] Yaroshevich, I., Zhuk, V., Karabanov, K., Matveev, V., Konopelko, V., Vasilevsky, L., Lukashevich, A. 2012. Indoor radon and radon component of radiation doses of the population in different areas of Belarus. *Beloruskaya Nauk* 56, 92–97.
- [Zub16] Zubair, M., Kassar, A.A., Hamouda Ishag, A.M., Ansari, A.A., Hussain Aljassmi, A.A., 2016. Radiation Measurement in the University of Sharjah. *Int J Magn Nucl Sci.* 2(5), 33-38. doi: [dx.doi.org/10.19070/2577-4387-160006](https://doi.org/10.19070/2577-4387-160006).